INVESTIGATION OF HARMONICS ON POWER DISTRIBUTION SYSTEM

A DISSERTATION

Submitted in partial fulfillment of the requirements for the award of the degree of

MASTER OF TECHNOLOGY

in

ELECTRICAL ENGINEERING

(With Specialization in Power Apparatus & Electric Daives Engineering)

By

BHARAT SINGH RAJPUROHIT

DEPARTMENT OF ELECTRICAL ENGINEERING
INDIAN INSTITUTE OF TECHNOLOGY, ROORKEE
ROORKEE-247 667 (INDIA)

June, 2005

CANDIDATE'S DECLARATION

I hereby declare that work which is being presented in this dissertation entitled **"INVESTIGATION OF HARMONICS ON POWER DISTRIBUTION SYSTEM"** in partial fulfillment of the requirement for the award of degree of Master of Technology with specialization in **Power Apparatus and Electric Drives**, submitted in the department of Electrical Engineering, Indian Institute of Technology Roorkee, Roorkee, is an authentic record of my work under supervision of **Dr. G. K. Singh,** Professor, Department of Electrical Engineering, Indian Institute of Technology Roorkee, Roorkee.

The matter embodied in this dissertation work has not been submitted by me for the award of any other degree or diploma.

Date: June 29, 2005

Place: Roorkee

(B. S. Rajpurohit)

This is to certify that the above statement made by the candidate is correct to the best of my knowledge and belief.

Date: 29/06/05

Place: Roorkee

(Dr. G. K. Singh)
Professor
Indian Institute of Technology
Roorkee, Roorkee-247667
(India)

ACKNOWLEDGEMENTS

I wish to express my profound sense of gratitude and intentness to **Dr. G. K Singh Professor, Department of Electrical Engineering, Indian Institute of Technology Roorkee, Roorkee** for their unfailing inspiration, whole hearted co-operation, excellent guidance and supervision for the completion of this dissertation. The valuable discussions with him gave me many important impulses that contributed considerably to both my technical and personal development. The acre with which hey examined the manuscript is thankfully acknowledged.

My heartfelt gratitude and indebtness goes to **my teachers** of Power Apparatus & Electric Drives, with their encouraging and caring words, constructive criticism and suggestions have contributed directly or indirectly in a significant way towards completion of this dissertation.

I am indebted to all **my classmates** from Power Apparatus & Electric Drives group for taking interest in discussing my problems and encouraging me. Thanks are also due to those who helped me directly or indirectly in my endeavor.

(Bharat Singh Rajpurohit)

ABSTRACT

Investigation of harmonics on power distribution system is presented, i.e. qualitative overview study of the distribution power system with the goal of understanding harmonics waveform distortion within it, and to provide a detailed analysis, that gives quantitative answers to the distortion due to the specific sources of harmonics and to take preventive measures for control of the same is done and presented in this work.

A complete analytical model for the most common load type, i.e. single-phase power electronic load, is derived and investigation of the cumulative harmonic current characteristics of a large number of such loads is done. This model is then used to investigate the impact of 1) interaction due to shared source impedance, 2) variation in power level, and 3) variations in circuit parameters, on individual and cumulative current harmonics. Derivation of harmonic domain models suitable for the study of conventional three-phase, six pulse harmonic converters is performed. Modulation theory based on switching functions and discrete convolutions are the cornerstone of these models. Inrush current phenomenon, arising during transformer energization, and containing a slowly decaying transient response, with connection to harmonic domain technique is presented.

A need to reduce the harmonics and reactive power in the system has occurred mostly due to large use of power electronic apparatus. The comparison of the technologies developed for handling harmonic and reactive power reveals that the strategy of hysteresis current control provides best results with regard to THD confirming well to IEEE – 519 standards. But the major limitation is the high and variable switching frequency of operation of the devices, which results in complexity in design of filters needed to meet the EMI standards. This led to selection of control techniques suitable for APF which employing constant switching frequency. Hence adaptive hysteresis band current controller is proposed and modeled. Analytical results are presented to show the effectiveness of the proposed shunt active filter.

CONTENTS

1. INTRODUCTION

The development of technology over the years, especially the progress of power electronics applications, has brought about many technical conveniences and economical profits, but it has simultaneously created new challenges for power system operation studies. Driven by challenging environmental constraints, liberalization of the energy market and privatization of the power supply industry, power systems are more and more often operating at their maximal performance limits - and frequently beyond them - to maximize asset utilization. To avoid serious functional problems from occurring under these conditions, the system's secure and reliable operation needs to be maintained regarding various aspects of power system operation. One of the main topics of special concern is an aspect of wide power quality area which deals with, among others, voltage characteristics, one of which is analysis and control of harmonics.

Since the quality of electrical power, e.g. the voltage at the point of common coupling, has become an important feature of consumer goods on the market, the interest in finding, describing and above all, in forecasting system behavior grows continuously. On the one hand, an extensive use of power electronic loads, especially in distribution networks, introduces new inconveniences to proper system operation and demands an analytical method to forecast serious harmonic problems before they occur. On the other hand, the development of standards can help to keep the disturbances within the limits, which simultaneously influences the proper voltage waveform within the system. Obviously, in standards, the tendency in the setting up compatibility levels, e.g. for the voltage harmonics, shows a direct convergence to the increasing number of harmonic sources [1].

The facts that conventional power supply systems are designed to operate with sinusoidal waveforms and electric utilities strive to supply customers with reliable power of good "quality" that does not represent a damaging threat to their equipment conflicts with the steep development that the power electronic industry has undergone lately. This incoherent development results in the introduction of appliances that are more sensitive to the quality of power supplied and simultaneously, during their normal operation they introduce distortion to the steady-state current and voltages. These circumstances have set the basis for paying considerable attention to the quality of electrical power, intensely addressing the issue of voltage distortion, a major form of which is harmonic distortion [2].

1.1 AIM AND STRUCTURE OF WORK

The aim of this work is to do investigation of harmonics on power distribution system, i.e. to do qualitative overview study of the distribution power system with the goal of understanding harmonics waveform distortion within it, and to provide a detailed analysis, that gives quantitative answers to the distortion due to the specific sources of harmonics and to take preventive measures for control of the same. The qualitative analysis enables one to get a general outlook of the studied power system from the harmonics point of view. It can be of special interest in cases of widespread systems.

Since distribution systems are operating nowadays with a high content of power electronic-based equipment that draw distorted currents and cause self-generated interference in the supply voltage, polluting it and propagating the distortion within the system, the need to understand the phenomena is stronger than ever because the damaging effects of harmonics can no longer be ignored [3]. The proper system arrangement avoiding capacitor failure or transformer and neutral conductor overheating demand analytical methods which require proper mathematical models to assure reliable system operation both in existing and in planned distribution systems [4].

Moreover, the detailed analysis of the distribution system in which many types of non-linear loads have a big influence on the quality of voltage should be done, and it makes a whole overview of the potential problems that can arise. Therefore, it is very important to know in advance how the power system, especially the distribution network, as in case of this work, will behave under distorted conditions.

Within the text, the work is structured in the following way.

The introductory part of Chapter 2 is devoted to understanding power system harmonics. The first section covers the brief history of power system harmonics, how harmonics first comes into picture and what are the methods of analysis given at that time. Authentic bibliography of starting period of identification of harmonics and its problem is also given in this section. The second section includes a concise review of the modeling and analysis of harmonics in power networks. Three domains of harmonic analysis: Time, frequency and harmonic domain are discussed in terms of complexity, computation time and accuracy with merits and demerits of each over others. The third section of this chapter covers the description of existing harmonic standards, i.e. IEC 61000, IEEE 519 and EN 50160, in details. This part builds a comprehensive basis for considerations presented in the next chapters of this work.

In Chapter 3, a description of the causes and effects of harmonics are presented. What are the sources of harmonics and how they inject the harmonics in system are presented in first section. Harmonic generation by Power electronic equipments is presented in nutshell. In second section, impacts of harmonics on system voltage, power factor, conductors, transformers and capacitor banks with effect on consumer's equipment, power system protection and interference on communication is discussed.

Chapter 4 is dedicated to present the modeling and simulations of various harmonic sources with investigations of harmonics on distribution systems, so that the analysis and planning of distribution system becomes effective or 'proactive' rather than 'reactive'. The first section is devoted to single-phase power electronic loads and investigation of the cumulative harmonic current characteristics of a large number of such loads. A complete analytical model for the most common load type is derived. This model is then used to investigate the impact of 1) interaction due to shared source impedance, 2) variation in power level, and 3) variations in circuit parameters, on individual and cumulative current harmonics. The thrust of second section is on the derivation of harmonic domain models suitable for the study of conventional three-phase, six pulse harmonic converters. Modulation theory based on switching functions and discrete convolutions are the cornerstone of these models.

With reference to power system harmonics, it was largely in Germany in the 1920s and 1930s when the subject of waveform distortion caused by static converters was developed. The most influential source of converter theory published during that period in English language is the book by Rissik, H. (1935),'The mercury Arc current converter', Pitman ,England. A classical paper on harmonic generation by static converter was written by J.C.Read (1945) 'The calculation of rectifier and inverter performance characteristics' [2].

In 1910, an additional harmonic problem arose as a result of harmonic interference in communication circuits sharing a common right-of-way with power lines [6]. At that time, a reduction in harmonic distortion was achieved through series of practices such as improved generator and transformer designs, improvements in grounding methods and the use of suitable three phase transformer connections. Transmissions lines were kept as short as possible following generator modifications.

Such measures were technically and economically successful thanks to the operational and structural properties of the early power networks. From the utility viewpoint, harmonic distortion was no longer considered to be a problem and for several decades the phenomenon was generally ignored within the power community. This apathy among power engineers began to change when significant resonance problems were encountd, the problem being traced to the harmonics generated by the recent introduction of static drives. In fact, traction applications had been using thyristor and diodes since the late 1960, a trend that was exacerbated in the following decade with the development of faster, cheaper and more reliable power electronics valves.

During the 1950s and 1960s the study of converter harmonics was advanced in the field of high voltage direct current transmission. During this period a large number of papers were published. These are summarized in a book by Kimbark, E.W. (1971).'Direct Current Transmission', Wiley Interscience, which contains 60 references in the field of power system harmonics. In the past few years the subject has been regularly discussed in international meetings and extensive bibliographies are produced from time to time.

2.2 Harmonic Analysis

Harmonic analysis is the process of calculating the magnitudes and phases of the fundamental and higher order harmonics of the periodic waveform. Orthogonal series expansions play a key role in solving a wide range of problems encountered in physics and engineering. Fourier, Hartley, Walsh etc., have been used to approximate non-linear characteristics with good results. They can be used to solve differential equations, resorting only to algebraic means. Because of their very interesting characteristics and high efficiency as integration solvers, they have been researched widely in different engineering fields such as system identification and control.

Harmonic studies are an important component of power system analysis and design. They are used to quantify the distortion in voltage and current waveforms at various points in a power system. Interest in the analysis of harmonics and their effect dates back to the early 1900's but since the late 1970's the subject has gained increasing attention due to the wide-spread use of static power converters. In general there are three main tendencies in the modeling philosophy: studies in time domain, frequency domain, and harmonic domain that can be viewed as a restriction of frequency domain modeling to integer frequencies but with all non-linear interactions modeled [7].

Time domain simulation consists of differential equations representing the dynamic behavior of the interconnected power system components. Mostly, calculations in time domain are used for simulations of transients and non-stationary disturbances in different time ranges. In studies of load non-linearity there also exists time domain models that accommodate both steady-state and dynamic behavior. However, they include parameter derivation procedure and describe only small loads, like a fluorescent lamp or a desktop computer [8]. The resulting system of equations, generally non-linear, is solved using numerical integration. The derivation of harmonic information from time domain programs involves solving for the steady-state and then applying the FFT. For applying the FFT, the basic idea is that the measurements should be made within a 200 ms time window, which means that in the scope of this standard the time window has a width of 10 (for a 50 Hz system) or 12 (for a 60 Hz system) fundamental periods. The sampled data are then subjected to the DFT or, in general, to its smarter version FFT, which results in a 5 Hz resolution of FFT-bins at the output of the FFT processor [9].

Frequency domain simulation in its simplest form provides a direct solution for the effect of specified individual harmonic injections throughout a linear system, without considering the harmonic interaction between the network and the non-linear components. The most commonly used model involves the use of single phase analysis, a single harmonic source and a direct solution [3]. The supply of three-phase fundamental voltage at points of common coupling is well balanced within strict limits, and under these conditions load flow studies are normally carried out on the assumption of perfect symmetry of network components. The same assumption is often made for the harmonic frequencies, even though there is no guarantee from the utilities of harmonic symmetry. The simulations based on models that did not account for the supply-voltage dependency of non-linear loads are very often burden with errors [10]. Therefore, such studies are eligible only for qualitative analysis.

To achieve better accuracy *harmonic domain* analysis, also called iterative harmonic analysis, is often performed. The increased power ratio of modern power electronic devices in relation to system short circuit power means that the principle of superposition that is used in frequency domain simulations does not apply. The harmonic injection from each source will, in general, be a function of that from other sources and the actual system state. Accurate results can only be obtained iteratively solving non-linear equations that describe the steady state as a whole. In many cases, it can be assumed that there are no other frequencies present apart from the fundamental frequency and its harmonics. This type of analysis, in harmonic domain, can be viewed as a restriction of frequency domain modeling to integer frequencies but with all non-linear interactions modeled. Standard methods are employed to obtain a set of accurate non-linear equations which describe the system steady-state mainly at the fundamental frequency [11]. After partitioning the system into linear regions and non-linear devices, these devices are described by isolated equations, depending on given boundary conditions to the linear system [12]. Then, the system solution is predominantly a solution for the boundary conditions for each non-linear device.

Within the text, the work is structured in the following way.

The introductory part of Chapter 2 is devoted to understanding power system harmonics. The first section covers the brief history of power system harmonics, how harmonics first comes into picture and what are the methods of analysis given at that time. Authentic bibliography of starting period of identification of harmonics and its problem is also given in this section. The second section includes a concise review of the modeling and analysis of harmonics in power networks. Three domains of harmonic analysis: Time, frequency and harmonic domain are discussed in terms of complexity, computation time and accuracy with merits and demerits of each over others. The third section of this chapter covers the description of existing harmonic standards, i.e. IEC 61000, IEEE 519 and EN 50160, in details. This part builds a comprehensive basis for considerations presented in the next chapters of this work.

In Chapter 3, a description of the causes and effects of harmonics are presented. What are the sources of harmonics and how they inject the harmonics in system are presented in first section. Harmonic generation by Power electronic equipments is presented in nutshell. In second section, impacts of harmonics on system voltage, power factor, conductors, transformers and capacitor banks with effect on consumer's equipment, power system protection and interference on communication is discussed.

Chapter 4 is dedicated to present the modeling and simulations of various harmonic sources with investigations of harmonics on distribution systems, so that the analysis and planning of distribution system becomes effective or 'proactive' rather than 'reactive'. The first section is devoted to single-phase power electronic loads and investigation of the cumulative harmonic current characteristics of a large number of such loads. A complete analytical model for the most common load type is derived. This model is then used to investigate the impact of 1) interaction due to shared source impedance, 2) variation in power level, and 3) variations in circuit parameters, on individual and cumulative current harmonics. The thrust of second section is on the derivation of harmonic domain models suitable for the study of conventional three-phase, six pulse harmonic converters. Modulation theory based on switching functions and discrete convolutions are the cornerstone of these models.

Third section has presented inrush current phenomenon, arising during transformer energization, and containing a slowly decaying transient response, with connection to harmonic domain technique. Conclusions and results are presented for each section.

Chapter 5 is dedicated to the elimination and/or control of harmonics form power system. In first section the passive filter is introduced with classifications and design flowchart. The second section is devoted to the Active Power Filters. It contains the analysis of Active power filter in detail. Classification of Active filter is presented based on several criteria. Shunt Active power filter (SAF) is modeled and simulated by giving the system equations with application of proposed adaptive hysteresis band current controller. Necessary analytical results are presented to show the effectiveness of the proposed SAF.

2. Understanding Power System Harmonics

In an ideal electrical power system, the voltage and current have perfect sinusoidal waveform and the energy is supplied at a single and constant frequency of specified voltage level and of constant magnitude. However none of these conditions is fulfilled in practice [2].

The deviation from perfect sinusoids is generally expressed in terms of harmonic components. The harmonics are defined as "a sinusoidal component of a periodic wave or quantity having a frequency that is an integral multiple of the fundamental frequency, i.e. the main frequency generated by generators" [5].

Power system harmonic distortion is not a new phenomenon and containing it to acceptable proportion has been a concern of power engineers from the early days of alternating current. The recent growing concern for this problem results from the increasing number and power ratings of the highly non liner power electronic devices used in the control of power apparatus and systems.

2.1 BRIEF HISTORY

To put the subject in historical perspective, it is necessary to go to back to the 18th and 19th centuries when various mathematicians, and in particular J.B.J. Fourier (1768-1830), set up the basis for harmonic calculations [2].

Alternating-current systems technology was new in 1893, and this was the first time an electrical applications problem was addressed using harmonic analysis as a tool. The engineers were grappling with a motor heating problem at Hartford, Conn. To identify its cause and resolve the problem, those engineers conducted harmonic analysis of various electric waveforms throughout the power systems to which the motor was connected. Ultimately, the source of motor heating was traced to transmission line resonances [4].

With reference to power system harmonics, it was largely in Germany in the 1920s and 1930s when the subject of waveform distortion caused by static converters was developed. The most influential source of converter theory published during that period in English language is the book by Rissik, H. (1935),'The mercury Arc current converter', Pitman ,England. A classical paper on harmonic generation by static converter was written by J.C.Read (1945) 'The calculation of rectifier and inverter performance characteristics' [2].

In 1910, an additional harmonic problem arose as a result of harmonic interference in communication circuits sharing a common right-of-way with power lines [6]. At that time, a reduction in harmonic distortion was achieved through series of practices such as improved generator and transformer designs, improvements in grounding methods and the use of suitable three phase transformer connections. Transmissions lines were kept as short as possible following generator modifications.

Such measures were technically and economically successful thanks to the operational and structural properties of the early power networks. From the utility viewpoint, harmonic distortion was no longer considered to be a problem and for several decades the phenomenon was generally ignored within the power community. This apathy among power engineers began to change when significant resonance problems were encountd, the problem being traced to the harmonics generated by the recent introduction of static drives. In fact, traction applications had been using thyristor and diodes since the late 1960, a trend that was exacerbated in the following decade with the development of faster, cheaper and more reliable power electronics valves.

During the 1950s and 1960s the study of converter harmonics was advanced in the field of high voltage direct current transmission. During this period a large number of papers were published. These are summarized in a book by Kimbark, E.W. (1971).'Direct Current Transmission', Wiley Interscience, which contains 60 references in the field of power system harmonics. In the past few years the subject has been regularly discussed in international meetings and extensive bibliographies are produced from time to time.

2.2 Harmonic Analysis

Harmonic analysis is the process of calculating the magnitudes and phases of the fundamental and higher order harmonics of the periodic waveform. Orthogonal series expansions play a key role in solving a wide range of problems encountered in physics and engineering. Fourier, Hartley, Walsh etc., have been used to approximate non-linear characteristics with good results. They can be used to solve differential equations, resorting only to algebraic means. Because of their very interesting characteristics and high efficiency as integration solvers, they have been researched widely in different engineering fields such as system identification and control.

Harmonic studies are an important component of power system analysis and design. They are used to quantify the distortion in voltage and current waveforms at various points in a power system. Interest in the analysis of harmonics and their effect dates back to the early 1900's but since the late 1970's the subject has gained increasing attention due to the wide-spread use of static power converters. In general there are three main tendencies in the modeling philosophy: studies in time domain, frequency domain, and harmonic domain that can be viewed as a restriction of frequency domain modeling to integer frequencies but with all non-linear interactions modeled [7].

Time domain simulation consists of differential equations representing the dynamic behavior of the interconnected power system components. Mostly, calculations in time domain are used for simulations of transients and non-stationary disturbances in different time ranges. In studies of load non-linearity there also exists time domain models that accommodate both steady-state and dynamic behavior. However, they include parameter derivation procedure and describe only small loads, like a fluorescent lamp or a desktop computer [8]. The resulting system of equations, generally non-linear, is solved using numerical integration. The derivation of harmonic information from time domain programs involves solving for the steady-state and then applying the FFT. For applying the FFT, the basic idea is that the measurements should be made within a 200 ms time window, which means that in the scope of this standard the time window has a width of 10 (for a 50 Hz system) or 12 (for a 60 Hz system) fundamental periods. The sampled data are then subjected to the DFT or, in general, to its smarter version FFT, which results in a 5 Hz resolution of FFT-bins at the output of the FFT processor [9].

Frequency domain simulation in its simplest form provides a direct solution for the effect of specified individual harmonic injections throughout a linear system, without considering the harmonic interaction between the network and the non-linear components. The most commonly used model involves the use of single phase analysis, a single harmonic source and a direct solution [3]. The supply of three-phase fundamental voltage at points of common coupling is well balanced within strict limits, and under these conditions load flow studies are normally carried out on the assumption of perfect symmetry of network components. The same assumption is often made for the harmonic frequencies, even though there is no guarantee from the utilities of harmonic symmetry. The simulations based on models that did not account for the supply-voltage dependency of non-linear loads are very often burden with errors [10]. Therefore, such studies are eligible only for qualitative analysis.

To achieve better accuracy *harmonic domain* analysis, also called iterative harmonic analysis, is often performed. The increased power ratio of modern power electronic devices in relation to system short circuit power means that the principle of superposition that is used in frequency domain simulations does not apply. The harmonic injection from each source will, in general, be a function of that from other sources and the actual system state. Accurate results can only be obtained iteratively solving non-linear equations that describe the steady state as a whole. In many cases, it can be assumed that there are no other frequencies present apart from the fundamental frequency and its harmonics. This type of analysis, in harmonic domain, can be viewed as a restriction of frequency domain modeling to integer frequencies but with all non-linear interactions modeled. Standard methods are employed to obtain a set of accurate non-linear equations which describe the system steady-state mainly at the fundamental frequency [11]. After partitioning the system into linear regions and non-linear devices, these devices are described by isolated equations, depending on given boundary conditions to the linear system [12]. Then, the system solution is predominantly a solution for the boundary conditions for each non-linear device.

Summarizing, time domain simulation involving non-linear load behavior requires its mathematical description, e.g. in form of differential equations, which for most types of non-linear load are either difficult to establish or unknown. The drawback is also the lack of power flow constraints, i.e. constant power specification at load buses at the fundamental frequency. The analysis in frequency domain can be built on the standard information including impedances of system elements and the characteristic (spectrum) of the current (or in some cases voltage) injected by non-linear loads bringing fast solutions and an overview, qualitative analysis of the system. But the drawbacks here are considerable errors resulting from the non-linear nature of the harmonic phenomenon itself, and the difficulties in the giving back of the interaction between harmonic source and the network. The harmonic domain is a novel approach and due to the giving back of the load-network interaction it is predestined for quantitative studies. Realistic harmonic domain evaluations are carried using computer calculations. These methods of direct frequency domain evaluation techniques based on self- and mutual convolutions. Convolutions represent a cleaner way of carrying out these operations, avoiding the errors introduced by numeric interpolations and aliasing due to the FFT algorithms.

2.3 Existing Harmonic Standards

The organization widely recognized as the curator of electric power quality standards is the IEC (International Electrotechnical Commission), based in Geneva. The IEC has defined a series of standards, called Electromagnetic Compatibility (EMC) Standards, to deal with power quality issues. The IEC 61000 series includes harmonics and inter-harmonics as one of the conducted low-frequency electromagnetic phenomena. A widespread standard is the IEEE 519-1992 document, which provides guidelines on harmonics and places the responsibility for ensuring power quality on both the utility and consumer [13]. European standard EN 50160 describes electricity as a product, including its shortcomings. It gives the main characteristics of the voltage at the customer's supply terminals in public low-voltage and medium-voltage networks under normal operating conditions [1].

The EN 50160 Gives limits for Harmonic Distortions.

Harmonic Distortion: For harmonic voltage components up to order 25, values are given which shall not be exceeded during 95% of the 10 minute averages obtained in one week. The total harmonic distortion shall not exceed 8% during 95% of the week. The following limits for the low-voltage supply have been reproduced in Table 2.1.

Table 2.1 Harmonic Voltage Limits According to EN 50160

Order	Relative Voltage (%)	Order	Relative Voltage (%)
3	5	15	0.5
5	6	17	2
7	5	19	1.5
9	1.5	21	0.5
11	3.5	23	1.5
13	3	25	1.5

The IEC 61000 Series [2] This section provides a concise description of the documents of the IEC series, which provide internationally accepted information for the control of power system harmonic (and inter-harmonic) distortion.

- *IEC 61000 1-4* Provides the rationale for limiting power frequency conducted harmonic and inter-harmonic current emissions from equipment in the frequency range up to 9 kHz.
- *IEC 61000 2-1 Outlines* the major sources of harmonics in three categories of equipment: power system equipment, industrial loads and residential loads.
- *IEC 61000 2-2* Contains a section on the compatibility levels of the harmonic and inter-harmonic voltage distortion in public low-voltage power industry systems.
- *IEC 61000 2-4* Provides harmonic and inter-harmonic compatibility levels for industrial plant. It also describes the main effects of inter-harmonics.
- *IEC 61000 2-12* Similarly to 61000 2-4, this document deals with compatibility levels for low-frequency conducted disturbances, in this case relating to medium voltage power supply systems. It also covers the subject of injected signals such as those used in ripple control.
- *IEC 61000 3-2* and *3-4* Contain limits for harmonic current emissions by equipment with input currents of 16 A and below per phase. It also specifies the measurement circuit, supply source and testing conditions as well as the requirements for the instrumentation.
- *IEC 61000 3-6* First, indicates the capability levels for harmonic voltages in low- and medium-voltage networks as well as planning levels for MV, HV and EHV power systems. It then makes an assessment of emission limits for distorting loads in MV and HV power systems.
- *IEC 61000 3-12* Provides limits for the harmonic currents produced by equipment connected to low-voltage systems with input currents equal to and below 75 A per phase and subject to restricted connection.
- *IEC 61000 4-7* This is perhaps the most important document of the series, covering the subject of testing and measurement techniques. It is a general guide on harmonic and inter-harmonic measurements and instrumentation for power systems and equipment connected thereto.

IEEE 519-1992 Recognizing the problems caused by nonlinear loads, the IEEE Standards board approved a revised and renamed Standard 519 in the fall of 1992. As indicated by the title, IEEE Standard 519 is a "recommended practice," which means it is not a law or rule for all utility-customer interfaces, but it may be used as a design guideline for new installations. The standard makes the customer responsible for limiting the harmonic currents injected into the power system and the utility responsible for avoiding unacceptable voltage distortion.

IEEE Standard 519 defines harmonic current limits (shown in Table 2.2) for individual customers at the point of common coupling (PCC). Because voltage distortion is caused by the amount of harmonic currents in the system, larger customers are capable of causing more voltage distortion than smaller ones. Recognizing this, the standard allows a higher current THD for smaller customer's loads. The short-circuit ratio (SCR) is used to differentiate customer size.

Table 2.2 Harmonic Current Distortion Limits Allowed by IEEE Standard 519 (V<69kV)

SCR	h<11	11-15	17-21	23-33	h>33	%THD
<20	4.0	2.0	1.5	0.6	0.3	5.0
20-50	7.0	3.5	2.5	1.0	0.5	8.0
50-100	10.0	4.5	4.0	1.5	0.7	12.0
100-1000	12.0	5.5	5.0	2.0	1.0	15.0
>1000	15.0	7.0	6.0	2.5	1.4	20.0

When the load of was shorted, the only impedance limiting the current was the system impedance. That current is called the available short-circuit current, and is generally high since the system impedance is much lower than the load impedance. SCR is defined as the "average maximum demand (load) current" for the facility divided by the available short-circuit current. The maximum load current drawn by a large customer would be a higher fraction of the available short-circuit current, so the large customer's SCR would be lower. The lower the SCR, the more stringent are the IEEE 519 limitations on harmonic currents.

IEEE Standard 519 also provides limits for specific ranges of frequencies, as shown in Table 2.2. Higher-order harmonics are constrained to have lower amplitudes for two reasons. First, higher-order harmonics cause greater voltage distortion than lower-order harmonics, even if they have the same amplitude, because the system inductive reactance is proportional to frequency. Second, interference with telecommunication equipment is more severe for higher-frequency harmonics. Note that Table 2.2 applies only to odd harmonics; even harmonics are limited to 25% of the values for the ranges they would occupy in Table 2.2.

The utility is required by Standard 519 to maintain acceptable levels of voltage distortion (shown in Table 2.3). Below 69 kV, individual harmonic components in the voltage should not exceed 3% of the fundamental, and the voltage THD must be less than 5%. Higher voltages have even lower limits, but those apply primarily to utility interconnections.

Table 2.3 Harmonic Voltage Distortion Limits

Bus Voltage at PCC	Individual Harmonic Voltage Distortion	Total Voltage Harmonic Distortioin
V> 69kV	3.0	5.0
69kV< V<161kV	5.0	2.5
V>161kV	1.0	1.5

3. CAUSES AND EFFECTS OF HARMONICS

3.1 Causes of Harmonics

As previously mentioned the first considerations made at the end of the 19th century identified transformers and rotating machinery as the main source of the waveform distortion since they use magnetic materials that are operated very close to - and often in - the non-linear region for economic purposes. However, the development of technology over decades, especially the underlined growth of the use of switched power semiconductor devices has resulted in rapid proliferation of the harmonics within power systems, so that the harmonics introduced by rotating machinery are considered negligible compared to those introduced by power electronic devices. Transformers can in some circumstances inject certain portions of harmonic to the system.

The term *linear load* indicates that the load current follows the general shape of the applied voltage waveform. Heating elements, motors and incandescent bulbs are examples of linear loads. As can be deduced, *non-linear loads* draw currents that do not generally track with the voltage waveform. This non-linear current flow occurs because most modern electronic devices require direct current (DC) power for operation. Since voltage supplied to end-users by utility companies and energy providers is alternating current (AC), electronic equipment must employ a mechanism to convert the voltage to DC. These mechanisms are called converters.

The most common single-phase converter is the switch-mode power supply. This device is most often found in electronic equipment such as personal computers, printers and copiers. Some fluorescent lighting also utilizes this type of power supply.

The most common three-phase converter is the variable speed motor drive, sometimes referred to as an adjustable speed drive. This device takes AC voltage, rectifies it to DC, and then inverts the voltage back to AC. When converting the DC back to AC, the AC signal is varied in either voltage or frequency (or both) to control the speed of motors. These types of drives are used to control the speed of, for example, fans and pumps in large industrial operations.

The creation of non-linear currents is not dependent on the single-phase or three-phase nature of the device. The fact that we are converting AC to DC produces the non-linear currents. A basic understanding of how this conversion from AC to DC produces harmonic currents is given:

The terminal voltage supplied by the power distribution system is first rectified and applied to a storage capacitor that is an integral component of the converter. In the first half of the cycle, this large capacitor is charged to the average value of the terminal voltage. As the electronic device draws DC power from the converter, the capacitor discharges to some lower voltage limit determined by the converter design. As the capacitor reaches the lower limit of its charge, it begins to charge again-this time in the second half of the voltage cycle. The device draws DC power again. And again, the capacitor discharges and recharges. Now the converter is in its next cycle and just repeats the process.

This operation allows AC current to be drawn from the power system only when the rectified supply voltage is greater than the capacitor's voltage. So the current flow created by the power supply is actually *pulses* and not continuous throughout the voltage cycle. In the presence of system impedance this current causes a non-sinusoidal voltage drop and therefore, produces voltage distortions at the load terminals i.e. later contain harmonics.

For general purposes the harmonic sources can be divided into three categories [11]:

1) A large number of distributed non-linear components of small rating (i.e. mass-products), consists mainly of: single phase diode bridge rectifiers, power supply of low voltage appliances (Switch Mode Power Suppliers: SMPS in TV sets, PCs and other IT equipment), and gas discharged lamps.

2) Large and continuously randomly varying non-linear loads, refers mainly to electric metal-melting arc furnaces with power rating in tens of MW connected directly to the transmission network. The furnace arc impedance is randomly

variable and extremely asymmetrical, where the carbon electrodes in contact with steel have dissimilar impedances between the positive and negative flows of current. The same character has resistance welding, where the copper electrodes and the steel being welded have dissimilar impedances between the positive and negative flows of current, and

3) Large static power converters and transmission system level power electronic devices. Static Power Converters are used more extensively for controlling loads. There are many forms of SPC: rectifiers, inverters, cycloconverters, single-phase, three-phase, twelve-pulse, six-pulse, but all have the same character, they are all non-linear, so that they require current from the power system that is non-sinusoidal.

The analysis of power system with large loads 2) and 3) is well described in [4], [11] and the connection of such is mainly subjected to network operator requirements, so that the level of distortion can be obtained analytically. Unlike 2) and 3), the big amount of loads of small rating 1) makes it difficult to analyze its effects directly; therefore it is up to the network structure to ensure the proper operation of those devices in the electromagnetic environment. This demands that the new methods acquire system structure characteristic regarding the effects of potential harmonics injecting loads.

Currently, a strong trend in decreasing the amount of linear, resistive loads can be observed. Like with the air conditioners which are replaced by the power electronic controlled ones the danger of resonance is increasing. This is why the description of the electromagnetic environment of the power system under normal operating conditions has become an issue recently, and why harmonics, one of several forms of energy pollution, are of special interest and world wide research tremendously increases on this topic.

3.2 Effects of Harmonics

3.2.1 Introduction

Once the harmonic sources are clearly defined, they must be interpreted in terms of their effects on the rest of the system and on personnel and equipment external to the power system.

Each element of the power system must be examined for its sensitivity to harmonics as a basis for recommendations on the allowable levels. The main effects of voltage and current harmonics within the power system are [2]:

- The possibility of amplification of harmonic levels resulting from series and parallel resonances.
- A reduction in the efficiency of the generation, transmission and utilization of electric energy.
- Ageing of the insulation of electrical plant components with consequent shortening of their useful life.
- Malfunctioning of system or plant components.

Among the possible external effects of harmonics are degradation in communication systems performance, excessive audible noise and harmonic-induced voltage and currents.

3.2.2 Effects of Harmonics on the System voltage

Harmonic currents drawn from the power system by nonlinear loads create harmonic voltages across the system impedance, and their effect can be significant for higher-order harmonics because inductive reactance increases with frequency. The load voltage is the difference between the source voltage and the voltage drop across the system impedance. Since the voltage drop across the system impedance contains harmonic components, the load voltage may become distorted if the nonlinear loads are a large fraction of the system capacity.

As discussed earlier, the current pulse drawn by the rectifier occurs only when the AC source voltage is near its peak. This means the voltage drop across the source impedance will be large when the source voltage is near its peak and essentially zero during the remainder of the half-cycle. Thus, the voltage delivered to the load will be "flattened" by the subtraction of the system impedance voltage drop. Voltage distortion affects the nonlinear load that created the harmonics and any other load that is connected in parallel with it.

3.2.3 Effects of Harmonics on the System Power Factor

Addition of harmonic currents to the fundamental component increases the total r.m.s. current. Because they affect the r.m.s. value of the current, harmonics will affect (reduces) the power factor of the circuit. The apparent power of the circuit would be found by multiplying the r.m.s. voltage magnitude by the r.m.s. current magnitude. Power factor, is then defined as the ratio of the real power to the apparent power. Since the voltage consists of a single component, the power is a series of terms consisting of the voltage times each harmonic component of current, but only first term of series indicates real power being delivered to the load.

Low power factor results in higher losses in the system due to higher I^2R losses. In fact, both I and R increase in this case because the r.m.s. current is higher due to the harmonics and because skin effect causes higher resistance in the conductors.

3.2.4 Effects of Harmonics on Static Power Plant

A. Transmission System

The flow of harmonic currents in the transmission network produces two main effects. One is the additional power loss caused by the increased r.m.s. value of the current waveform, i.e.

$$\sum_{n=2}^{\infty} I_n^2 R_n$$

where I_n is the nth harmonic current and R_n, the system resistance at that harmonic-frequency. Skin and proximity effects are functions of frequency and raise the value of the a.c. resistance of the cable, thus increasing the conductor I^2R losses.

The second effect of the harmonic current flow is the creation of harmonic voltage drops across the various circuit impedances. This means in effect that a 'weak' system (of large impedance and thus low fault level) will result in greater voltage disturbances than a 'stiff' system (of low impedance and high fault level).

In the case of transmission by cable, harmonic voltages increase the dielectric stress in proportion to their crest voltages. This effect shortens the useful life of the cable. It also increases the number of faults and therefore the cost of repairs.

The effects of harmonics on Corona starting and extinction levels are a function of peak-to-peak voltage. The peak voltage depends on the phase relationship between the harmonics and the fundamental. It is thus possible for the peak Voltage to be above the rating while the r.m.s. voltage is well within this limit.

B. Transformers

The primary effect of power system harmonics on transformers is the additional heat generated by the losses caused by the harmonic content of the load current. Other problems include possible resonances between the transformer inductance and system capacitance, mechanical insulation stress (winding and lamination) due to temperature cycling and possible small core vibrations.

The presence of harmonic voltages increases the hysteresis and eddy current losses in the laminations and stresses the insulation. The increase in core losses due to harmonics depends on the effect that the harmonics have on the supply voltage and on the design of the transformer core.

The flow of harmonic currents increases the copper losses; this effect is more important in the case of converter transformers because they do not benefit from the presence of filters, which are normally connected on the a.c. system side. Apart from the extra rating required, converter transformers often develop unexpected hot spots in the tank.

Guidelines for transformer derating to lake into account the harmonic content are given in the ANSI/IEEE standard C57.110 based on a derating factor [reference] expressed as

$$k = \sqrt{\frac{\sum_h \left(I_h^2 h^2\right)}{\sum_h I_h^2}}$$

In terms of the above K factor, the following expression is used to determine the derated (or maximum allowed) current:

$$I_{\max} = \sqrt{\frac{1 + P_{EC.R}}{1 + kP_{EC.R}}}\left(I_R\right)$$

where I_R is the fundamental r.m.s. current under rated load conditions and $P_{EC.R}$ is the ratio of eddy-current loss to rated I^2R loss (I being the total r.m.s. Current).

C. Capacitor Banks

The presence of voltage distortion increases the dielectric loss in capacitors, the total loss being expressed by

$$\sum_{n=1}^{\infty} C(\tan\delta)\omega_n V_n^2$$

where $\tan\delta = R/(1/\omega C)$ is the loss factor, $\omega_n = 2\Pi f_n$ and V_n is the r.m.s. voltage of the n^{th} harmonic.

The additional thermal stress of capacitors directly connected to the system (i.e. without series inductance) is assessed approximately with the help of a special capacitor weighted THD factor defined as

$$THD_c = \frac{\sqrt{\sum_{n=1}^{N}(n.V_n^2)}}{V_1}$$

One reason harmonics are a problem for capacitors is because capacitive impedance decreases as frequency increases. Thus, as our currents increase in harmonic order, the capacitors will act more and more as a short. This basically means that the capacitors attract the high frequency harmonics. The result is that the capacitors will become overloaded because of the increased current flow. Another problem between capacitors and harmonics is the possibility for resonance. This condition occurs when the inductive and capacitive reactances of a system are equal and cancel each other. When resonance occurs, the only effective impedance is the system resistance. This implies that the system sees a lower than expected impedance value. Therefore, the currents are less impeded, and effective amplification can occur. Resonance will cause severe and destructive damage to capacitors and to other parts of the system as well. These capacitors are rated according to over current limiting standards, such as ANSI/IEEE 18-1980, typical values being 15% in the UK, 30% in Europe and 80% in the USA.

3.2.5 Effect of Harmonics on Consumer Equipment

This is a broad subject discussed in many journal articles; a selected bibliography on the topic can be found in a paper by the IEEE Task Force on the Effects of Harmonics on Equipment [14]. A concise summary of the main effects is made below:

- T*elevision receivers* Harmonics which affect the peak voltage can cause changes in TV picture size and brightness. Inter-harmonics cause amplitude modulation of the fundamental frequency; even a 0.5% inter-harmonic level can produce periodic enlargement and reduction of the image of the cathode ray tube.
- *Fluorescent and mercury arc lighting* These appliances sometimes have capacitors which, with the inductance of the ballast and circuit, produce a resonant frequency. If this corresponds to a generated harmonic, excessive healing and failure may result. However, the resonant frequency of most lamps is in the range 75-80 Hz and should not interact with the power supply. Audible noise is another possible effect of harmonic voltage distortion.
- *Computers* There are designer-imposed limits to as to acceptable harmonic distortion in computer and data processing system supply circuits. Harmonic rate (geometric) measured in vacuum must be less than -3% (Honeywell, DEC) or 5% (IBM). CDC specifies that the ratio of peak to effective value of the supply voltage must equal 1.41 ±0.1.
- *Power electronic equipment* Notches in the voltage waveform resulting from current commutations may affect the synchronization of other converter equipment or any other apparatus controlled by voltage zeros. Harmonics could theoretically affect thyristor-controlled variable-speed drives of the same consumer in several ways: (i) voltage notching (causing brief voltage dips in the supply) can cause maloperation via a thyristor through misfiring; (ii) harmonic voltages can cause the firing of the gating circuits at other than the required instant; (iii) resonance effects between different equipment can result in over-voltages and hunting.

3.2.6 Effects of Harmonics on Rotating Machines

Non-sinusoidal voltages applied to electrical machines may cause overheating. Motors are not normally derated so long as the harmonic distortion remains within the 5% normally recommended by the regulations. Above that limit they will often experience excessive heating problems. On the positive side, motors contribute to the damping of the system harmonic content by virtue of the relatively high X/R ratio of their blocked rotor circuit.

Harmonic voltages or currents give rise to additional losses in the stator windings, rotor circuits, and stator and rotor laminations. The losses in the stator and rotor conductors' are greater than those associated with the dc resistances because of eddy currents and skin effect.

Leakage fields set up by harmonic currents in the stator and rotor end-windings produce extra losses. In the case of induction motors with skew rotors the flux changes in both stator and rotor and high frequency can produce substantial iron loss. The magnitude of this loss depends upon the amount of skew, and the iron-loss characteristics of the laminations.

3.2.7 Harmonic Interference with Ripple Control Systems

Ripple signals are often used for the remote control of street lighting circuits and for load reduction (such as domestic hot water heaters) during peak times of the day.
Electricity suppliers have in the past experienced some practical difficulties with their ripple control equipment, as a result of harmonic interference. . Since ripple relays are essentially voltage-operated (high-impedance) devices, harmonic interference can cause signal blocking or relay maloperation if present in sufficient amplitude. The exact amplitude at which the voltage harmonic will affect the relay is a function of the relay detection circuit (sensitivity and selectivity) and the proximity of the ripple injection frequency of the interfering harmonic.

3.2.8 Harmonic Interference with Power System Protection

Harmonics can distort or degrade the operating characteristics of protective relays depending on the design features and principles of operation. Digital relays and algorithms that rely on sample data or zero crossings are particularly prone to error when harmonic distortion is present.

Current harmonic distortion can also affect the interruption capability of circuit breakers and fuses. Possible reasons are higher di/dt at zero crossings, the current sensing ability of thermal magnetic breakers and a reduction in the trip point due to extra heating of the solenoid. The fuses, being thermally activated, are inherently r.m.s. overcurrent devices; the fuse ribbons are also susceptible to the extra skin effect of the harmonic frequencies.

3.2.9 Interference with Communications

Noise on communication circuits degrades the transmission quality and. can interfere with signaling. At low levels noise causes annoyance and at high levels loss of information, which in extreme cases can render a communication circuit unusable.

The continuously changing power transmission environment demands regular reconsideration of the interference problem when telephone lines are placed in the vicinity of the power system.

4. Modeling and Analysis of Harmonic Sources

This chapter is dedicated to present the modeling and simulations of various harmonic sources with investigations of harmonics on distribution systems, so that the analysis and planning of distribution system becomes effective or 'proactive' rather than 'reactive'. The first section is devoted to single-phase loads, their modeling using Gauss-Seidel approach, and calculations of Attenuation and Diversity factor for large number of such loads. The thrust of second section is on the derivation of harmonic domain models suitable for the study of conventional three-phase, six pulse harmonic converters. Modulation theory based on switching functions and discrete convolutions are the cornerstone of these models. Third section has presented inrush current phenomenon, arising during transformer energization, and containing a slowly decaying transient response, with connection to harmonic domain technique. Conclusions and results are presented for each section.

4.1 Single-Phase Power Electronic Loads

Widely distributed single-phase power electronic loads are an increasingly important source of harmonics in power distribution systems. The objective of this section is to investigate the cumulative harmonic current characteristics of a large number of such loads. A complete analytical model for the most common load type is derived. This model is then used to investigate the impact of 1) interaction due to shared source impedance, 2) variation in power level, and 3) variations in circuit parameters, on individual and cumulative current harmonics. The findings of this section are that

- *Diversity* and *Attenuation* are very important factors in predicting the behavior of distributed single-phase power electronic loads, especially for the higher-order harmonics, and that
- due to these two factors, the commonly-used fixed current injection method, using arithmetic sums of harmonic current magnitudes, can significantly overestimate the cumulative harmonic currents produced by these loads.

4.1.1 Introduction

Harmonic currents generated by single-phase power electronic loads such as desktop computers and television sets are, individually, too small to cause any appreciable distortion in distribution feeders. However, as the number of these loads increases, and as larger nonlinear loads such as adjustable-speed drive (ASD) heat pumps and electric vehicle battery chargers proliferate, the cumulative harmonics may become very significant.

Most of these loads employ the capacitor-filtered diode-bridge rectifier, shown in Fig. 4.1, as their power supply [15]. The input current wave shape is characterized by a pulsed current which flows during the charging period of the smoothing capacitor. This current is rich in harmonics, and its total harmonic distortion (THD) is typically in the range of 100%.

Distributed single-phase power electronic loads are usually treated as fixed harmonic current injectors in distribution system studies. Their current harmonics are characterized by normalized Phasors $|I_h/I_1|\angle\theta_h$ where the fundamental current component I_l is varied proportionally with load power. Fixed harmonic current injection leads to an overestimation of the resulting voltage harmonics because it neglects phase angle dispersion of individual current harmonics.

In this section, a complete analytical model is derive for calculating the harmonic components of the input current of a capacitor-filtered diode bridge rectifier, using circuit parameters and load level as input variables. Then this model is use to investigate the harmonics attenuation that results when several power electronic loads share a common source impedance, and to study the diversity of current harmonics caused by variations in power level and circuit parameters [16-19]. It is shown that these phenomena significantly affect the cumulative current harmonics produced by distributed loads.

4.1.2 Single-Phase Capacitor-Filtered Diode Bridge Rectifier

The circuit model for harmonic analysis of a single-phase power electronic load is shown in Fig.4.1.

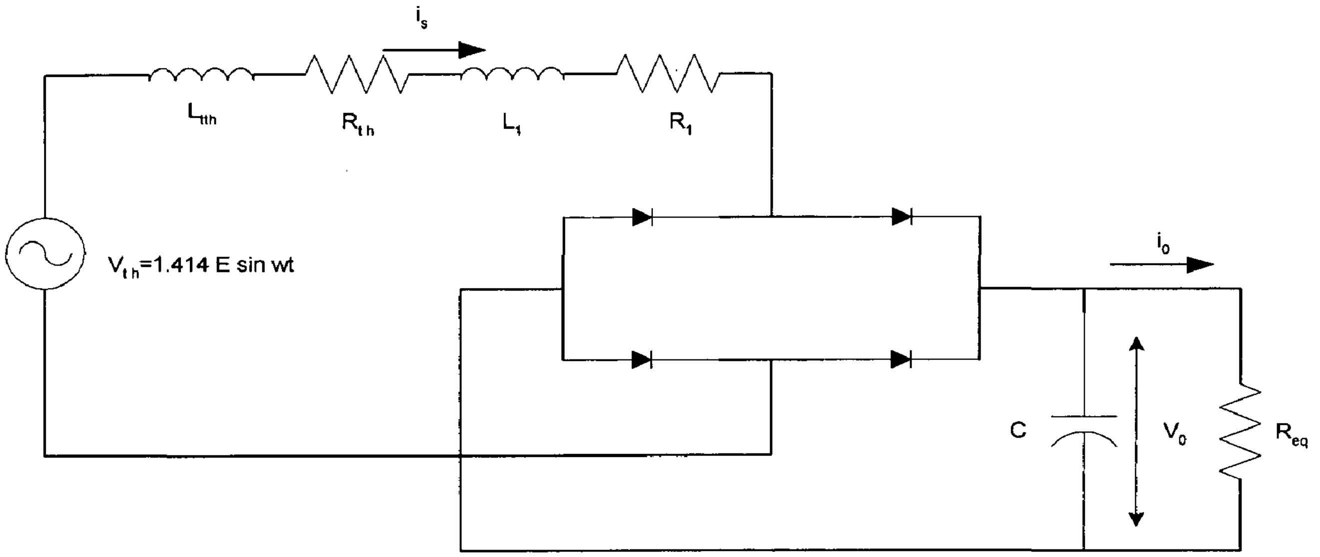

Fig.4.1 Capacitor-Filtered Diode Bridge Rectifier Model

The various circuit components are

V_{th}: Thevenin equivalent system voltage,

R_{th},L_{th}: Thevenin equivalent system impedance parameters,

R_1, L_1: Local line impedance parameters,

C: Smoothing Capacitor,

R_{eq}: Equivalent load resistance.

The analytical expressions for output voltage V_0 (θ) and input current i_s(θ) are derived in terms of circuit parameters and forcing function V_{th} (θ). The circuit is solved for both real and imaginary roots.

4.1.3 Circuit Analysis

The circuit operates in two modes - charging and discharging. Input current flows only during the charging mode, which corresponds to ($\theta_1 \leq \theta \leq \theta_2$) in Figure 4.2.

During the charging mode, $i_s(\theta)$ flows through the diodes and charges the capacitor. The circuit equations are

$$V_{th}(\theta) = R_t i_s + \omega L_t \frac{di_s}{d\theta} + V_0(\theta) \tag{4.1}$$

$$i_s(\theta) = \omega C \frac{dV_0}{d\theta} + \frac{V_0(\theta)}{R_{eq}} \tag{4.2}$$

where $R_t = R_{th} + R_1$, $L_t = L_{th} + L_1$.

Equations (1) and (2) can be expressed in matrix form as

$$\frac{d}{d\theta}\left[\dot{Y}\right] = \alpha Y + \beta V \tag{4.3}$$

where

$$Y = \begin{bmatrix} i_s(\theta) \\ V_0(\theta) \end{bmatrix}, V = [V_{th}(\theta)] = [1.414E\sin(\theta)],$$

$$\alpha = \begin{bmatrix} -R_t/\omega L_t & -1/\omega L_t \\ 1/\omega C & -1/\omega CR_{eq} \end{bmatrix} = \begin{bmatrix} -\alpha_1 & -\alpha_2 \\ \alpha_3 & -\alpha_4 \end{bmatrix},$$

$$\beta = \begin{bmatrix} 1/\omega L_t \\ 0 \end{bmatrix} = \begin{bmatrix} \alpha_2 \\ 0 \end{bmatrix}$$

Laplace transforming (4.3), and rearranging terms yields

$$Y(s) = (sI - \alpha)^{-1} Y(\theta_1) + (sI - \alpha)^{-1} \beta V(s) \tag{4.4}$$

Where the initial value of Y (θ_1) is

$$Y(\theta_1) = \begin{bmatrix} i_s(\theta_1) \\ V_0(\theta_1) \end{bmatrix} = \begin{bmatrix} 0 \\ 1.414E\sin(\theta_1) \end{bmatrix} \tag{4.5}$$

The solution for $i_s(\theta)$ and $V_0(\theta)$ can be obtained by applying an inverse Laplace transform to (4.4). However, depending upon the value of the circuit parameters, the characteristics roots of $(sI-\alpha)^{-1}$ can be real or complex.

If $(\alpha_1-\alpha_4) < 2\sqrt{(\alpha_2\alpha_3)}$, then the roots are complex and are given by $S_{1,2} = a \pm jb$, where $a = -(\alpha_1+\alpha_4)/2$, $b = \sqrt{((\alpha_2\alpha_3) - (1/4)(\alpha_1-\alpha_4)^2)}$.

Inverse transforming (4.4) then gives the following expression for $i_s(\theta)$ and $V_0(\theta)$ during the charging period $(\theta_1 \le \theta \le \theta_2)$:

$$i_s(\theta) = \sqrt{2}E\alpha_2 \frac{e^{a(\theta-\theta_1)}}{b}[\{-\sin(\theta_1)+C_2a+C_3\}\sin\{b(\theta-\theta_1)\}+C_2b\cos\{b(\theta-\theta_1)\}]$$
$$+\sqrt{2}E\alpha_2[-C_2\cos(\theta-\theta_1)+C_4\sin(\theta-\theta_1)] \quad (4.6)$$

$$V_0(\theta) = \sqrt{2}E\frac{e^{a(\theta-\theta_1)}}{b}[\{(a+\alpha_1)\sin(\theta_1)+\alpha_2(C_5a+C_6)\}\sin\{b(\theta-\theta_1)\}+\{b\sin(\theta_1)+\alpha_2C_5b\}\cos\{b(\theta$$
$$+\sqrt{2}E\alpha_2[-C_5\cos(\theta-\theta_1)+C_7\sin(\theta-\theta_1)] \quad (4.7)$$

If $(\alpha_1-\alpha_4) > 2\sqrt{(\alpha_2\alpha_3)}$, then the roots are complex and are given by $S_{1,2} = a \pm b$, where

$a = -(\alpha_1+\alpha_4)/2$, $b = \sqrt{((1/4)(\alpha_1-\alpha_4)^2 - (\alpha_2\alpha_3))}$.

Inverse transforming (4.4) then gives the following expression for $i_s(\theta)$ and $V_0(\theta)$ during the charging period $(\theta_1 \le \theta \le \theta_2)$:

$$i_s(\theta) = \frac{\sqrt{2}E\alpha_2}{2b}\left[e^{(a+b)(\theta-\theta_1)}\{-\sin(\theta_1)+(C_2a+C_2b+C_3)\}+e^{(a-b)(\theta-\theta_1)}\{\sin(\theta_1)-(C_2a-C_2b+C_3\right.$$
$$+\sqrt{2}E\alpha_2[-C_2\cos(\theta-\theta_1)+C_4\sin(\theta-\theta_1)] \quad (4.8)$$

$$V_0(\theta)=\frac{\sqrt{2}E}{2b}\left[\begin{array}{l} e^{(a+b)(\theta-\theta_1)}\{(a+b+\alpha_1)\sin(\theta_1)+\alpha_2(C_5a+C_5b+C_6)\}+ \\ e^{(a+b)(\theta-\theta_1)}\{(a-b+\alpha_2)\sin(\theta_1)+\alpha_2(C_5a-C_5b+C_6)\}\cos\{b(\theta-\theta_1)\}\end{array}\right]$$
$$+\sqrt{2}E\alpha_2[-C_5\cos(\theta-\theta_1)+C_7\sin(\theta-\theta_1)] \tag{4.9}$$

By defining B = (($\alpha_2\alpha_3$) – (1/4) (α_1-α_4)^2), $C_1 \ldots C_7$ become,

$$C_1=\frac{1}{4a^2+(a^2+B-1)^2},$$
$$C_2=C_1[\{2a-\alpha_4(a^2+b-1)\}\sin(\theta_1)-(a^2+B-1+2a\alpha_4)],$$
$$C_3=C_1[(a^2+b)(a^2+B-1+2a\alpha_4)\sin(\theta_1)+\{(3a^2+1-B)\alpha_4+2a(a^2+B)\}\cos(\theta_1)],$$
$$C_4=C_1[(1-a^2-B-2a\alpha_4)\sin(\theta_1)+\{\alpha_4(a^2+B-1)-2a\}\cos(\theta_1)],$$
$$C_5=\alpha_3C_1[(1-a^2-B)\sin(\theta_1)+2a\cos(\theta_1)],$$
$$C_6=\alpha_3C_1[2a(a^2+B)\sin(\theta_1)+(3a^2+1-B)\cos(\theta_1)],$$
$$C_7=\alpha_3C_1[-2a\sin(\theta_1)+(a^2+B-1)\cos(\theta_1)]$$

During the discharging mode ($0 \le \theta \le \theta_1$, $\theta_2 \le \theta \le \Pi$), the diodes are off, and the capacitor discharges through equivalent load resistance R_{eq}. The analytical expressions for input current $i_s(\theta)$ and $V_0(\theta)$ are given by

$$i_s(\theta_2)=0 \tag{4.10}$$
$$V_0(\theta)=V_0(\theta_2)\exp[(\theta_2-\Pi-\theta)\alpha_4],(0\le\theta\le\theta_1) \tag{4.11}$$
$$V_0(\theta)=V_0(\theta_2)\exp[(\theta_2-\theta)\alpha_4],(\theta_2\le\theta\le\Pi) \tag{4.12}$$

4.1.4 Solution Procedure

Conduction angles θ_1 and θ_2 can be determined by simultaneously solving the following two boundary conditions:

$$i_s(\theta_2) = 0 \quad (4.13)$$

$$V_0(\theta_2)\exp[(\theta_2 - \Pi - \theta_1)\alpha_4] = \sqrt{2}E\sin(\theta_1) \quad (4.14)$$

It is found the Newton-Raphson method to be unsuitable for solving (4.13) and (4.14) because they have multiple zero crossings, accurate initial estimates are difficult to obtain, and angles θ_1 and θ_2 vary widely between 0° and 180°, depending upon circuit parameters and operating power level. This difficulty overcame by solving for θ_1 and θ_2 using a simpler Gauss-Seidel approach, which is

a) Find an initial value of θ_1 for which $i_s(\theta)$ has a zero crossing between θ_1 and 180°,
b) Solve (4.13) for θ_2, using the bisection method,
c) Using θ_2 from b), solve (4.14) with bisection to obtain an updated value of θ_1,
d) Repeat steps b) and c) until both (4.13) and (4.14) are satisfied.

This technique has proven to be very effective, reaching convergence in 5 to 6 iterations, and it is rather insensitive to the initial value chosen for θ_1 in step a).

Now, consider the case where output power P_{out} is known instead of R_{eq}. In this case, R_{eq} is found after using the following iterative procedure:

1) Estimate a starting value of R_{eq} from $R_{eq} = 1.5\ E^2 / P_{out}$.
   (1.5 is a compromise between the "stiff capacitor" value of 2.0, and the "no capacitor" value of 1.0),
2) Calculate θ_1 and θ_2 using the method described above,
3) Calculate numerical values of $i_s(\theta)$ and $V_0(\theta)$, and the rms value of $V_0(\theta)$, (defined as V_{0rms}),
4) Check $\left|\frac{V_{0,rms}^2}{R_{eq}} - P_{out}\right| \le \varepsilon$ for convergence,

5) If not converged, update R_{eq} using $R_{eq} = \frac{V_{0,rms}^2}{P_{out}}$, and continue from step (2) until convergence is reached.

The solution technique is applied to a typical single phase capacitor filtered diode bridge rectifier having $R_t = 0.6517\ \Omega$, $X_t = 0.6517\ \Omega$, $C = 4200\ \mu F$, $E = 240$ V, and $P_{out} = 3000$ W, and we compute the waveforms shown in Figure 4.2. Conduction angles i.e. θ_1 and θ_2 are 57.41° and 142.30°. Total Harmonic Distortions (THD %) of source current is found to be 86.90%.

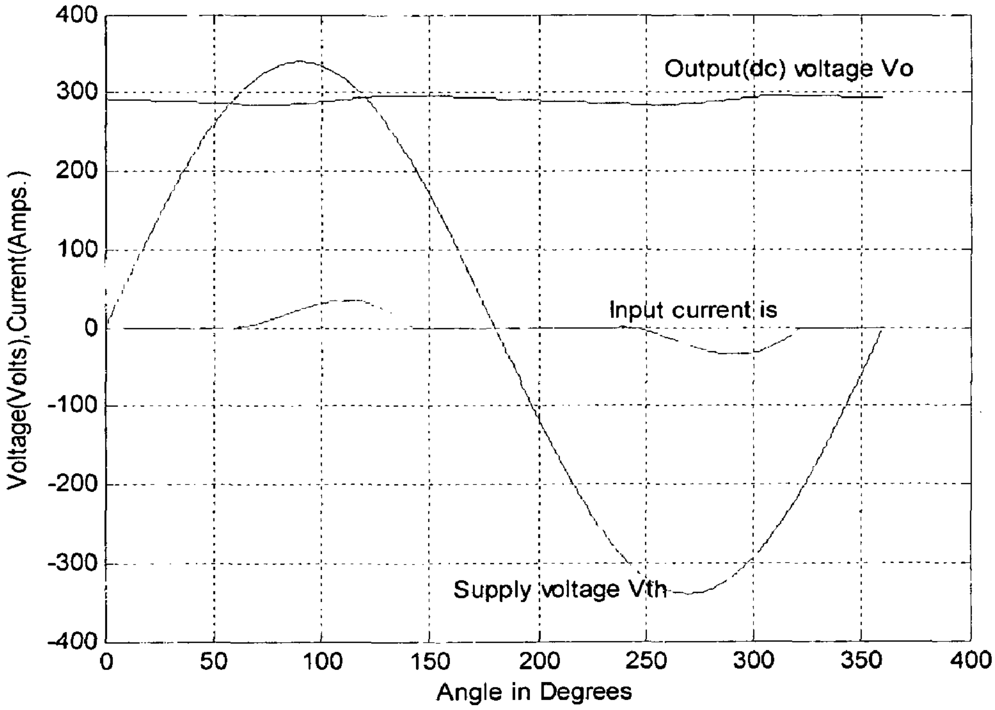

Fig. 4.2 Supply Voltage $V_{th}(\theta)$, Input Current $i_s(\theta)$ and output voltage $V_0(\theta)$

4.1.5 Harmonics Characteristics

We now examine the effect of circuit parameters and load level on the magnitudes and phase angles of harmonic currents. Load is same single phase capacitor filtered diode bridge rectifier used above, with variation of power level from 20-100%.

Load power affects the shape of the current pulse in Figure 4.2 as follows: as power increases, the pulse becomes wider, taller, and more skewed to the right. The corresponding effect on current harmonics is given in Figures 4.3 and 4.4, where the variations in percent magnitudes and phase angles are plotted for the 20-100% power range. Note that as power increases, there is an attenuation effect on harmonic current magnitudes (in percent of fundamental), and a significant impact on phase angles, especially for higher-order harmonics. Similar variations occur with changes in system impedance magnitude and X/R ratio [16].

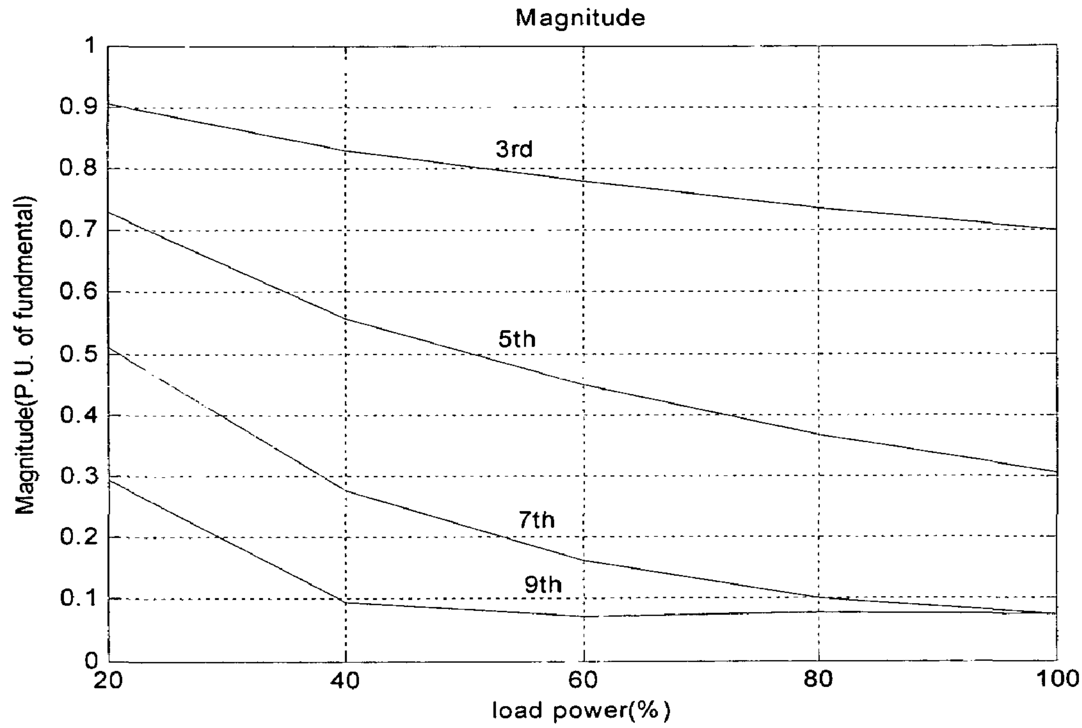

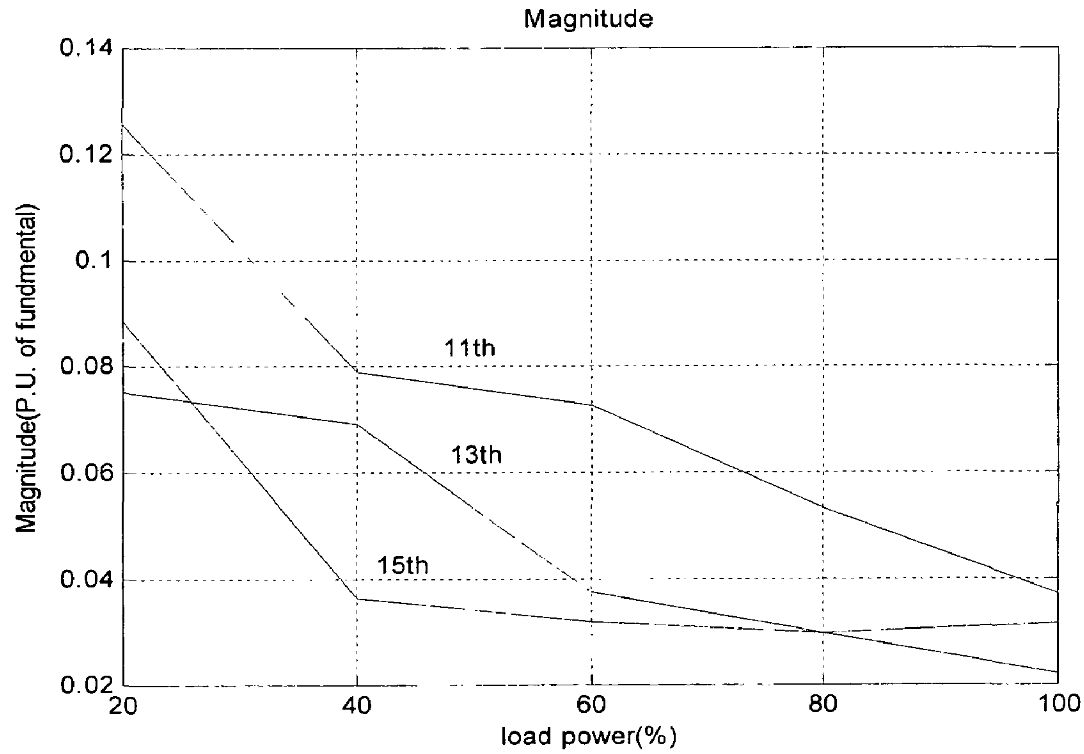

Fig. 4.3 Variation Of Magnitude Of harmonic Component with Load Power

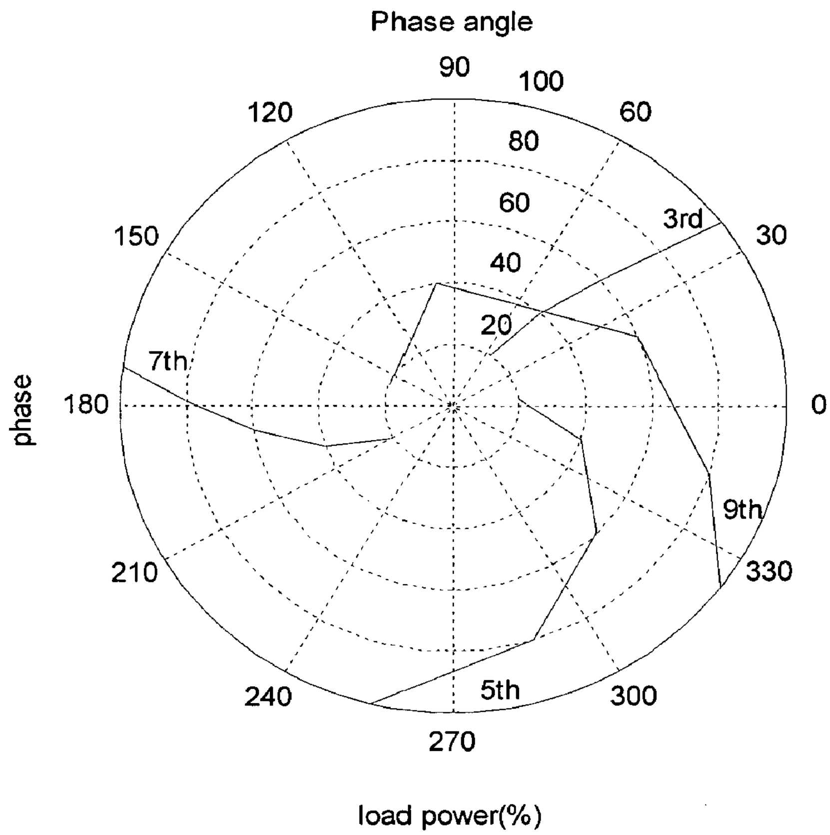

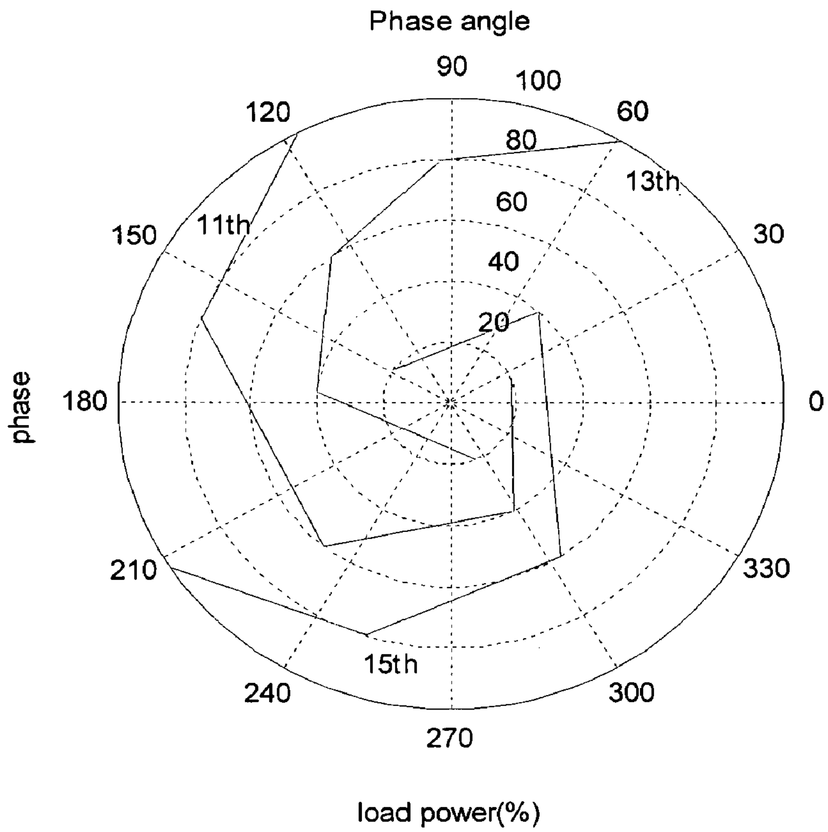

Fig. 4.4 Variation of Phase of harmonic Component with Load Power

The magnitude reductions in Figure 4.3 imply that there will be an attenuation effect when a number of identical loads are served through shared system impedance. The phase angle variations in Figure 4.4 make possible significant cancellation due to the circulation of harmonic currents among multiple loads with different power levels, especially for higher-order harmonics. If attenuation and cancellation are ignored, as in a simple application of fixed harmonic current injection, harmonics-related problems may be overestimated. This overestimation may be unimportant when studying the harmonics impact of one nonlinear load, but can be very significant for a group of loads. The significance of attenuation and cancellation are examined in the following sections.

4.1.6 ATTENUATION DUE TO SHARED SYSTEM IMPEDANCE

Consider the case shown in Fig. 4.5 where N identical 100 W power electronic loads share a common system impedance. Because of the magnitude variation in Fig. 4.3, the harmonic content of total current i_s depends on N. In the method of fixed harmonic current injection, it is customary to assume a fixed spectrum for each load, independent of N, and to apply superposition. Potential error of this technique by defining the following *Attenuation Factor* [16]:

$$AF_h = \frac{I_h^N}{N \cdot I_h^1} \tag{4.15}$$

Where

I_h^N = Resultant current for harmonic h for N units operating in parallel.

I_h^1 = Current for harmonic h when N=1.

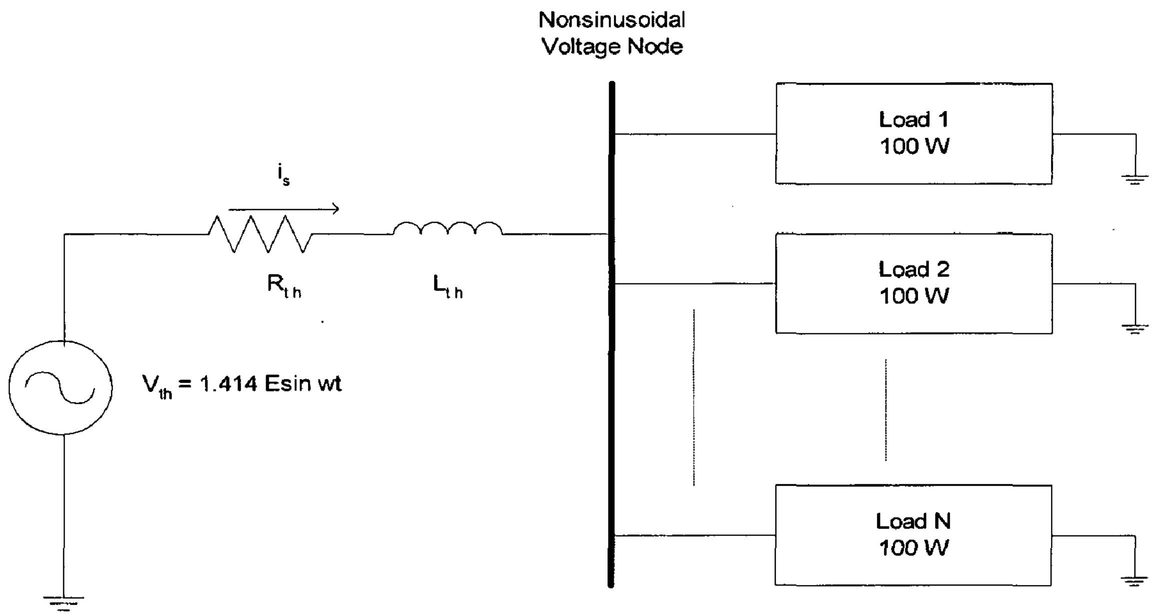

Fig. 4.5 N Identical Units with a Shared Thevenin Equivalent System Impedance

Each unit in this study is rated 100W, 220V 50Hz, and has a 370μF smoothing capacitor. The equivalent system impedance of the shared bus is chosen to be (0.4 + j0.25) Ω.

The *Attenuation factors* with 5, 10 and 15 loads operating in parallel are shown in Fig. 4.6. Note that, in general, the attenuation due to a shared system impedance is more pronounced for higher-order harmonics, and tends to increase with N. The increase in the 11^{th} and onwards attenuation factors is not important since current magnitudes tend to decrease as 1/h.

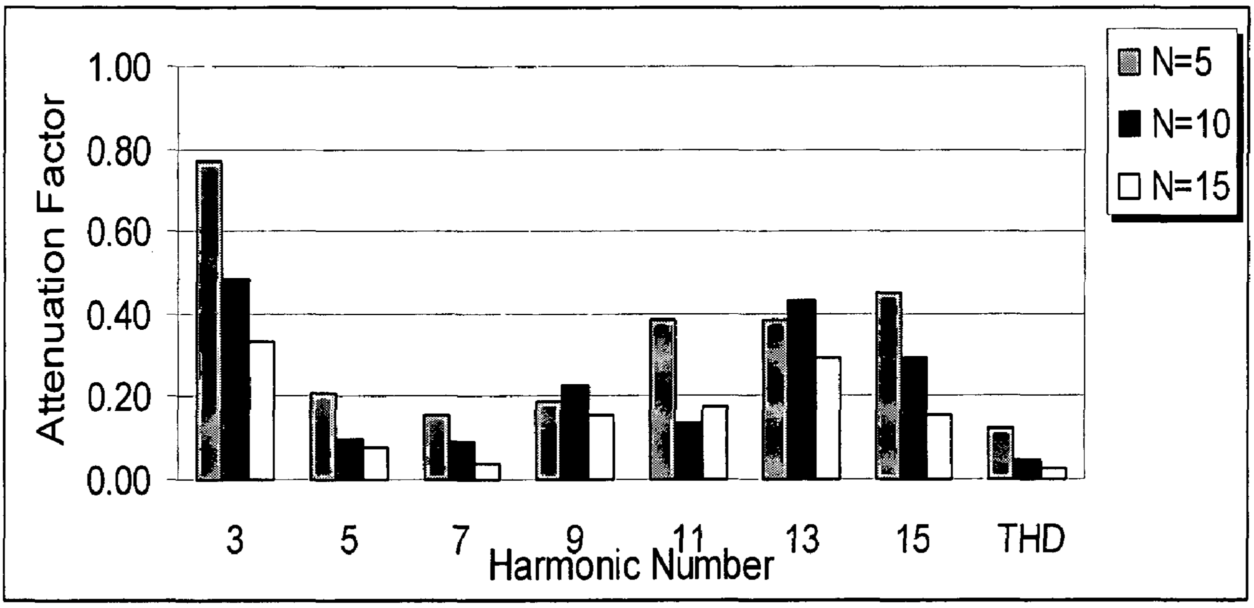

Fig.4.6 Attenuation Factor for Harmonic Currents due to Shared System Impedance.

4.1.7 DIVERSITY DUE TO PHASE ANGLE VARIATION

Phase angle dispersion of individual current harmonics. As illustrated in Fig. 4.4, occurs mainly due to the following three types of variations:

1. Power Level,
2. Line Impedance magnitude and
3. Line Impedance X/R ratio.

In order to access the impact of each of these on the cumulative harmonic currents produced by N non linear loads, simulation is performed in MATLAB™. The loads are connected in parallel to a common stiff bus, as shown in Fig. 4.7, each load is rated 220 V, 3kW.

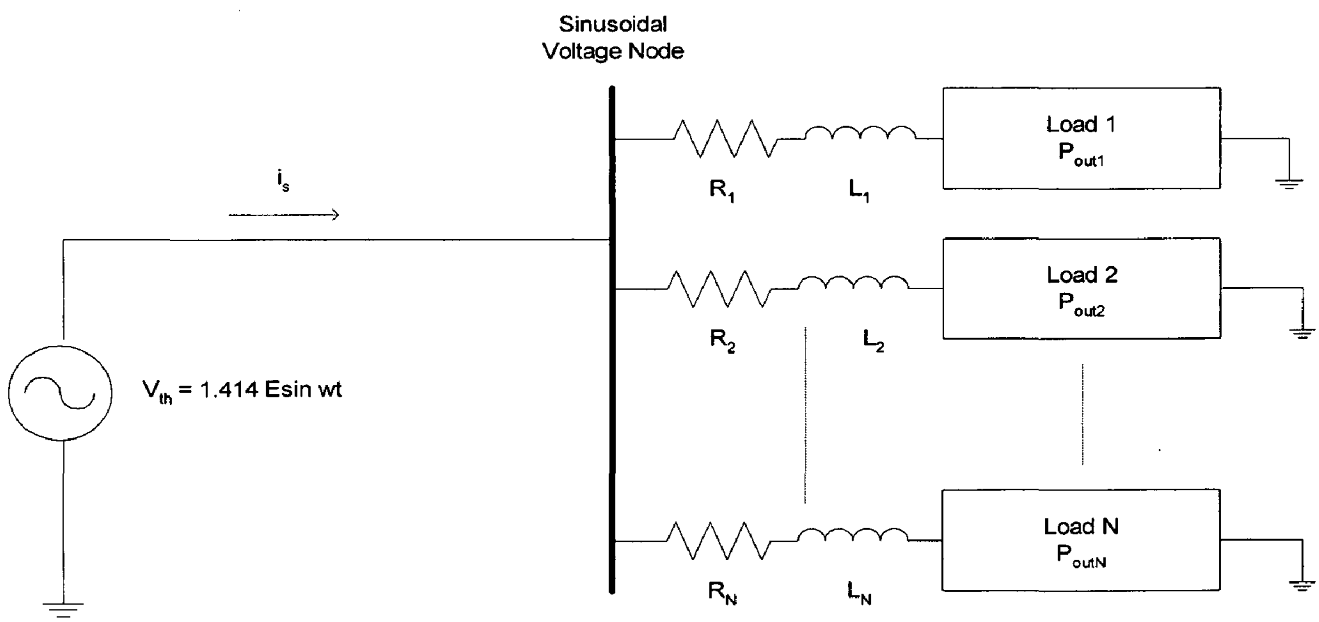

Fig. 4.7 N Identical Parallel Loads Sharing a Common Stiff Bus

In order to quantify the effect of phase angle dispersion on total current i_s, the current harmonics *Diversity Factor* is defined in [16], which is

$$DF_h = \left| \frac{\text{Phasor Sum of Currents of harmonic h}}{\text{Algebraic Sum of Currents of Harmonic h}} \right|$$

$$= \left| \sum_{i=1}^{N} I_h^i \Big/ \sum_{i=1}^{N} \left| I_h^i \right| \right| \qquad (4.16)$$

where

$I_h^i = \left| I_h^i \right| \angle \theta_h^i =$ Harmonic current of order h injected by the i_{th} load (of N loads)

The *Diversity Factor* ranges between 0 and 1. A small value implies a significant amount of cancellation due to the circulation of harmonic currents among individual loads.

4.1.8 PARAMETERS VARIATIONS

First effect of power variation is studied by randomly varying the power level of individual loads while holding their impedances and smoothing capacitor at fixed values. The power levels are uniformly distributed over a 20%-100% range. For each simulation *Diversity Factor* is calculated using (4.16).

In a similar fashion, other parameters, Impedance Magnitude, X/R Ratio, Capacitor values individually and then all parameters simultaneously varied to observe the effect on mean harmonic current diversity factors for N =5. Nominal values of P, Z, X/R, and C are chosen as 3.0 kW, 4% (on a 5 kVA, 240 V base), 1.0, and 4200 U.F, respectively. The ranges of variation are as follows: impedance magnitude, 2 - 10%; X/R ratio, 0.1-5.0; capacitance, 1000 -9000 μF.

The simulation results are shown in Table 4.1, along with the power variation. Z variation has the greatest effect on diversity factor, X/R yields similar results to P, and C variation has little effect. In general, diversity factor decreases with harmonic order. All four parameters also simultaneously vary uniformly within their respective ranges given above. The diversity factors for this composite variation are also given in Table 4.1.

Table 4.1: Mean Harmonic Current Diversity Factors due to Individual and Combined Variations of Circuit Parameters (Power P, Impedance Magnitude Z, Impedance X/R ratio, Smoothing Capacitor C).

Harmonic Number h	DF_h Due to P	DF_h Due to Z	DF_h Due to X/R	DF_h Due to C	DF_h Due to Composite P,Z.X/R,C
3	0.997586	0.988725	0.842483	0.986675	0.754039
5	0.985669	0.924293	0.614225	0.954981	0.577446
7	0.801639	0.330814	0.529752	0.841473	0.396687
9	0.656244	0.567505	0.382990	0.884986	0.461237
11	0.704064	0.062414	0.431705	0.758184	0.689791
13	0.342297	0.069586	0.489308	0.753166	0.563993

4.1.9 CONCLUSIONS

This section of chapter investigates the cumulative harmonic current characteristics of a large number of single-phase power electronic loads that employ conventional diode bridge rectifiers and DC smoothing capacitors. This section also examines the effects of shared impedance, as well as variations in power level, impedance magnitude, X/R ratio, and smoothing capacitance.

It is shown that there is significant attenuation of current harmonics above the 3rd multiple when a number of identical loads, such as televisions and desktop computers, share a common source impedance. The THD of current in this case is approximately one-half of that obtained using superposition of individual load currents. However, the 3rd harmonic, which is responsible for most harmonic-related neutral conductor overloading problems, experiences only slight attenuation (i.e., 0.7 - 0.8).

By defining a current harmonic diversity factor, it is also shown that the cumulative harmonic currents for the 9th multiple and above experience appreciable phase cancellation due to individual and/or composite variations in power level, impedance magnitude, impedance X/R ratio, and smoothing capacitance. Since the 3rd and 5th harmonics show little phase cancellation, the THD of the summed current is only slightly less than that obtained by using superposition.

The mean harmonic diversity factors shown in Table 4.1 were calculated for ranges of circuit parameter variations that are likely to be encountered by these types of loads in actual distribution systems.

The attenuation and diversity factors calculated in this section give an indication of how much the commonly-used fixed current injection method, using arithmetic sums of harmonic current magnitudes, can overestimate the cumulative harmonic currents produced by distributed single-phase power electronic loads.

4.2 THREE PHASE CONVERTER

The thrust of this section is on the derivation of harmonic domain models suitable for the study of conventional three-phase, six pulse harmonic converters. Modulation theory based on switching functions and discrete convolutions are the cornerstone of these models.

4.2.1 INTRODUCTION

The main sources of harmonic current are at present the phase angle controlled rectifiers and inverters. The derivation of the harmonic currents produced by static power converters requires accurate information of the a.c. voltage waveforms at the converter terminals, converter configuration, and type of control, a.c. system impedance and DC circuit parameters [2].

When the rectifier is working under non ideal conditions such as unbalanced ac excitation , unbalanced firing angle control unbalanced ac impedance as well as pre existing harmonics in the ac supply a wide range of non characteristic harmonics will be generated on both the ac side and dc side of rectifier these non characteristic harmonics can not be calculated with the classical equations since the key assumption of the classical model is that there is infinite inductance on the de side of the rectifier and zero commutating reactance on the ac side the former assumption means that at the end of commutation period the current waveform will be perfectly flat topped. This is an assumption that often does not conform to realistic converter design and operation.

Traditionally the calculation of non characteristic harmonics has been carried out using general time domain simulations and very cumbersome and yet contrived methods based on analytical expressions [20].

In this section the theory presented in [21] is used to model six pulse rectifiers in order to calculate non characteristic harmonics. This method uses switching functions for each phase of the converter which incorporates the conduction states of the thyristors in each phase. The analysis is carried out entirely in the harmonic domain where the harmonic admittance matrix of the rectifier is obtained.

The harmonic converter models given in this section build up incrementally, starting with the simplified case where no commutation effects are included. This simplicity is used to illustrate the simple relationship that exists between the AC and DC voltages and switching functions.

The matrix structure of three-phase equivalent admittance matrix gives the cross-coupling between phases and between harmonics.

4.2.2 Effect of AC Side Inductance

In practice the existence of reactance in the commutation circuit causes conduction overlap of the in-coming and out-going phases.

The Fig.4.8 shows the effect of finite commutating reactance on the ac line current drawn by the converter it causes gradual rise time and fall time governed by the angle μ.The angle μ is termed the overlap angle the length of this commutation period is function of magnitude of ac system inductance and thyristor firing angle alpha where the larger firing angle results in lower commutation angles the figure shows ac current waveform where the instant of thyristor switching is delayed by firing angle α .

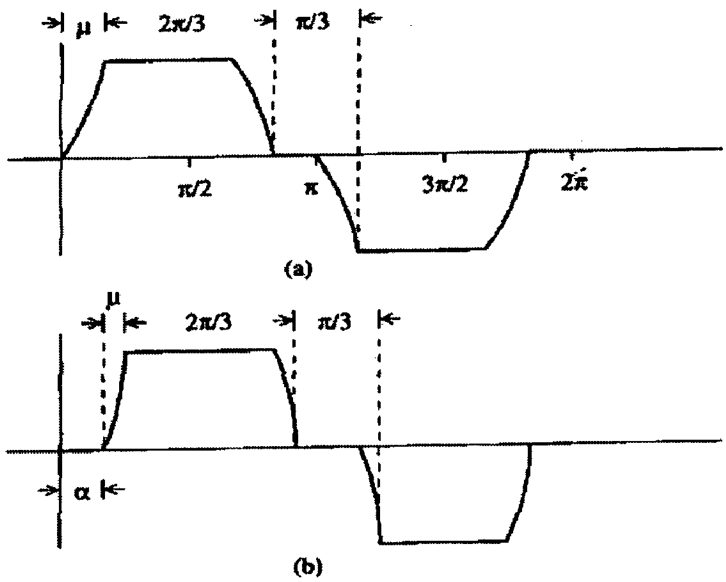

Fig. 4.8 Effect of the phase control and overlap over the AC current waveform

The current waveform has now lost the even symmetry with respect to the centre of the idealized rectangular pulse. Using as a reference the corresponding commutating voltage (i.e. the zero voltage crossing) and assuming a purely inductive commutation circuit, the following expression defines the commutating current.

$$i_c(t) = \frac{V}{1.414X_c}(\cos\alpha - \cos\omega t) \tag{4.17}$$

Where X_c is the reactance (per phase) of the commutation circuit, which is largely determined by the transformer leakage reactance.

At the end of commutation $i_c(t) = i_{dc}(t)$ and $\omega t = \mu$, and (4.17) becomes

$$i_{dc}(t) = \frac{V}{1.414X_c}(\cos\alpha - \cos(\alpha + \mu)) \tag{4.18}$$

Dividing (1) by (2)

$$i_c(t) = i_{dc}(t)\left(\frac{(\cos\alpha - \cos\omega t)}{(\cos\alpha - \cos(\alpha + \mu))}\right) \tag{4.19}$$

and this expression applies for $\alpha < \omega t < \alpha + \mu$.

The rest of the positive current pulse is defined by

$$i(t) = i_{dc}(t) \text{ for } \alpha + \mu < \omega t < \alpha + 2\Pi/3 \tag{4.20}$$

and

$$i_c(t) = i_{dc}(t) - i_{dc}(t)\left(\frac{(\cos(\alpha + 2\Pi/3) - \cos\omega t)}{(\cos(\alpha + 2\Pi/3) - \cos(\alpha + 2\Pi/3 + \mu))}\right) \tag{4.21}$$

for $\alpha + 2\Pi/3 < \omega t < \alpha + 2\Pi/3 + \mu$

The negative current pulse still possesses half-wave symmetry and therefore only odd-ordered harmonics are present. These can be expressed in terms of the delay (firing) and overlap angles and their magnitudes, related to the fundamental components, are illustrated in Fig. 2, for the 5th, 7th, 11th and 13th harmonic respectively [2].

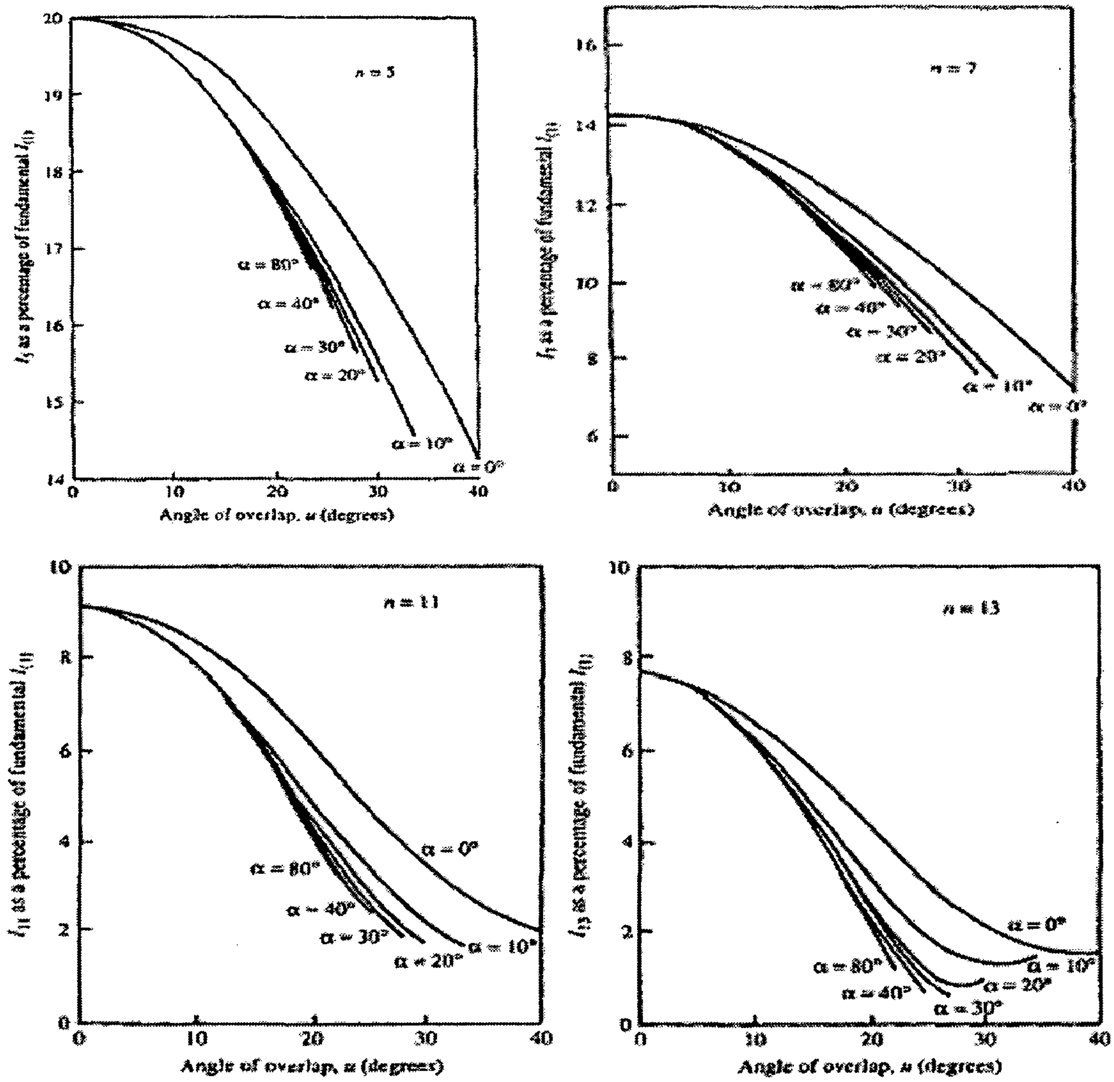

Fig. 4.9 Variation of 5th, 7th, 11th and 13th harmonic current in relation to angle of delay and overlap

In summary, the existence of system impedance is seen to educe the harmonic content of the waveform, the effect being much more pronounced in the case of uncontrolled rectification. With large firing angles the current pulses are practically unaffected by ac system impedance.

4.2.3 Rectifier Operation Using Switching Functions

The theory of converter modulation provides a simple alternative for the calculation of converter harmonics [22]. It uses switching functions to relate the voltages and currents that exist on both sides of the converter the ac side and the dc side.

The six pulse thyristor bridge is shown in Fig.4.10 (a) it consist of an arrangement of six thyristor valves with the firing sequence indicated by the numbers on the side of thyristors. In this case the valves are connected on the ac side to secondary side of a star connected; three phase winding, whereas on the dc side they are connected to load. No overlap exists for this case. The Fig. 4.10 (b) shows the input ac voltage and six switching functions, s_1 (t), s_2 (t), s_3 (t), s_4 (t), s_5 (t) and s_6 (t), which represent the conduction periods of the thyristors. A switching function takes a value of one when the thyristor is conducting and a value of zero when it ceases to conduct.

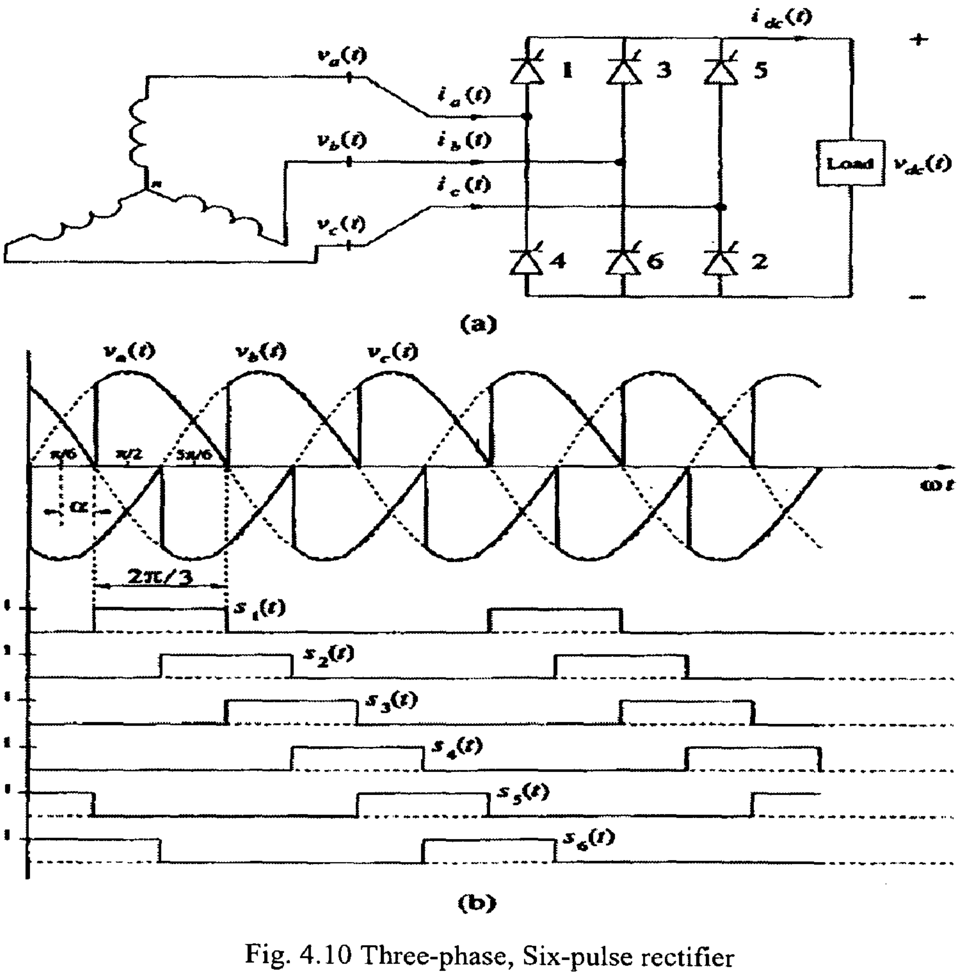

Fig. 4.10 Three-phase, Six-pulse rectifier

A basic analysis of switching functions shown in Fig. 4.10 (b) help to understand their role in the calculation of harmonics. In this case, thyristor 1 is turned on at ($\Pi/6+\alpha$).It should be noted that thyristor 6 is already conducting and that thyristor 5 has ceased to conduct owing to natural commutation. It is said then that thyristor 1 commutes with thyristor 5. It is important to realize that during interval $(\Pi/6+\alpha) \leq \omega_o t \leq (\Pi/2+\alpha)$ thyristors 6 and 1 conduct and that line to line voltage v_{ab} (t) appears across the load. At $\omega_o t = (\Pi/2+\alpha)$, thyristor 2 is turned on and thyristor 6 turns off owing to natural commutation. During the interval $(\Pi/2+\alpha) \leq \omega_o t \leq (5\Pi/6+\alpha)$, thyristors 1 and 2 conduct and the line-to-line conduction period: 1-2, 2-3, 3-4, 4-5, 5-6, 6-1. Assuming steady state conditions this basic switching mechanism continues for as long as the converter is in operation.

It should be noted from closer examination of Fig. 4.10 (b) that $s_1(t)$ is responsible for the positive contribution of $v_a(t)$ to $v_{dc}(t)$ and that $s_4(t)$ is responsible for the negative contribution of $v_a(t)$ to $v_{dc}(t)$. Similarly $s_3(t)$ and $s_6(t)$ are responsible for the positive and negative contributions of $v_b(t)$ to $v_{dc}(t)$, respectively. Also $s_5(t)$ and $s_2(t)$ are responsible for the positive and negative contributions of $v_c(t)$ to $v_{dc}(t)$ respectively. In this situation the relationship between the ac and dc voltages is given by the following expression:

$$v_{dc}(t) = [s_1(t) - s_4(t)]\, v_a(t) + [s_3(t) - s_6(t)]\, v_b(t) + [s_5(t) - s_2(t)]\, v_c(t) \tag{4.22}$$

The relationships between the ac and dc converter currents may be taken to be the dual relationships of those in the voltages,

$$\begin{aligned} i_a(t) &= [s_1(t) - s_4(t)]\, i_{dc}(t) \\ i_b(t) &= [s_3(t) - s_6(t)]\, i_{dc}(t) \\ i_c(t) &= [s_5(t) - s_2(t)]\, i_{dc}(t) \end{aligned} \tag{4.23}$$

The (4.22) and (4.23) describe very well the periodic steady state operation of the three phase six pulse rectifier in cases where no overlap is assumed to exist.

4.2.4 Effect of Ac Side Inductance in Modeling

The effect of finite ac inductance on the current commutation, as opposed to the zero inductance assumed in previous section may be included in the switching functions. However the resulting switching functions will be far more complex than cases where the overlap is neglected, since the ac current during commutation is a function of system impedance, firing angle and dc current. It has been suggested that a simplifying approach that would reduce complexity while still yielding a satisfactory answer would be to use a linear rising function during the commutation period [22]. This approach is presented in the section.

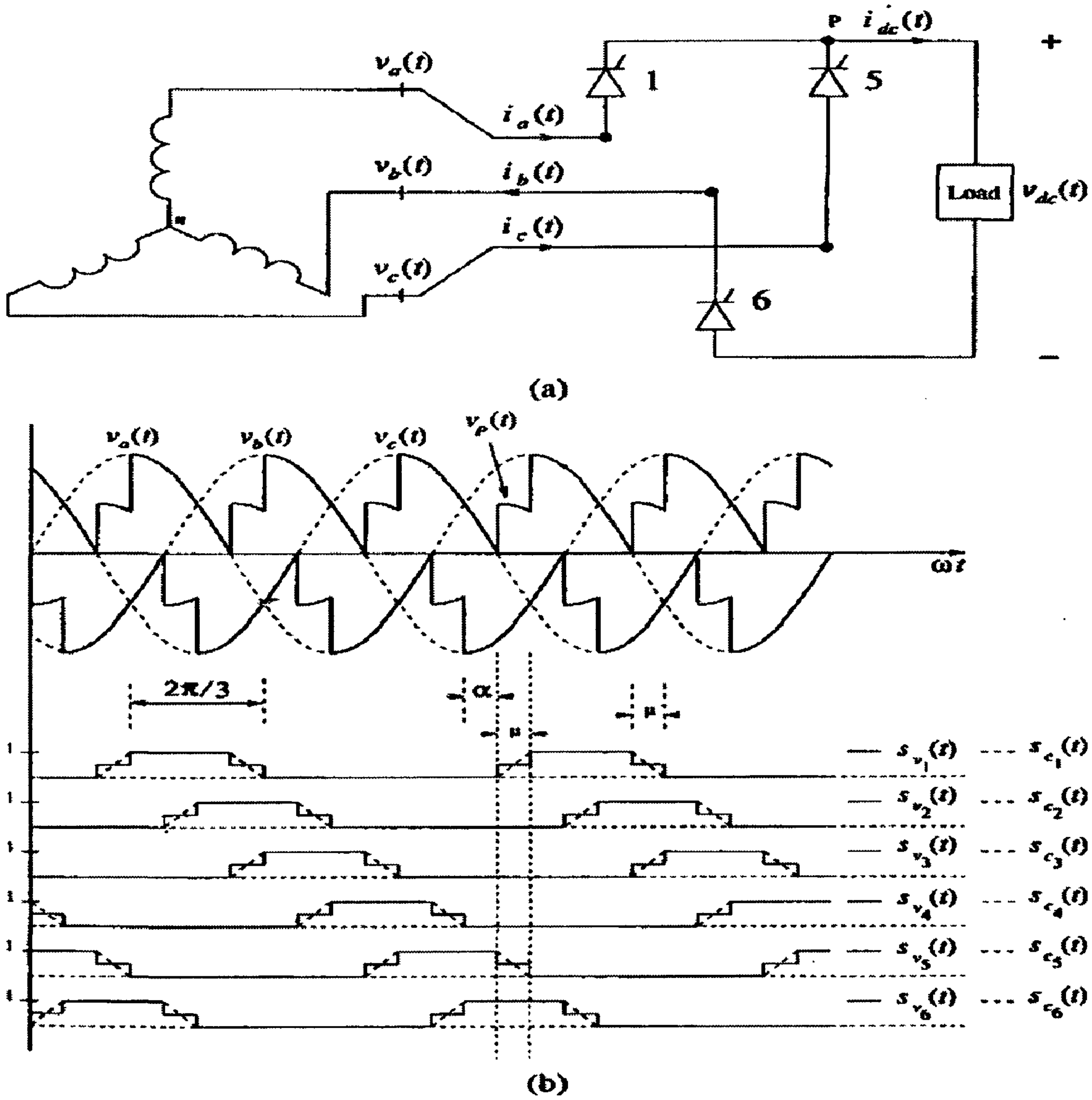

Fig. 4.11 Three-phase, Six-pulse rectifier, with Commutation effect

With reference to Fig. 4.11 and assuming that thyristors 5 and 6 have been previously conducting, at $\omega_o t = \alpha$ the current begins to commutate from thyristor 5 to thyristor 1.The instant when $v_a(t)$ becomes more positive than $v_c(t)$ is chosen at the time origin $\omega_o t = 0$. During the current commutation interval μ thyristors 1 and 5 conduct simultaneously and the phase voltage $v_a(t)$ and $v_c(t)$ are shorted together through the ac side inductance in each phase. The current $i_a(t)$ builds up from 0 to $i_{dc}(t)$ where as $i_c(t)$ decreases from $i_{dc}(t)$ to 0, at which instant the current commutation from thyristor 5 to thyristor 1 is completed. Under such conditions the voltage waveform during commutation interval μ is given by

$$v_p(t) = \frac{v_a(t) + v_c(t)}{2} \tag{4.24}$$

In order to incorporate such effects in the switching functions the relevant voltages are averaged during the commutation interval. For the currents the switching functions are represented by stepped functions.

The relationship between the voltages on the ac and dc sides of the rectifier is given by the following expression:

$$v_{dc}(t) = [s_{v1}(t) - s_{v4}(t)]\, v_a(t) + [s_{v3}(t) - s_{v6}(t)]\, v_b(t) + [s_{v5}(t) - s_{v2}(t)]\, v_c(t) \tag{4.25}$$

For the currents the relationship is as follows:

$$\begin{aligned} i_a(t) &= [s_{c1}(t) - s_{c4}(t)]\, i_{dc}(t) \\ i_b(t) &= [s_{c3}(t) - s_{c6}(t)]\, i_{dc}(t) \\ i_c(t) &= [s_{c5}(t) - s_{c2}(t)]\, i_{dc}(t) \end{aligned} \tag{4.26}$$

4.2.5 Thyristor Switching Functions

The harmonic contents of the six switching functions of figure associated with the ideal operation of the six pulse rectifier are given by:

$$S_0 = \frac{1}{3}$$
$$S_n = \frac{1}{n\Pi}\sin\left(\frac{n\Pi}{3}\right)e^{-jn\left(\phi_r+\phi_p+\Pi/2+\alpha\right)} \qquad (4.27)$$

Where

Φ_r is the shift angle of the ac voltage supply with respect to the reference $v_a(t)=V_a \sin \omega_0 t$

Φ_p is the sequence phase angle required to fire the thyristors i.e. 0 for thyristor 1; Π/3 for thyristor 2; 2 Π /3 for thyristor 3; Π for thyristor 4; 4 Π /3 for thyristor 5; 5 Π /3 for thyristor 6.

A more realistic operation of the converter should include the representation of the commutation overlap angle. From Fig. 4.11 the harmonics of the six switching functions for the voltages are:

$$S_{v0} = \frac{1}{3}$$
$$S_{vn} = \frac{1}{2n\Pi}\left(\sin n\left(\frac{\Pi}{3}-\frac{\mu}{2}\right)+\sin n\left(\frac{\Pi}{3}+\frac{\mu}{2}\right)\right)e^{-jn\left(\phi_r+\phi_p+\Pi/2+\alpha\right)} \qquad (4.28)$$

Similarly the six switching functions for the currents are:

$$S_{c0} = \frac{1}{3}$$
$$S_{cn} = \frac{1}{2n\Pi}\left(\cos n\left(\frac{\Pi}{3}-\frac{\mu}{2}\right)-\cos\left(\frac{\Pi}{3}+\frac{\mu}{2}\right)\right)e^{-jn\left(\phi_r+\phi_p+\Pi/2+\alpha\right)} \qquad (4.29)$$

It should be pointed out that when the converter is working under unbalanced supply conditions the commutation overlap for each phase will differ. This means that the switching function for each phase will have a different wave shape and therefore would need to be expressed by different equations. In this case the calculation of the harmonics becomes more elaborated. In order to simplify the analysis, the average commutation overlap due to positive sequence voltage may be used [22].

4.2.6 Model in the Harmonic Domain

The harmonic domain model of the three phase six pulse rectifier presented below is based on the relationships between the harmonic voltages and currents in both the ac and dc sides of the rectifier [4]. The equations which take into account the overlap angle, i.e. (4.25) and (4.26), are represented in the harmonic domain by

$$\mathbf{V}_{dc} = [\mathbf{S}_{v1} - \mathbf{S}_{v4}]\,\mathbf{V}_a + [\mathbf{S}_{v3} - \mathbf{S}_{v6}]\,\mathbf{V}_b + [\mathbf{S}_{v5} - \mathbf{S}_{v2}]\,\mathbf{V}_c(t) \tag{4.30}$$

and

$$\begin{aligned} \mathbf{I}_a &= [\mathbf{S}_{c1} - \mathbf{S}_{c4}]\,\mathbf{I}_{dc} \\ \mathbf{I}_b &= [\mathbf{S}_{c3} - \mathbf{S}_{c6}]\,\mathbf{I}_{dc} \\ \mathbf{I}_c &= [\mathbf{S}_{c5} - \mathbf{S}_{c2}]\,\mathbf{I}_{dc} \end{aligned} \tag{4.31}$$

Equations (4.30) and (4.31) contain harmonic coefficients of the voltages and currents existing in both sides of the converter. The harmonic coefficients of AC and DC voltages and currents are related by the harmonic content of the switching functions. This is a general representation that caters for the incorporation network and operational imbalances, pre existing harmonic distortion in the ac supply and unbalanced converter operation.

It should be noted that the vector products in (4.30) and (4.31) equations represent mutual convolutions, where the switching functions become matrices with Toeplitz structures and entries obtained from (4.28) and (4.29).

It is not difficult to appreciate from the (4.30) that if ac voltages contain imbalances and non characteristic harmonics their effects will be reflected in the harmonic content of $\mathbf{V}_{dc}$.

For the converter circuit to have practical meaning the admittance of the dc loads requires explicit representation,

$$\mathbf{I}_{dc}=\mathbf{Y}\ \mathbf{V}_{dc} \tag{4.32}$$

The harmonic coefficients of $\mathbf{I}_{dc}$ are a function of the voltage $\mathbf{V}_{dc}$ and the load admittance $\mathbf{Y}$, which clearly indicates that the dc component and the ripple of $i_{dc}(t)$ are represented explicitly in the relation. It should also be noted that the load in above equation may take any composition as long as it is static.

Using (4.30) and (4.32), the equivalent three phase six pulse rectifier circuit as seen from the ac side is obtained:

$$\mathbf{I}_{abc}=\mathbf{Y}_{rect}\ \mathbf{V}_{abc} \tag{4.33}$$

where the matrix Y_{rect} represents the three phase six pulse rectifier equivalent admittance matrix.

The current and voltage vectors are given by

$$I_{abc} = \begin{bmatrix} I_a \\ I_b \\ I_c \end{bmatrix}, V_{abc} = \begin{bmatrix} V_a \\ V_b \\ V_c \end{bmatrix} \tag{4.34}$$

and the admittance matrix by

$$\mathbf{Y}_{rect} = \mathbf{S}_c\ \mathbf{Y}_l\ \mathbf{U}_u\ \mathbf{S}_v \tag{4.35}$$

where

$$S_c = \begin{bmatrix} S_{c1} - S_{c4} & 0 & 0 \\ 0 & S_{c3} - S_{c6} & 0 \\ 0 & 0 & S_{c5} - S_{c2} \end{bmatrix}$$

$$Y_l = \begin{bmatrix} Y & 0 & 0 \\ 0 & Y & 0 \\ 0 & 0 & Y \end{bmatrix}$$

$$U_u = \begin{bmatrix} U & U & U \\ U & U & U \\ U & U & U \end{bmatrix}$$

$$S_v = \begin{bmatrix} S_{v1} - S_{v4} & 0 & 0 \\ 0 & S_{v3} - S_{v6} & 0 \\ 0 & 0 & S_{v5} - S_{v2} \end{bmatrix}$$

where U is the identity matrix.

It should be mentioned that if no commutation angle is considered, then the switching functions $s_v(t)$ and $s_c(t)$ are both equal to s(t), which in the harmonic domain becomes $\mathbf{S}_c = \mathbf{S}_v = \mathbf{S}$ with entries obtained from (4.27).

The three-phase, Six-pulse rectifier model in the form of a harmonic transfer admittance matrix, $\mathbf{Y}_{rect}$, is both flexible and comprehensive. It caters for imbalances in the thyristors firing angles, commutation effect and a variety of static loads.

4.2.7 MODELING RESULTS

A six-pulse, three-phase rectifier feeds a load Z = R+jX. In its turn, the rectifier is fed form a sinusoidal, three phase balanced voltage source of 1 p.u. magnitude. Simulations were carried out for two different representations of the rectifier: (i) With no commutation angle, (ii) With commutation angle. Conditions for distorted and unbalanced voltage source can be considered, individually and simultaneously for same simulations.

(i) With no commutation angle:

Neglecting the commutation angle, with $\alpha = 20^{o}$, and h=100, three different loading conditions are considered (R+jX= 0.5 +j0.1, 0.5 +j 100, 0.5).Results are presented for the most relevant converter parameters.

Table 4.2 Neglecting Commutation, Sinusoidal Source

	R=0.5,X=100	R=0.5,X=0.1	R=0.5
V_{dc}	1.5542	1.5542	1.5542
I_{dc}	3.1085	3.1085	3.1085
I_{1rms}	2.4237	2.4301	2.4293
I_{rms}	2.5342	2.5407	2.5525
V_{rms}	0.7071	0.7071	0.7071
V_{1rms}	0.7071	0.7071	0.7071
PF	0.8987	0.9002	0.9047
THD_I	30.53%	30.51%	32.25%
THD_V	0%	0%	0%
S	1.7919	1.7965	1.8049
P	1.6104	1.6193	1.6328
Q_H	0.5862	0.5806	0.5336
D_H	0.5234	0.5242	0.5540

The results show that the DC components of V_{dc} and I_{dc} are a function only of the resistance but not the reactance, which is an expected result. The main waveforms of rectifier operation are shown in Fig. 4.12-4.13 for a load of Z = 0.5 + j0.1.Voltage and current of DC side is shown with ac side current and its harmonic spectrum.

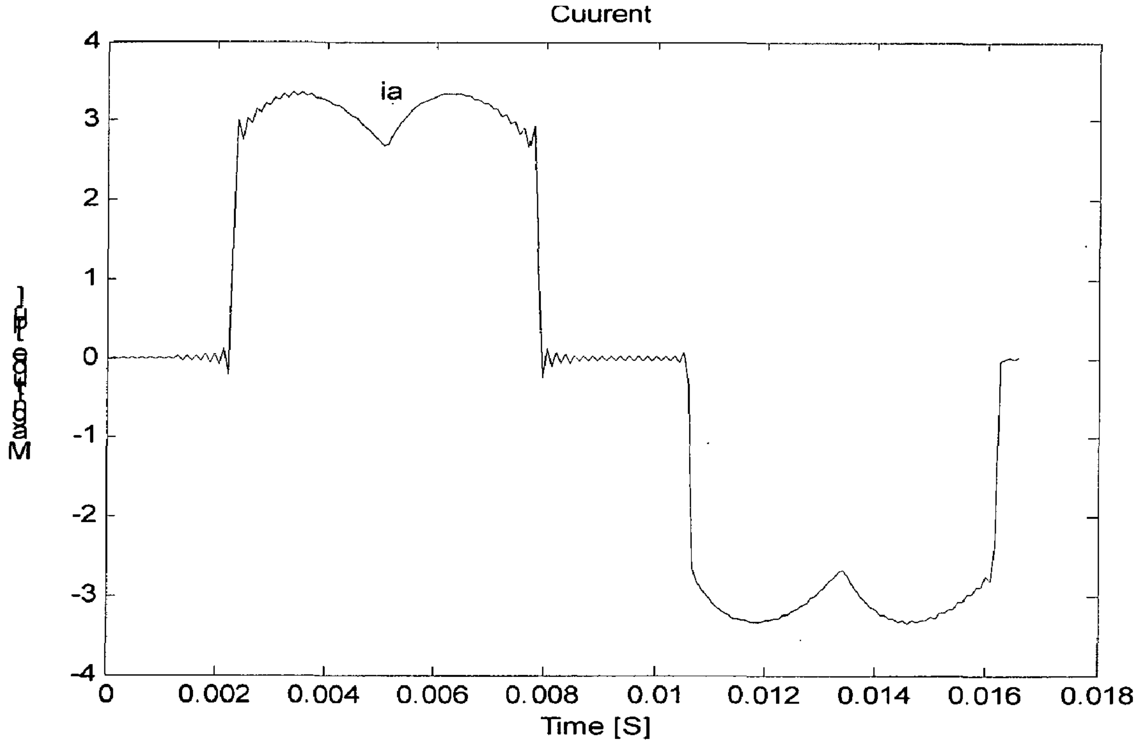

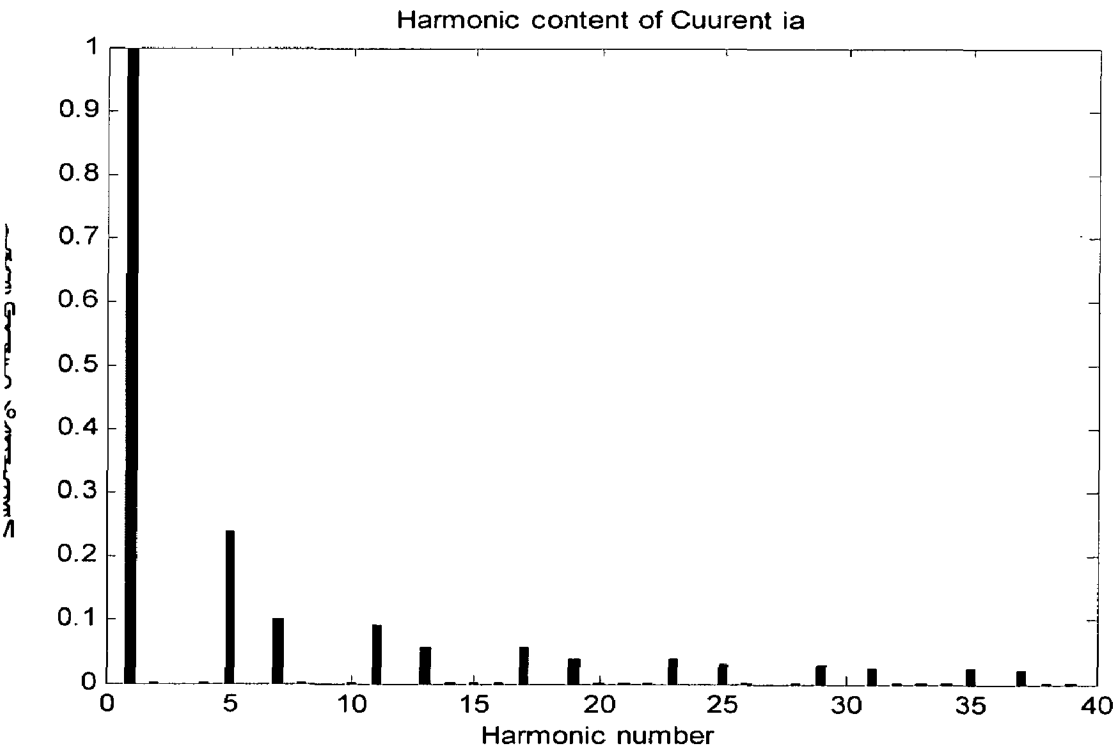

Fig.4.12 AC line Current waveform with harmonic spectrum

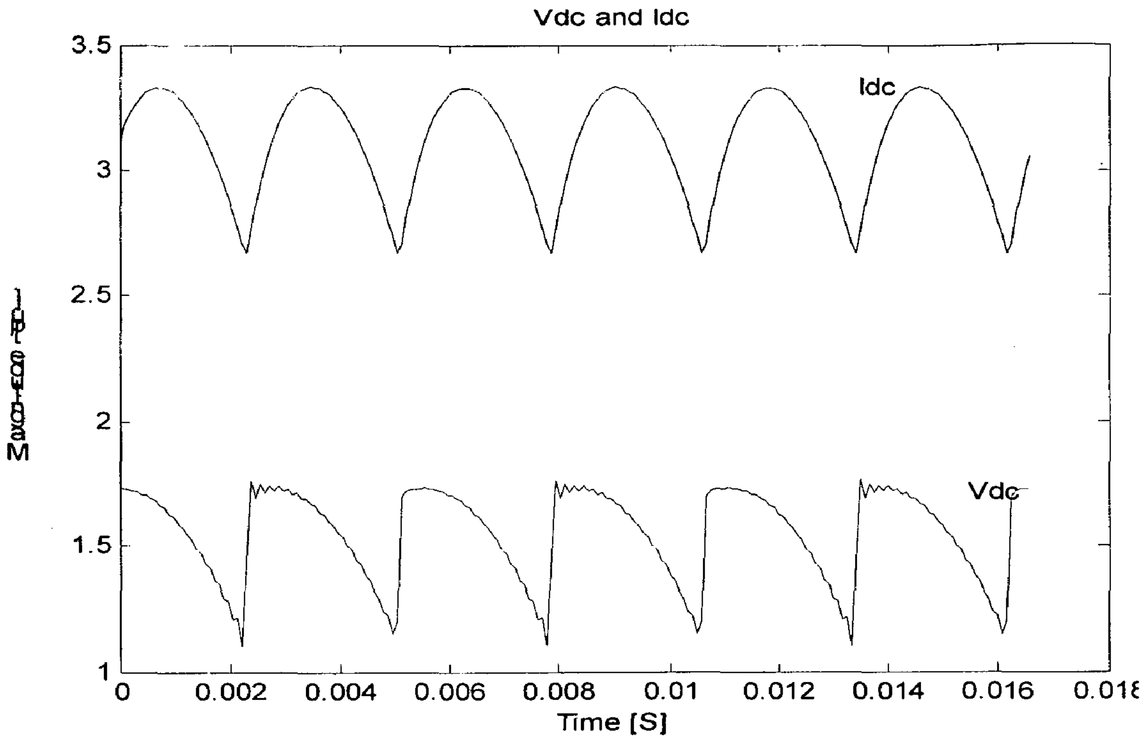

Fig.4.13 DC side Voltage and Current Waveforms

Fig. 4.14 shows the structure of $\mathbf{Y}_{rect}$, with no commutation .The matrix structure shows that the three-phase rectifier impedance has a very strong inter-coupling between phases and between harmonics. In this harmonic domain $\mathbf{Y}_{rect}$ is a skew Hermitian matrix.

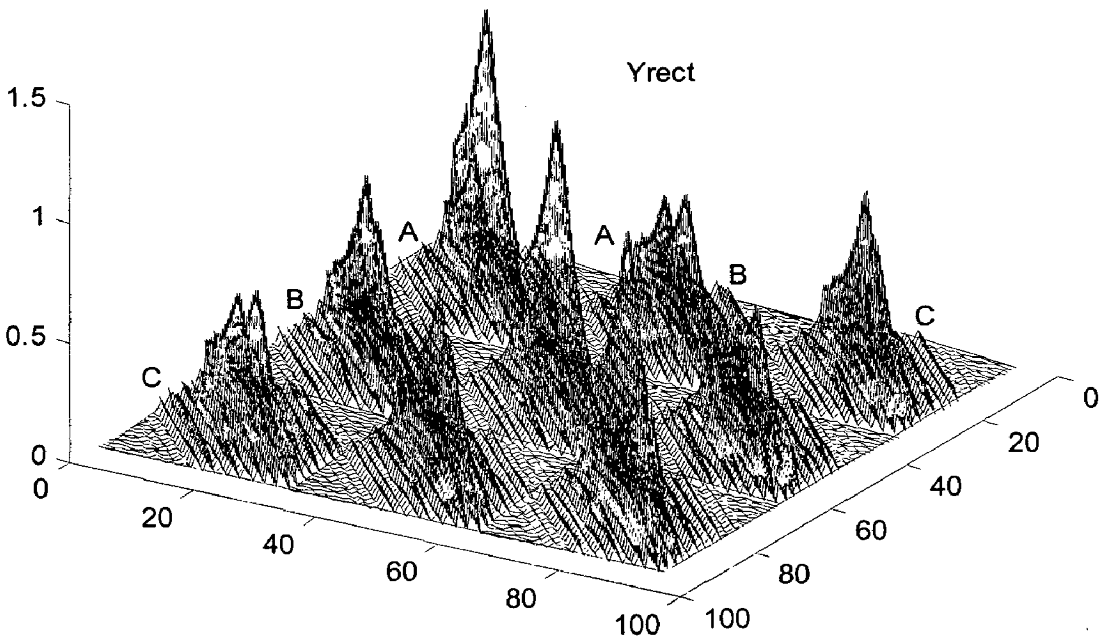

Fig. 4.14 Three-phase rectifier equivalent admittance matrix $\mathbf{Y}_{rect}$, without commutation.

(ii) This case assumes a commutation angle μ=10°, a firing angle α=20°, and uses a more complex model.

The relevant converter parameters are shown in Table 4.3. Three different loading conditions are considered as in case (i). It is seen from the result that the load reactance does not influence the DC variables. However, it has a more significant impact on the current THD.

Table 4.3 Neglecting Commutation, Sinusoidal Source

	R=0.5,X=100	R=0.5,X=0.1	R=0.5
V_{dc}	1.5483	1.5483	1.5483
I_{dc}	3.0966	3.0966	3.0966
I_{1rms}	2.4114	2.4174	2.4170
I_{rms}	2.4930	2.5033	2.5114
V_{rms}	0.7071	0.7071	0.7071
V_{1rms}	0.7071	0.7071	0.7071
PF	0.9089	0.9081	0.9107
THD_I	26.24%	26.89%	28.23%
THD_V	0%	0%	0%
S	1.7628	1.7701	1.7759
P	1.6023	1.6073	1.6172
Q_H	0.5862	0.5817	0.5528
D_H	0.4475	0.4596	0.4824

It is well known that one effect of commutation is to make the converter waveforms more sinusoidal, thus reducing harmonic distortion. This can be appreciated by comparing the relevant THD_I values in Table 4.2 and Table 4.3. The result presented in the later table includes commutation effect, and the THD_I values are shown to be consistently lower.

The main waveforms of rectifier operation are shown in Fig. 4.15-4.16 for a load of Z = 0.5 + j0.1. The AC side line currents, where the effect of the finite inductance on the DC side is clearly seen and its harmonic spectrum is also given. These currents also show the effect of commutation. Voltage and current of DC side is shown with the phase and line ac voltages, and the commutation voltages.

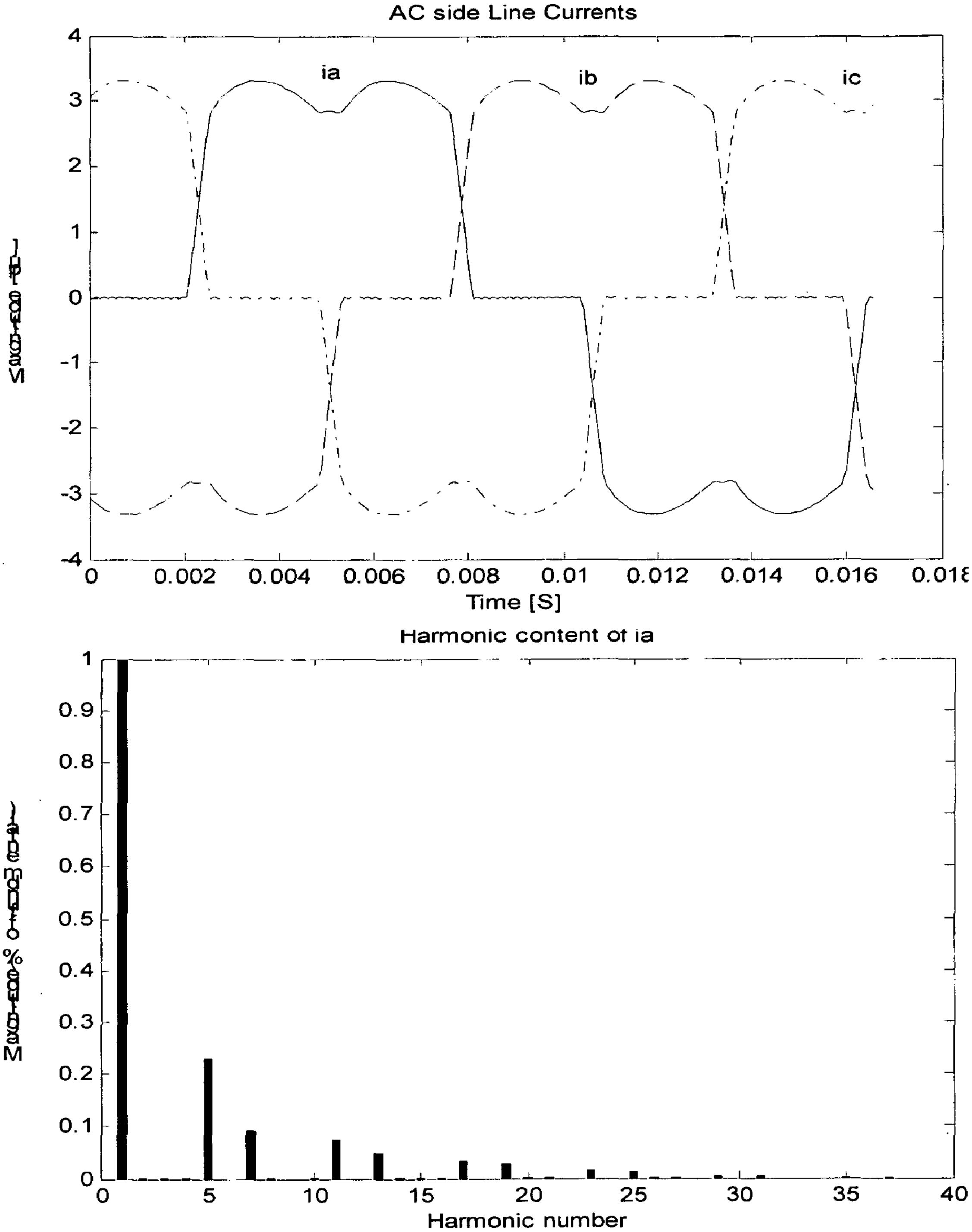

Fig.4.15 AC line Current waveform with harmonic spectrum

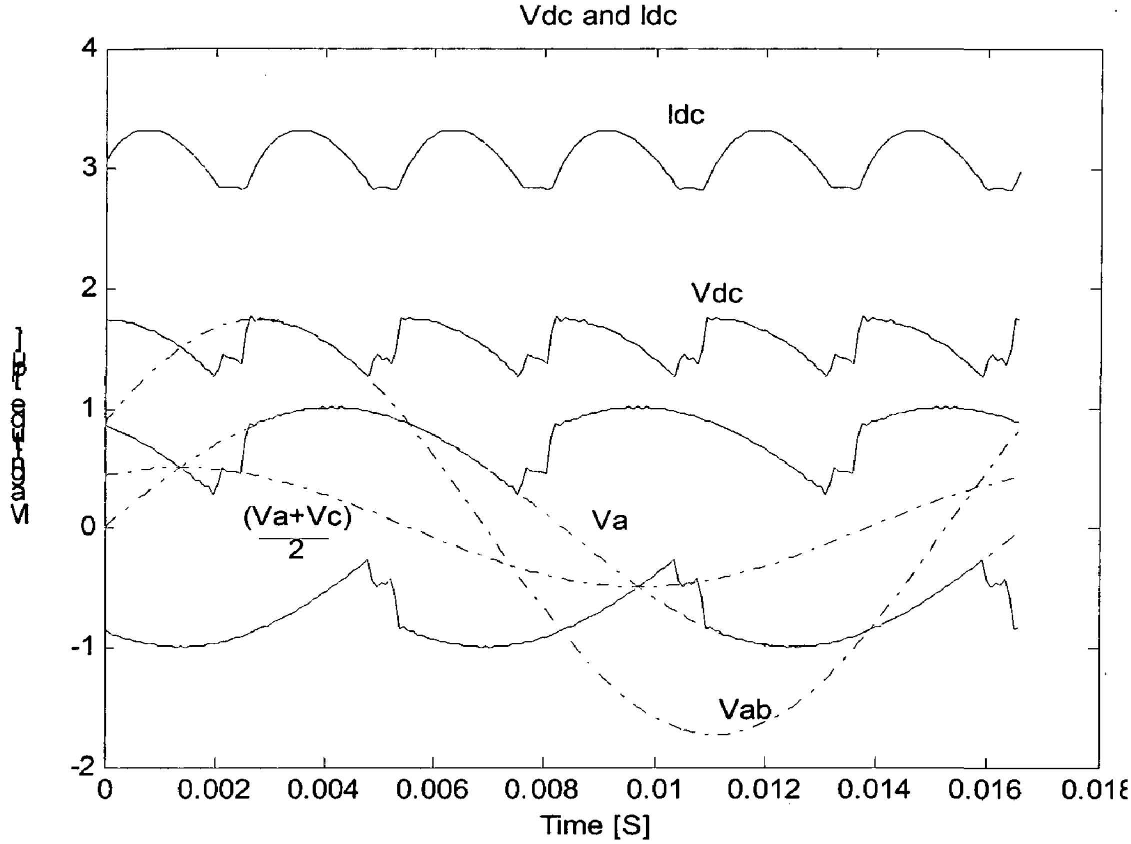

Fig.4.16 DC side Voltage and Current Waveforms with AC side phase, line and commutation voltages.

Fig. 4.17 shows the structure of $\mathbf{Y}_{rect}$, with considering commutation .The matrix structure shows that the three-phase rectifier impedance has a very strong inter-coupling between phases and between harmonics. In this harmonic domain $\mathbf{Y}_{rect}$ is a skew Hermitian matrix.

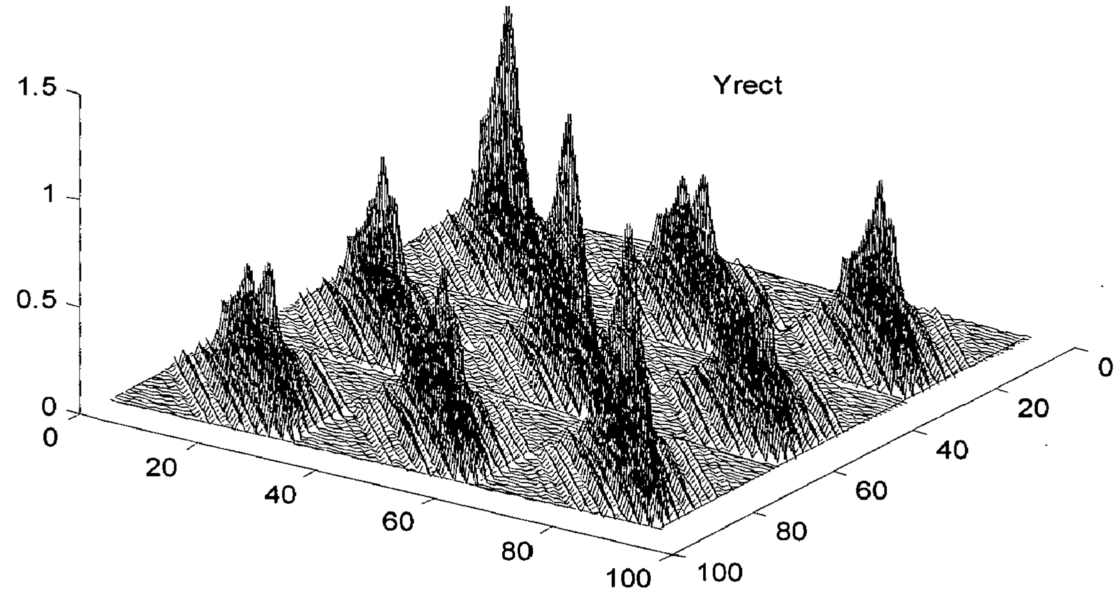

Fig. 4.17 Three-phase rectifier equivalent admittance matrix $\mathbf{Y}_{rect}$, with commutation.

4.2.8 CONCLUSION

The thrust of this section is on the derivation of harmonic domain models suitable for the study of conventional three-phase, six pulse harmonic converters. Modulation theory based on switching functions and discrete convolutions are the cornerstone of these models.

The harmonic converter models given in this section build up incrementally, starting with the simplified case where no commutation effects are included. This simplicity is used to illustrate the simple relationship that exists between the AC and DC voltages and switching functions. The MATLAB™ code is used for developing the model. The characteristic and non- characteristic harmonics are implicitly included in the model, together with DC ripple, ac and converter imbalances, and pre existing harmonics.

The model comes in the form of a harmonic admittance which shows a very strong cross-coupling between phases and between harmonics. Also, the harmonic interaction and frequency conversion that exists between the ac and DC sides of the converter are implicitly included. The effect of source impedance is presented in detail with effects on harmonics.

4.3 INRUSH CURRENT PHENOMENON

This section presents an important class of non-linear characteristics in electrical power circuits which are the magnetizing impedance of saturated power transformers. Saturated magnetic cores may generate harmonic currents during steady-state operation, as well as transient harmonic currents and temporary over-voltages following a major switching operation in the transformer's vicinity, with a critical case being the energization of transformer itself. The steady-state magnetizing currents of power transformer are only 1-2 % of the rated current but they may reach 10-20 times their rated value when transformers are switched on to source, exhibiting a current spectrum which is rich in harmonics. This transient phenomenon is termed *Inrush Currents*.

4.3.1 INTRODUCTION

Transformers used in distribution system and industrial facilities such as furnace installations are switched many times during a twenty-four-hour period. Each energization of the transformer will generate a transient inrush current rich in harmonics. This inrush current is dependent on the magnitude of the supply voltage at the instant the transformer is energized, the residual flux in the core of the transformer, and the impedance of the supply circuit. It includes both even and odd harmonics which decays with time until the transformer magnetizing current reaches a steady state.

The steady-state magnetizing currents of power transformers are only 1-2% of the rated current but they may reach 10-20 times their rated value when transformers are switched onto source. Owing to the slow attenuation of the transient, its effect may persist for several seconds before the steady state is reached, causing many adverse operating conditions. They are known to have caused unnecessary tripping of differential protection relays in the past [23].

Inrush currents may also give rise to long-term over-voltages in system configurations with pronounced parallel resonant points and low degree of damping [24]. In industrial systems such situations may occur when large power factor correction capacitors exist at the secondary side of the transformer which, when combined with the predominantly inductive impedance of the system at low harmonic frequencies, lead to a parallel resonant circuit of high impedance [25].

Moreover, if the ensuing parallel circuit is tuned to a harmonic frequency component of the inrush current then a voltage magnification will take place. In the long range, if over-voltages occur frequently then the life expectancy of the capacitors will be very much reduced.

HVDC schemes have also been reported to experience voltage magnifications due to the capacitive influence of the ac filters and the inductive impedance of the system at low harmonic frequencies [26]. The inrush phenomenon is intrinsically linked to saturated iron cores. Accordingly, accurate representations of transformers' magnetizing characteristics became of paramount importance in these studies. This has been a topic of active research in the past and many good methods are available in the open literature. For instance, a simple polynomial representation has been used with good results [27]. The appeal of this mathematical representation is that it is amenable to fast frequency domain evaluations via repeated convolutions.

The inrush phenomenon is of nonlinear nature and can only be reproduced by actual tests and computer simulations. However, the issue is not straightforward because the use of scale-down testing may not reflect accurately the attenuation observed in full-size transformers and numeric simulations are slow and prone to errors, particularly in the case of slowly attenuating transients [28]. The use of operational matrices, which overcomes some of the problems encountered with step-by-step time domain simulations, is a full frequency domain solution technique which solves the inrush phenomenon by assuming that the overall transient is part of a periodic train of transients [23].

Owing to the nonlinear nature of the application at hand, the problem must be solved by iteration. A harmonic Newton-Raphson method is used to solve the inrush problem to a specified accuracy, leading to very robust iterative solutions [29].

4.3.2 Transformer Energization Inrush Currents

Energization inrush currents occur when a system voltage is applied to a transformer at a specific time when the normal steady-state flux should be at a different value from that existing in the transformer core [25]. For the worst-case energization the flux in the core may reach a maximum of over twice the normal flux. For flux values much greater than normal, the core will be driven deep into saturation, causing very high-magnitude energization inrush current to flow [25]. The magnitude of this current is dependent on such factors as supply voltage magnitude at the time of energizing, source impedance, residual flux in the core, transformer size, and design. This initial energization inrush current could reach values as high as 25 times full-load current and will decay with time until a normal exciting current value is reached. Values of 8 to 12 times full-load current for transformers larger than 10 MVA with or without load tap changers have been measured during testing. The decay of the inrush current may vary from times as short as 20 to 40 cycles to as long as minutes for highly inductive circuits.

The inrush current produced during the energization of a transformer is a case where the distinction between harmonics and transients becomes less clear. The dynamic inrush-current waveform associated with transformer energizing operation includes both even and odd harmonics which decays with time until the transformer magnetizing current reaches steady state. The most predominant harmonics, during transformer energization, are second, third, fourth, and fifth in descending order of magnitude. Some typical magnitudes of the energization inrush-current harmonics are given in Table 4.4 [25].

TABLE 4.4. Typical Magnitudes of Energization Inrush-Current Harmonics

Harmonic	Magnitude X is between 5-12
2nd Harmonic	21.6% of X * $I_{Full\ lload}$
3rd Harmonic	7.2% of X * $I_{Full\ lload}$
4th Harmonic	4.6% of X * $I_{Full\ lload}$
5th Harmonic	2.8% of X * $I_{Full\ lload}$

Modern high-voltage power transformers with grain-oriented steel cores are designed operate in he region of 1.6-1.7T, and have a sharply defined knee. Hence, over-excitation of 20% and even 10% in some cases above the rated value will push the transformer deep into saturation. The magnetizing current of single phase iron cores will be symmetric in most cases, with the harmonic current spectrum containing no even harmonics and no DC term, just the fundamental frequency component and odd harmonics. For most practical purposes, harmonic terms in the magnetizing current above the 15^{th} are negligibly small and are not cause for no concern. Moreover, in most three-phase transformer applications at least one of the three-phase winding is delta connected to confine the zero-sequence harmonic currents within this winding , and only the 5^{th}, 7^{th}, 11^{th} and 13^{th} harmonic currents would normally deserve attention. However, some caution should be exercised because the delta connection will only be 100% effective if the power circuit is perfectly balanced. It is unavoidable that practical power networks will always contain asymmetries of one type or another.

A practical problem of greater concerns is the case when a DC component finds its way into the magnetic core, causing the transformer to saturate asymmetrically. The end result is that the harmonic spectrum of the magnetizing current becomes richer, containing in addition to the fundamental frequency component and odd harmonics, the even harmonics and the DC term. In practice, the DC term causing the asymmetrical core behaviour may come from a power electronic circuit fed directly from the transformer, such as a half-wave rectifier or a three-phase converter with unequal firing pulses. In the case of furnace transformers, it may come from asymmetric operation of the arc. It has been observed using simulations that the magnitude of the low-order harmonic currents increase linearly with the amount of direct current at the secondary of the transformer [4]. It has also been observed that the harmonic currents generated as a result of the spurious DC excitation are largely independent of AC excitations.

4.3.3 Inrush Currents Simulations

To gain some insight into magnetizing inrush currents and how they are calculated, the unloaded, single-phase transformers equivalent circuit shown in Fig. 4.18 is used.

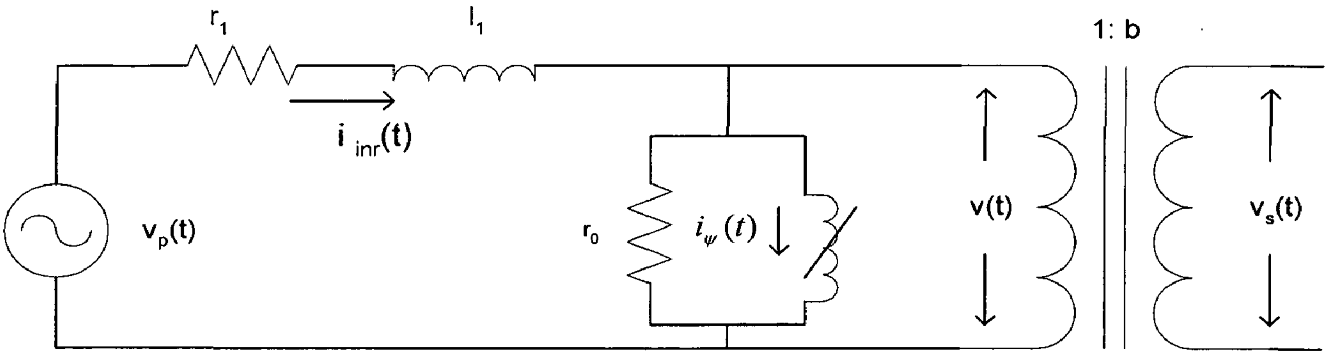

Fig. 4.18 Unloaded Single-Phase Transformer

In this particular case the non-linear characteristics is represented by the following polynomial equation [24]:

$$i_{\psi}(t) = 0.7576\psi(t) + 1.03 * 10^{7}\psi^{19}(t)$$

DC pre-magnetization is strictly speaking the effect of a remanent flux. However, the energization of a winding at a point different from the voltage peak will also result in a flux which is equivalent to the flux due to remanence, Inrush currents can be calculated following the basic premise. It is important to mention at this point that the attenuation of inrush currents is not affected by eddy current and hysteresis losses in the iron core [30]. The state equation below describes the circuit:

$$\begin{bmatrix} \dot{i}_{inr}(t) \\ \dot{\psi}(t) \end{bmatrix} = \begin{bmatrix} -(r_1 + r_0)/l_1 & 0 \\ r_0 & 0 \end{bmatrix} \begin{bmatrix} i_{inr}(t) \\ \psi(t) \end{bmatrix} + \begin{bmatrix} 1/l_1 & r_0 \\ 0 & -r_0 \end{bmatrix} \begin{bmatrix} v_p(t) \\ i_{\psi}(t) \end{bmatrix}$$

For this study $v_p(t) = 110 \cos(\omega_0 t - 42.97^{o})$, $f_0 = 50$ Hz was selected, and 200 cycles of simulation were selected. Initial conditions are assumed to be zero. The other transformer parameters are $r_l = 0.192\ \Omega$, $r_0 = 612.86\ \Omega$, $l_l = 0.9$mH. The state equations solved by using differential equation solver (ODE23) in MATLAB™.

4.3.4 SIMULATION RESULTS

Fig. 4.19 shows the inrush current evolution during the full simulation time. Further detail is provided at three different stages of the inrush current evolution in Fig 4:20. This result shows that the initial magnetizing current is much larger that can be the steady-state current, and takes a considerably long time to reach steady state.

This behaviour of the inrush current has been exploited to conduct simulation using harmonic domain techniques [31], arguing that the inrush current may be considered like a non-sinusoidal current in a quasi-steady-state condition if one only looks at a reduced number of cycles. This is particularly the case after the first few cycles have elapsed.

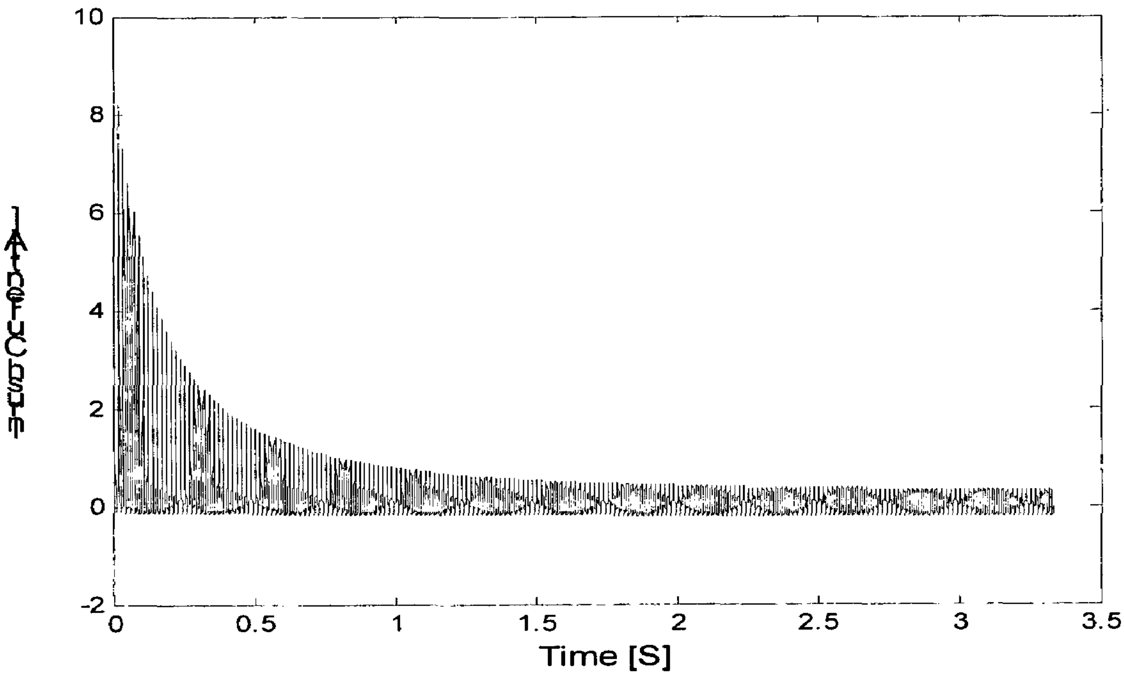

Fig. 4.19 Inrush Current

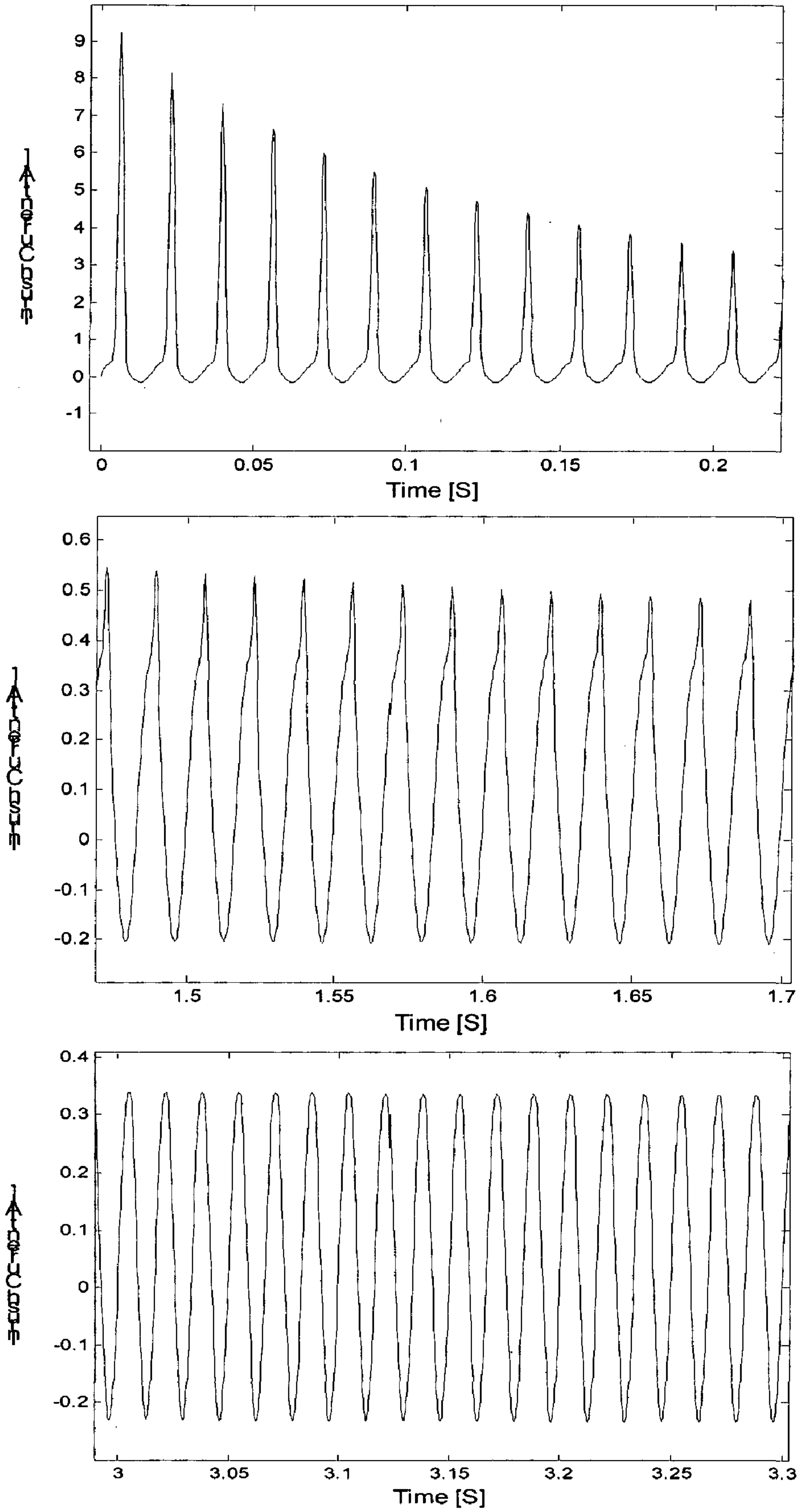

Fig. 4.20 Inrush Current (Enlargement of Fig. 4.19)

Fig. 4.21-4.22 shows the harmonic content of the inrush current at each cycle. This result shows the decay of the inrush current and its DC component, together with the harmonic terms. The slow decay of the harmonics suggests that the inrush current may be represented by a constant harmonic source for a limited number of consecutive cycles, i.e. window. This characteristic of slow attenuation has been used to establish a harmonic domain model [31] for the inrush current, where a pre-determined sequence of steady-state "images" is used to capture the complete picture of the inrush phenomenon.

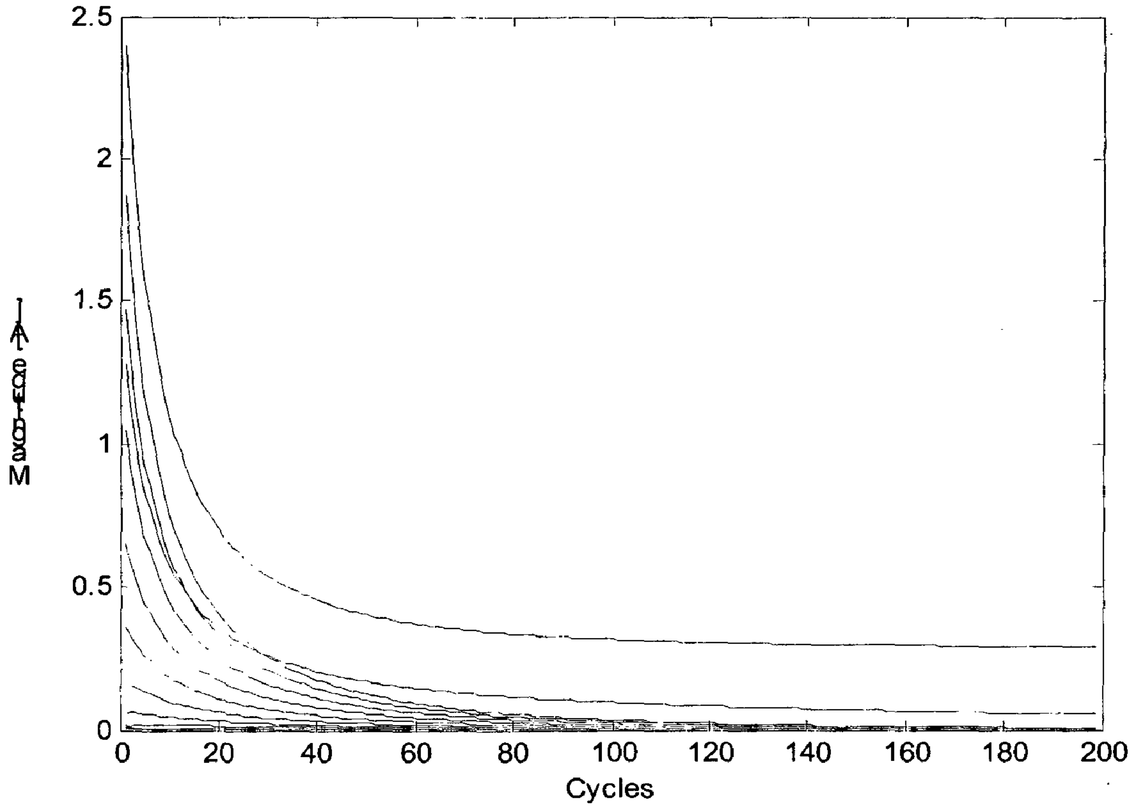

Fig. 4.21 Harmonic Content of the Inrush Current

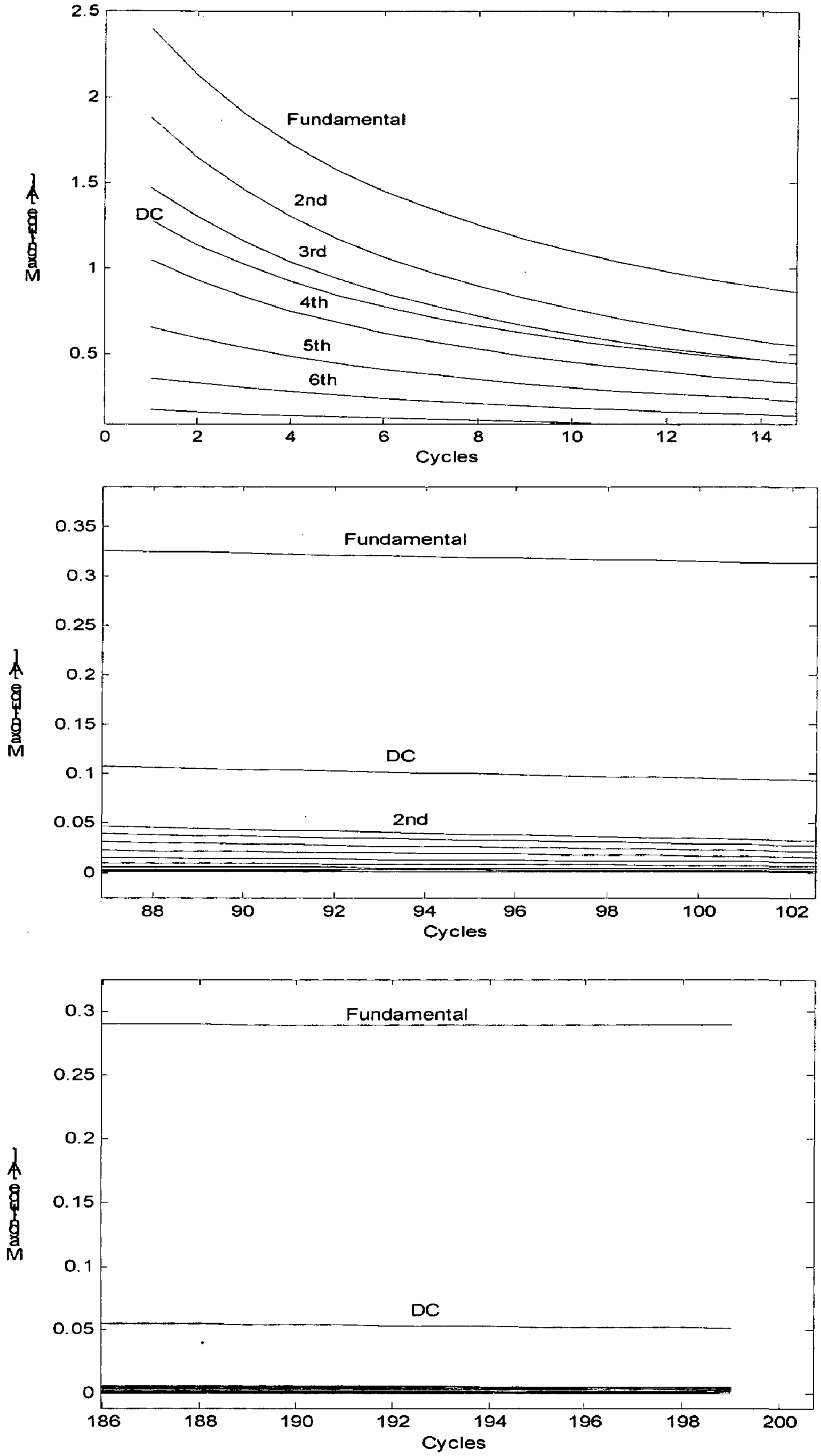

Fig. 4.22 Harmonic Content of the Inrush Current (Enlargement of Fig. 4)

5. ELIMINATION OF HARMONICS - PASSIVE & ACTIVE HARMONIC FILTERS

The primary object of a harmonic filter is to reduce the amplitude of one or more fixed frequency currents or voltages. In the past, utilities had the responsibility to provide a single frequency voltage waveform and customer loads had little effect on the voltage waveform. Now, however, power electronics are used widely and create non-sinusoidal currents that contain many harmonic components.

Odd-number harmonics (3rd, 5th, 7th, etc.) are of the greatest concern in the electrical distribution system. Even-number harmonics are usually mitigated because the harmonics swing equally in both the positive and negative direction.

Passive filters, consisting of tuned series L-C circuits, are the most popular. However, they require careful application, and may produce unwanted side effects, particularly in the presence of power factor correction capacitors.

The active filter concept uses power electronics to produce harmonic components that cancel the harmonic components from the nonlinear loads so that the current supplied from the source is sinusoidal. These filters are costly and relatively new.

These harmonics can be reduced or eliminated by the use of passive and active filters. In this chapter passive and active filters are presented.

5.1 PASSIVE HARMONIC FILTERS

5.1.1 INTRODUCTION

Passive harmonic filters are constructed from passive elements (resistors, inductors, and capacitors) and thus the name. These filters are highly suited for use in three-phase, four-wire electrical power distribution systems. They should be applied as close as possible to the offending loads, preferably at the farthest three to single-phase point of distribution. This will ensure maximum protection for the upstream system. Harmonics can be substantially reduced to as low as 30% by use of passive filters.

Passive filters can be categorized as parallel filters and series filters. A parallel filter is characterized as a series resonant and trap-type exhibiting low impedance at its tuned frequency. Deployed close to the source of distortion, this filter keeps the harmonic currents out of the supply system. It also provides some smoothing of the load voltage. This is the most common type of filter.

The series filter is characterized as a parallel resonant and blocking type with high impedance at its tuned frequency. It is not very common because the load voltage can be distorted.

5.1.2 Classification of Passive Filters [36, 37]

A. Series Passive Filters

When the only purpose of filters is to prevent a particular frequency from entering selected plant components or parts of a power system, series filters can be used. Series filters consist of a parallel inductor & capacitor and presents a large impedance to the relevant for such a solution, however, can not be used to eliminate harmonics from arising at the source because the production of harmonics by non-linear plant components is essential to their normal operation.

This configuration is popular for single-phase applications for the purpose of minimizing the 3rd harmonic. Other specific tuned frequencies can also be filtered. Fig. 5.1 shows the basic diagram of a series passive filter.

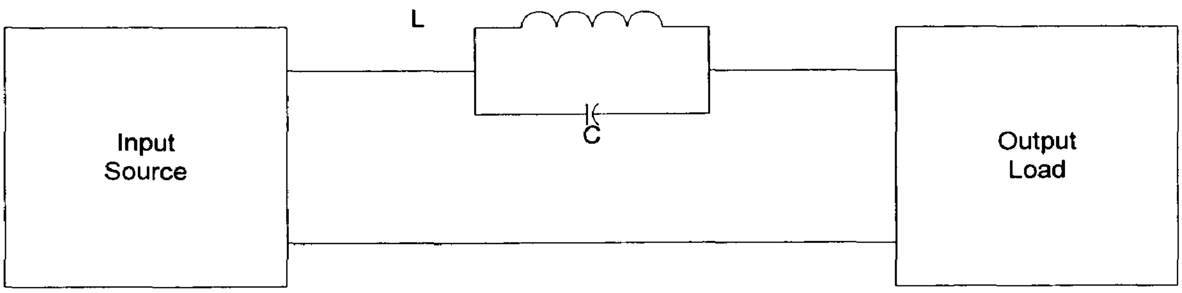

Fig 5.1 Series Passive Filter

The advantages of a series filter are that it:

- Provides high impedance to tuned frequency;
- Does not introduce any system resonance;
- Does not import harmonics from other sources;
- Improves displacement power factor and true power factor.

Some disadvantages are that it:

- Must handle the rated full load current;
- Is only minimally effective other than turned harmonic frequencies;
- Can supply nonlinear loads only.

B. Shunt Passive Filter

Passive shunt filter are a very popular-method to control the propagation of harmonics currents and as normally designed as a series combination of reactors and capacitors. Passive filters are also referred to as sinks because they absorb the harmonic currents. They present a low-impedance path to the harmonics to which it is tuned. Passive shunt filter are installed at the ac terminals of rectifiers, motor drives, UPS, & other nonlinear loads to reduce voltage and current distortion to acceptable limits at the point of connection.

The shunt passive filter is also capable of filtering specific tuned harmonic frequencies such as, 5th, 7th, 11th, etc. Fig. 5.2 shows a commonly used diagram of a shunt filter.

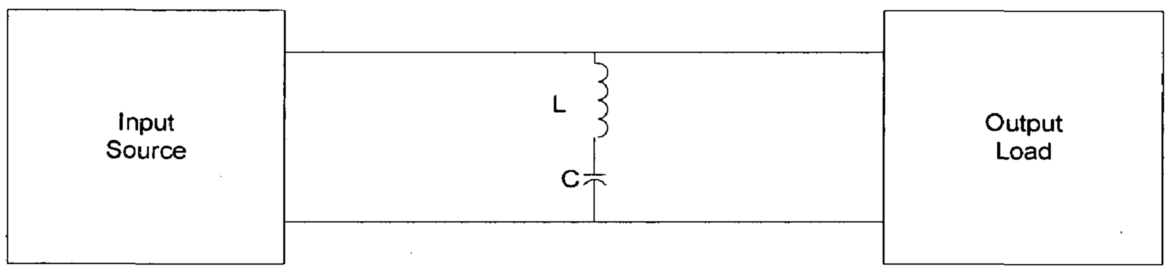

Fig 5.2 Shunt Passive Filter

The advantages of a parallel filter are that it:

- Provides low impedance to tuned frequency;
- Supplies specific harmonic component to load rather than from AC source;
- Is only required to carry harmonic current and not the full load current;
- Improves displacement power factor and true power factor.

Some disadvantages are that:

- It only filters a single (tuned) harmonic frequency;
- It can create system resonance;
- It can import harmonics form other nonlinear loads;
- Multiple filters are required to satisfy typical desired harmonic limits.

C. Series Passive AC Input Reactor

The basic configuration of series passive ac input reactor is shown in Fig. 5.3. This type filters all harmonic frequencies, by varying amounts.

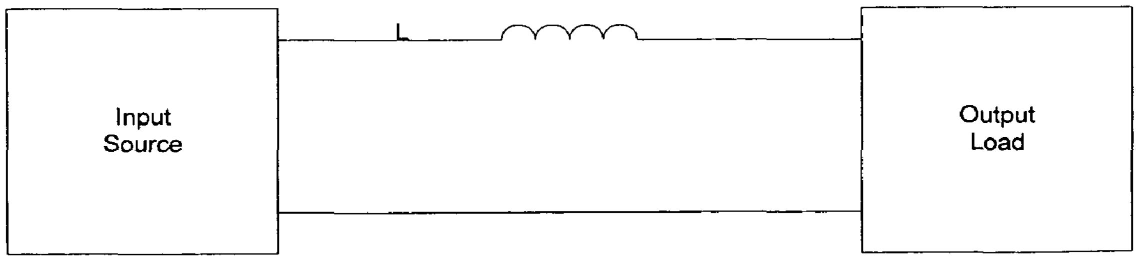

Fig. 5.3 Series Passive AC Input Reactor

The advantages of a series reactor are:

- Low cost;
- Higher true power factor;
- Small size;
- Filter does not create system resonance;
- It protects against power line disturbances.

Some disadvantages are that it:

- Must handle the rated full load current;
- Can only improve harmonic current distortion to 30 to 40-% at best;
- Only slightly reduces displacement power factor.

D. Low-Pass (Broadband) Filter

The basic configuration of the filter is shown in Fig. 5.4. It is capable of eliminating all harmonic frequencies above the resonant frequency.

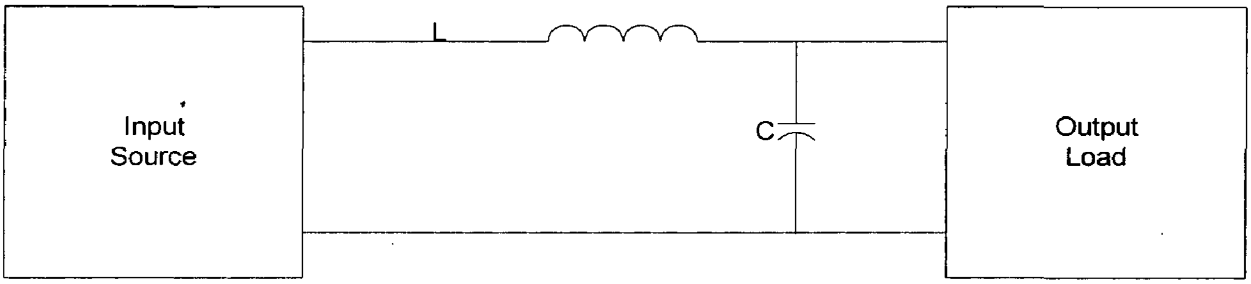

Fig. 5.4 Low Pass Filter

The specific advantages of a low-pass filter are that it:

- Minimizes all harmonic frequencies.
- Supplies all harmonic frequencies as opposed to the AC source supplying those frequencies;
- Does not introduce any system resonance;
- Does not import harmonics from other sources;
- Improves true power factor.

Some of the disadvantages are that it:

- Must handle the rated full load current;
- Can supply nonlinear loads only.

5.1.3 Passive Filter Design [36]

Filter design is normally carried out assuming static operating conditions, although in practice filter may be operated dynamically, switching them ON & OFF by sections, according to system requirements. For example switched filter are used in elevator drives, adjustable speed pump drives, reactive power compensator and HVDC converter stations.

The filter design process involves a number of steps that will ensure lowest possible cost and proper performance under the THD limits. Fig. 5.5 shows a flowchart of the entire design process.

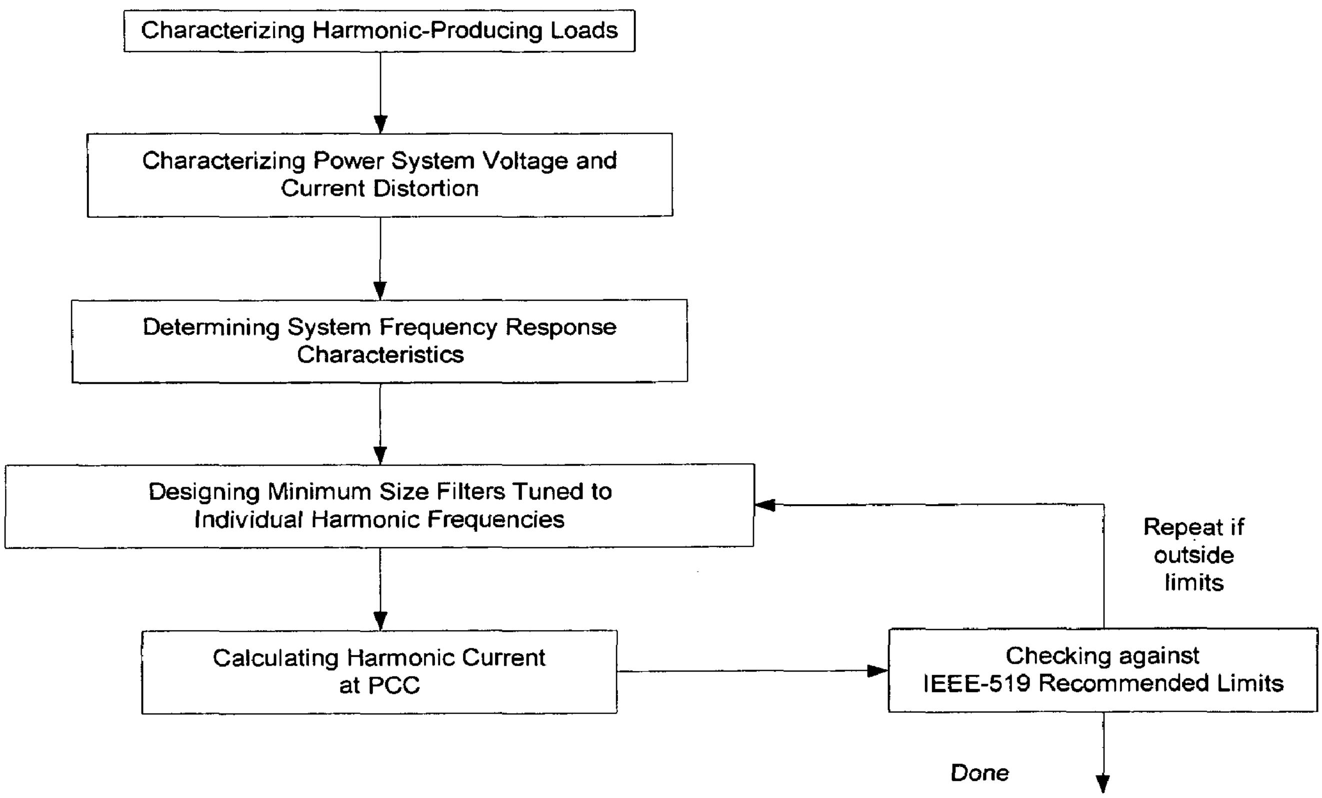

Fig. 5.5 Flowchart for Harmonic Filter Design

The size of a filter is defined as the reactive power that the filter supplies at fundamental frequency. It is substantially equal to the fundamental reactive power supplied by the capacitors. The total size of all the branches of a filter is determined by the reactive power requirements of the harmonic source and by how much this requirement can be supplied by the ac network.

The ideal criterion of filter design is the elimination of all detrimental effects caused by ware form distortion, including telephone interference. However, this criterion is unrealistic both for economic & technical reasons. From the technical point of view, it is very difficult to estimate in advance the distribution of harmonics throughout the ac network. On the economic side, the reduction of telephone interference can be achieved more economically taking some of the preventive measures in the telephone system and others in the power system.

A more practical criterion suggests reducing the problem to an acceptable level at the point of common coupling, with other consumers, the problem being expressed in terms of harmonic wattage, harmonic cement or both. A criterion based on harmonic voltage in more convenient to guarantee staying within a reasonable voltage limit than to limit the current level as the ac network impedance changes.

5.1.4 CASE STUDY [37]

Example: A 6-pulse connecter bridge is rated at 100kV, 100MW dc, operating at $\alpha = 15^{\circ}$. The bridge is connected to a 275kV, 50Hz, ac system via a 275/83 kV transformer with 15% leakage reactance. The secondary fundamental current is 780A and that of the primary 236A. The filters to be connected to the primary side, consists of resonant arms for the 5^{th}, 7^{th}, 11^{th} and 13^{th} and second order high pass arm.

Solution:

Reactive power requirement of the load:

MVA supplied = $\sqrt{3} \times \frac{83 \times 780}{1000} = 112.13 MVA$

MVAR supplied = $\sqrt{(112.13)^2 - (100)^2} = 50.73 MVAR$

For a total fitter size of 50 MVAR, and assuming that the capacitor is to be equally divided among the filter branch each filter branch requires 0.417μ F.

$$X_c = \frac{kV^3}{MVAR} = \frac{275^2}{50} = 1512.5\Omega$$

$$C = \frac{1}{\omega XC} = \frac{1}{2 \times \Pi \times 50 \times 1512.5} = 2.104 \times 10^{-6} F$$

$$C / branch = \frac{2.104}{5} = 0.420 \mu F$$

Standard value = 0.417 μ F.

If the capacitor temperature coefficient is 0.05% per degree design and inductor temperature coefficient is 0.01% per degree Celsius, ambient temp. is ±20°C and frequency tolerance is ±1%.

$$\delta = \frac{1}{100}\left\{1 + \frac{1}{2}[0.05 \times 20 + 0.01 \times 20]\right\} = 0.016$$

Let the ac system impedance be of any magnitude but its phase angle restricted to $\phi_a < 75$, at any frequency. The optimum value of Q is then obtained from equation.

$$Q = \frac{1+\cos\phi}{2\delta\sin\phi} = \frac{1+\cos 75}{2\times 0.016\times \sin 75} = 41$$

With Q and C known, L and R of the resonant arms can be determined:

For 5th arm,

$$Q = \frac{\omega_s L}{R}, \omega_s L = \frac{1}{\omega_s C}$$

$$L = \frac{1}{\omega_s^{\,2} C} = 0.972H, R = \frac{\omega_s L}{Q} = 37.25\Omega$$

For 7th arm,

$$L = \frac{1}{\omega_7^{\,2} C} = 0.496H, R = 26..6\Omega$$

For 11th arm,

$$L = \frac{1}{\omega_{11}^{\,2} C} = 0.201H, R = 16.94\Omega$$

For 13th arm,

$$L = \frac{1}{\omega_{13}^{\,2} C} = 0.144H, R = 14.32\Omega$$

The damped arm components are found by choosing m =1 and f_0= 850 Hz.

Since C has already been fixed to 0.417 μ F, the resulting values of L and R are

$$L = m^2 R^2 C$$

$$R = \frac{1}{2\Pi f_0} = \frac{1}{2\Pi \times 0.417\mu \times 85} = 450\Omega$$

$$L = 0.0844H$$

The complete circuit of the passive filter is shown in Fig. 5.6

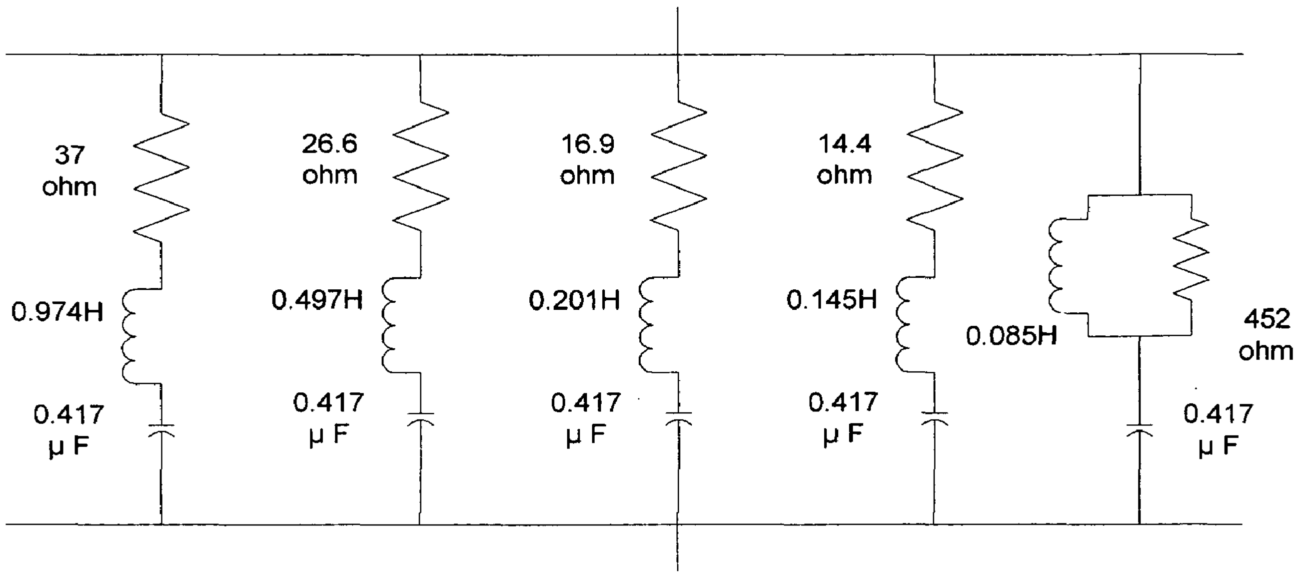

Fig 5.6 Example of a.c. filter design

5.2 ACTIVE HARMONIC FILTERS

5.2.1 INTRODUCTION

The traditional approach to harmonic reduction is by means of passive filters. Shunt passive filters, consists of tuned LC filter and/or high pass filter. These filters are also used to improve the input power factor to suppress harmonic. They have a low initial cost and high efficiency. However, shunt passive filters have such problems as to discourage their applications. A shunt passive filter (SPF) exhibits lower impedance at a tuned harmonic frequency than the source impedance to reduce the harmonic currents flowing into the source. In principle, filtering characteristics of the SPF are determined by the impedance ratio of the source and the shut passive filter. Therefore, the SPF has the following problems [37]:

- The source impedance, which is not accurately known and varies with the system configurations strongly influences filtering characteristics of the shunt passive filter.
- The shunt passive filter acts as a sink to the harmonic current flowing from the source. In the worst case, the SPF falls in series resonance with the source impedance.
- At a specific frequency a parallel resonance occurs between the source impedance and the SPF, which is called harmonic amplification.

Active power filter are used to compensate for reactive power, negative sequence harmonics and/or flicker in industrial power systems. The basic compensation principles were proposed in 1970 [38-40]. Over the last 10 years, due to development in semiconductor technology it has become possible to put them into practice.

Compensation principle:

Shunt active power filters compensate current harmonics by injecting equal-but-opposite harmonic compensating current. In this case, the shunt active power filter operates as a current source injecting the harmonic components generated by the load but phase shifted by 180°. As a result, components of harmonic currents contained in the load current are cancelled by the effect of the active filter, and the source current remains sinusoidal and in phase with the respective phase to neutral voltage. This principle is applicable to any type of load considered as an harmonic source. Moreover, with an appropriate control scheme, the active power filter can also compensate the load power factor. In this way, the power distribution system sees the non-linear load and the active power filter as an ideal resistor.

Fig.5.7 shows the basic principle of a Shunt Active Filters [SAF], which is controlled into a closed loop manner to actively shape the source current into the sinusoid. Fig.5.8 shows current & voltage waveforms in such a case. The load is assumed to be a 3-phase diode rectifier with an inductive load. The SAF injects the compensating current i_c into the source to cancel the harmonics contained in the load current I_L. Accordingly, a finite amount of impedance in the power system, which is usually inductive, seldom influences the filtering characteristics because the harmonic producing load can be considered a current source inductance on the dc side of a diode rectifier.

To put the shunt active conditioner into practical use, however the followings have to be solved.

1. Which voltage and/or current of v, is and it should we detect?
2. How should we decide or calculate the command of the compensating from the detected voltage and /or current? It is difficult to do it, especially in transient states or in such a case that it is always fluctuating
3. How should we realize .a large capacity non- sinusoidal current source with rapid current response, which can follow its command?

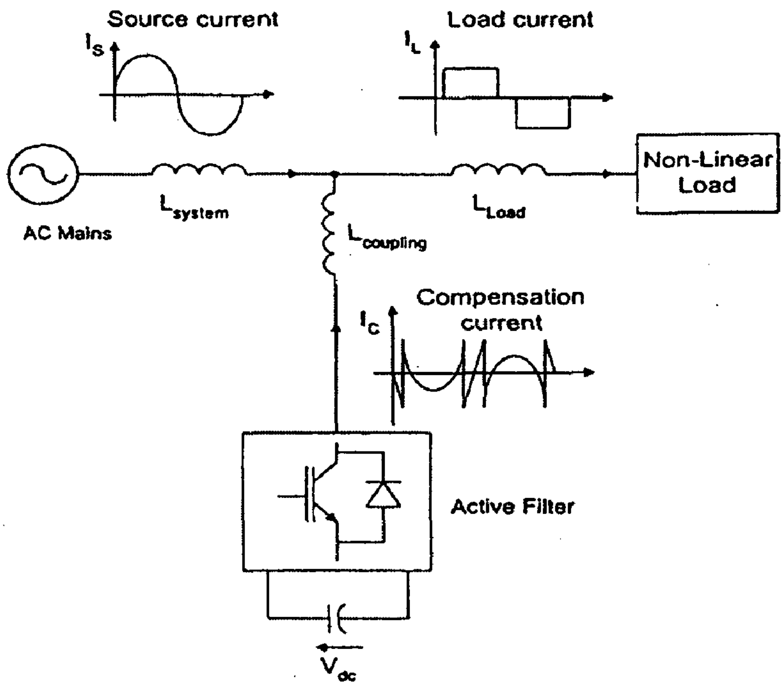

Fig. 5.7 Compensation Characteristics of SAF

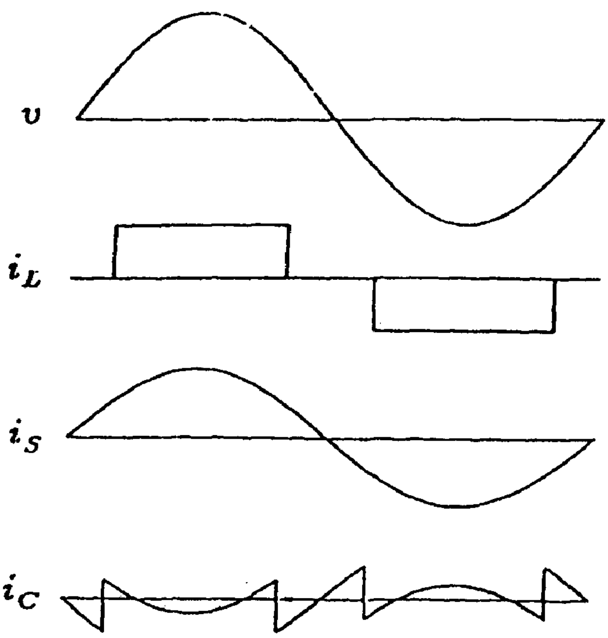

Fig. 5.8 Theoretical waveforms in Fig. 5.7

5.2.2 Classification of Active Filters [36]

Various types of APF have been proposed in technical literature [41-46]. Classification of APF is made from different points of view [47]. Active filters are divided into ac and dc filters. Active dc filters have been designed to compensate for current and/or voltage harmonics on the dc side of these converters for HVDC transmission systems [48-49] and on the DC link of a PWM rectifier/inverter for traction systems. However, emphasis is put on active ac filters. The basic principles of operation of active filters are outlined together with their general classifications [50].

A. Classification by objectives: *Who is responsible for installing active filter?*

The objective of "Who is responsible for installing active filters" classifies them into the following two groups:

- Active filters installed by individual consumers on their own premises near one or more identified harmonic producing loads.
- Active filters installed by electric power utilities in sub-stations and/or on distribution feeders. It is found that harmonic voltage increases due to "harmonic propagation" as a result of series and/or parallel resonance between the line inductors and shunt capacitors for p.f. correction installed on the distribution system. This implies that not only harmonic compensation but also harmonic damping is a viable & effective way of showing harmonic pollution in power systems. Hence utilities has the responsibly for actively damping harmonics propagation throughout the systems.

The main purpose of active filters installed by individual consumers is to compensate for current harmonics and or current imbalance of their own harmonics producing loads. On the other hand, the primary purpose of a filtration by utilities in the near future is to compensate for voltage harmonics and/or voltage imbalance, or to provide 'harmonic damping' throughout power distribution system. In addition, AFs have the function of harmonic isolation at the utility consumer point of common, coupling in power distribution systems.

B. Classification by System Configurations:

1. Shunt Active filters & Series Active Filters:

Fig.5.9 shows a system configuration of a shunt active filter (SAF) used alone, which is one of the most fundamental system configurations. The SAF is to draw a compensating current I_{AF} from the utility, so that it cancels current harmonics on the ac side of a general purpose thyristor rectifier [51-54] with a dc link inductor or a PWM rectifier with a dc link capacitor for traction system [55]. The shunt active filter has the capability of damping harmonic resonance between an existing passive filter and the supply impedance.

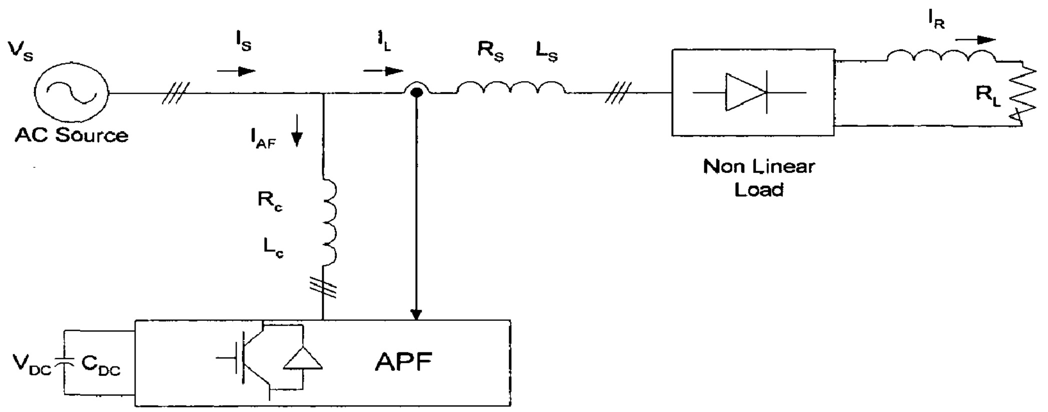

Fig. 5.9 Shunt Active Power Filter

Fig.5.19 shows a system configuration of a series active filter used alone. The series active filter is connected with the utility through a matching transformer, so that it is applicable to harmonic compensator of a large capacity diode rectifier with a dc link capacitor. Table 15.1 shows comparison between the shunt & series active filter. This concludes that series AF has a "dual" relationship in each item with the shunt AF [47, 56]

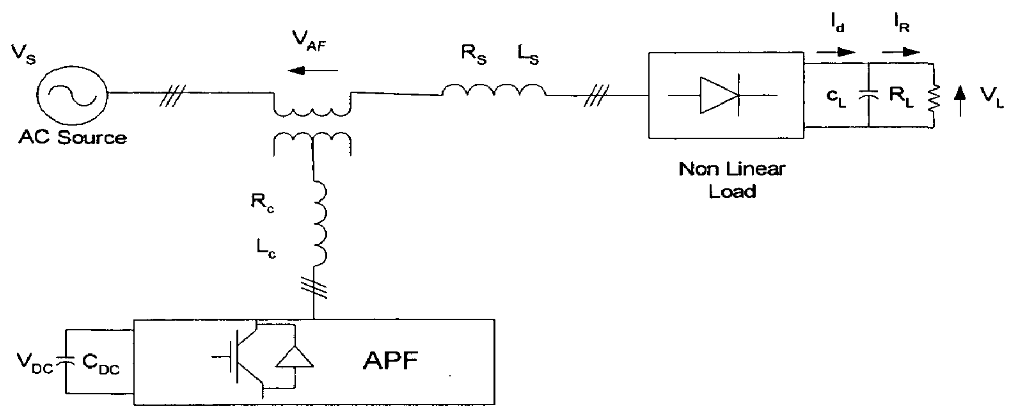

Fig. 5.10 Series Active Power Filter

Table 5.1 Comparisons of Shunt AF and Series AF

	Shunt Active Filter	Series Active Filter
System Configuration	**Fig. 5.18**	Fig. 5.19
Power Circuit of AF	**Voltage-fed PWM inverter with current minor loop**	Voltage-fed PWM inverter without current minor loop
AF act as	**Current Source: i_{AF}**	Voltage Source: v_{AF}
Harmonic producing load suitable	**Diode/Thyristor rectifiers with inductive loads, and cycloconverters**	Large capacity diode rectifiers with capacitive Loads
Additional function	**Reactive power compensation**	AC voltage regulation
Present situation	Commercial stage	Laboratory stage

2. Hybrid Active/Passive Filters:

Fig.5.11 through fig.5.13 shows three types of hybrid active/passive filters, the main purpose of which is to reduce initial costs and to improve efficiency. The shunt passive filter consists of one or more tuned LC filters and/or a high-pass filter. Table-5.2 shows comparisons among the three hybrid filters in which the active filters are different in function from the passive filters. Note that the hybrid filters are applicable to any current harmonic source, although a harmonic producing load is represented by a thyristor rectifier with a DC link inductor in Figures 5.11 through 5.13.

Such a combination of a shunt active filter and a shunt passive filter as shown in Fig.5.11 has already been applied to harmonic compensation of naturally commutated twelve-pulse cycloconverters for steel mill drives [57]. The passive filters absorbs 11^{th} and 13^{th} harmonic currents while the active filter compensates for 5^{th} and 7^{th} harmonic currents and achieves damping of harmonic resonance between the supply and the passive filter. One of the most important considerations in system design is to avoid competition for compensation between the passive filter and the active filter.

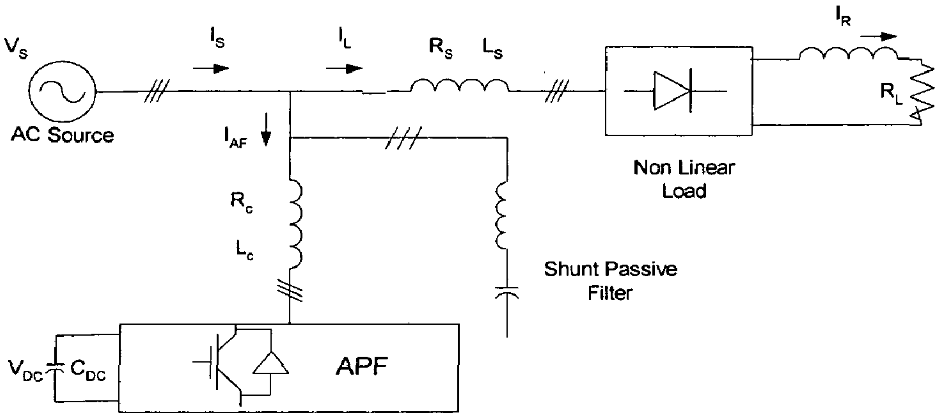

Fig. 5.11 Combination of Shunt Active Filter with Shunt Passive filter

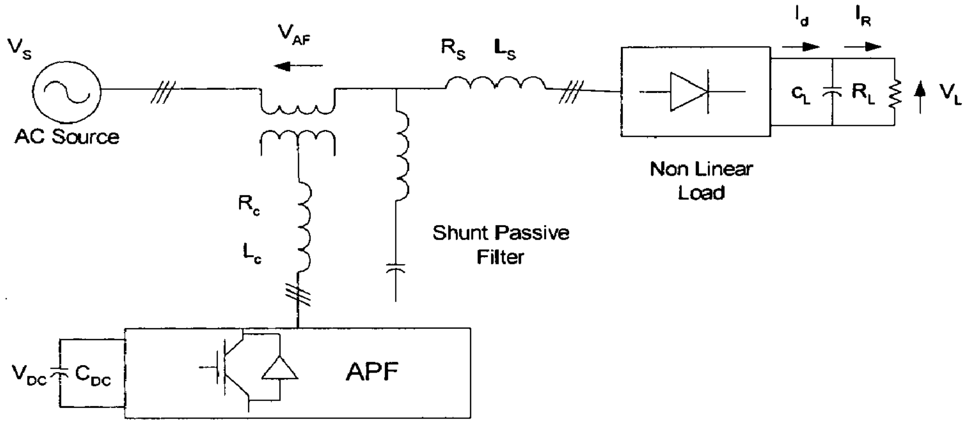

Fig. 5.12 Combination of Series Active Power Filterand Shunt passive filter

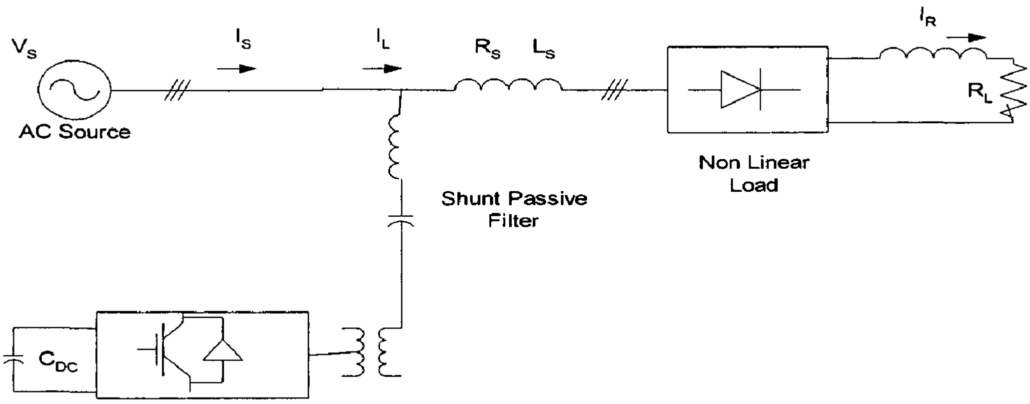

Fig. 5.13 Series Active Filter connected in series with Shunt Passive filter

The hybrid active filters, shown in Fig.5.12 [53] [58-59] and in Fig.5.13 [60-62] are right now on the commercial stage, not only for harmonic compensation but also for harmonic isolation between supply and load, and for voltage regulation and imbalance compensation. They are considered prospective alternatives to pure active filters used alone. Other combined systems of AF and PF or LC circuits have been proposed in [63].

Table 5.2 Comparisons of Hybrid Active/Passive Filters

	Shunt Active Filter +Passive Filter	Series Active Filter +Passive Filter	Series Active Filter Connected in series with SPF
System Configuration	**Fig. 5.20**	**Fig. 5.21**	Fig. 5.22
Power Circuit of AF	**Voltage-fed PWM inverter with current minor loop**	**Voltage-fed PWM inverter without current minor loop**	Voltage-fed PWM inverter with or without current minor loop
Function Of AF	**Harmonic Compensation**	**Harmonic Isolation**	Harmonic Isolation or Harmonic Compensation
Advantages	**General Shunt Fitter Applicable** **Reactive power controllable**	**Already existing Shunt Passive filters applicable** **No Harmonic current flowing through AF**	Already existing Shunt Passive filters applicable Easy protection of AF
Problems	**Share compensation in frequency domain between AF and PF**	**Difficult to protect AF against over current** **No reactive power control**	No reactive power control
Present status	Commercial stage	A few practical Applications	Commercial stage

C. Classification by Power Circuit:

There are two types of power circuits used for active filters: a voltage fed PWM inverter and a current fed PWM inverter as shown in fig.5.14 [64-65] & fig.5.15 [40] [66] respectively. These are similar to the power circuit used for ac motor drives.

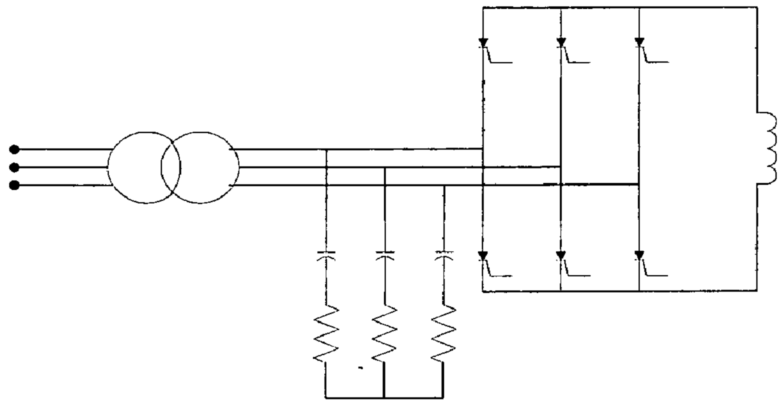

Fig.5.14 Current Source PWM inverter

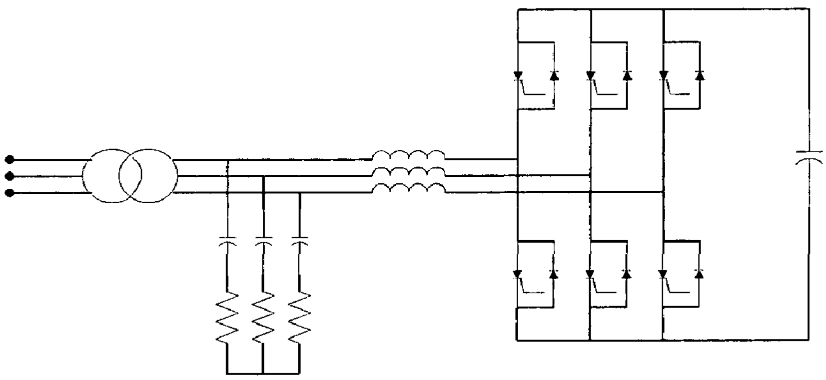

Fig. 5.15 Voltage-source PWM inverter

They are, however different in their behavior because the SAF acts as non-sinusoidal current source. The current source or voltage source PWM inverters which are used as a shunt active filter needs a dc reactor or a dc capacitor which plays an essential rolè as an energy storage element but it does not need any dc power supply on the dc side.

The reasons that the SAF can be controlled so as to supply the losses in the PWM inverter from the ac source voltage source PWM inverter is preferred over current source PWM inverter because of high η and lower initial cost [43]. In Japan, all the AFs put in use are voltage source PWM inverter. It is found that total losses is minimum in IGBT based VSI as compared to BJT based VSI & GTO based CSI-PWM.

D. Classification by Control Strategy:

The control strategy of active filter has a great impact not only on the compensation objective and required KVA rating of active filters, but also on the filtering characteristics in transient state as well as in steady state [63].

1. Frequency domain & Time-domain:

These are mainly two kinds of control strategies for extracting current or voltage harmonics from the corresponding distorted current or voltage, one is based on the Fourier analysis in the frequency domain [42], and the other is based on the theory of instantaneous reactive power in three phase circuits, which is called the p-q theory [67-68]. The concept of p-q theory in the time domain has already been applied.

2. Harmonic Detection Methods

Three kinds of harmonic detection methods in the time-domain have been proposed for shunt active filters acting as a current source i_{AF} .Taking into account the polarity of the currents i_s, i_L and i_{AF} in Fig.5.9 gives

Load-current detection: $i_{AF} = -i_{lh}$

Supply-current detection: $i_{AF} = -K_s.i_{sh}$

Voltage detection: $i_{AF} = -K_v.v_h$

The load-current detection is based on feed forward control, while supply-current detection and voltage detection are based on feedback control with gains of K_s and K_v, respectively. Load-current detection and supply-current detection are suitable for shunt active filters installed in the vicinity of one or more harmonic-producing loads by individual consumers. Voltage detection is suitable for shunt active filters that will be dispersed on power distribution systems by utilities, because the shunt active filter based on voltage detection is controlled in such a way to present infinite impedance to the external circuit for the fundamental frequency, and to present a resistor with low resistance of $1/K_v$ for harmonic frequencies [69].

Supply-current detection is the basic harmonic detection method for series active filters acting as a voltage source V_{AF}. Referring to Fig.5.10 yields,

Supply-current detection: $V_{AF} = G.\ i_{sh}$

The series active filter based on supply-current detection is controlled in such a way to present zero impedance to the external circuit for the fundamental frequency and to present at resistor with high resistance of G [Ω] for the harmonic frequencies. The series active filters shown in Fig.5.10 [45] and Fig.5.12 [63] are based on supply-current detection.

5.2.3 THREE-PHASE SHUNT ACTIVE FILTER

The shunt active power filter is a device that is connected in parallel to and cancels the reactive and harmonic currents from a non-linear load. The resulting total current drawn from the ac main is sinusoidal.

A hysteresis-band instantaneous current control PWM technique is popularly used because of its simplicity of implementation, fast current control response, and inherent peak current limiting capability. However, a current controller with a fixed hysteresis band has the disadvantage that the switching frequency varies in a band and, as a result, generates non-optimum current ripple in the load [70].

This section proposes an efficient adaptive hysteresis band current controller for shunt APF for harmonic elimination and reactive power compensation where band is programmed as a function of supply voltage, dc bus voltage and slope of reference compensator current wave to maintain the switching frequency constant.

The APF is realized using three single phase IGBT based PWM-VSI bridges with a common DC bus capacitor. An adaptive hysteresis band rule based carrier-less PWM current controller is used derive gating signals for the IGBTs. Source reference currents are derived using load currents, dc bus voltage and supply voltage. The commands current of APF are derived using source reference and load currents. A 3-phase diode rectifier with resistive loading is employed as the non-linear load. The APF is found effective to meet IEEE-519 standard recommendations on harmonics level.

A. INTORDUCTION

The hysteresis-band current control PWM method is popularly used for APF because of its simplicity of implementation. Besides fast current control response and inherent peak current limiting capability, the technique does not need any information about system parameters. However, the current controller with a fixed hysteresis band has the disadvantage that the switching frequency varies with in a band because peak-to-peak current ripple is required to be controlled at all points of the fundamental frequency wave.

Also the basic hysteresis technique exhibits also several undesirable features; such as device limitations, increased switching losses and uneven switching frequency that causes acoustic noise and difficulty in designing input filters [71].

The adaptive hysteresis band current controller is adapted by Bose (1990) [70] and applies to APF by Murat and Engin (2005) [72] using synchronous d-q-0 reference frame theory to determine the reference current, which is inefficient and difficult to implement.

In this section an efficient and simple control scheme is realized/ simulated to investigate the affects of hysteresis bandwidth to THD of supply current and switching frequency of APF. Adaptive hysteresis band current controller changes the hysteresis bandwidth as a function of supply voltage, dc bus voltage and reference compensator current variation to optimize switching frequency and THD of supply current.

B. SYSTEM CONFIGURATION AND CONTROL SCHEME

The basic building blocks of the conventional parallel APF are shown in Fig.5.16.The APF is composed of a standard 3 single phase voltage source inverter bridge with a common dc bus to facilitate the independent control of all the three phases of the APF. An adaptive hysteresis band rule based carrier-less PWM current controller is used derive gating signals for the IGBTs. The non-linear load is a dc resistive load supplied by the three phase uncontrolled bridge rectifier with an input impedance. The desired APF currents are estimated by sensing the load current, dc bus voltage and source voltage. The adaptive hysteresis current controller generates the switching signals to the IGBTs to force the desired currents into the APF phases.

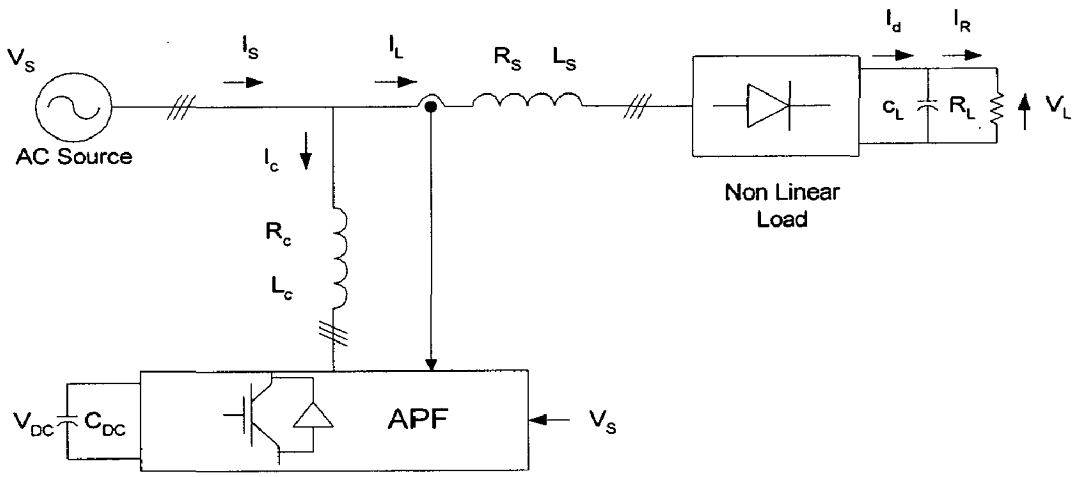

Fig. 5.16 Basic Building Block of the Active Power Filter

Fig. 5.17 shows the control scheme of the shunt APF [73] with adaptive hysteresis band width control. The ac source feeds fundamental active power component of load currents and another fundamental component of current to maintain the average capacitor voltage to desired value. This second component of supply current feeds losses in the VSI bridge such as switching losses, leakage current of capacitor, etc. under steady state conditions and to regulate the stored energy on the dc bus of the APF under transient conditions imposed on the system.

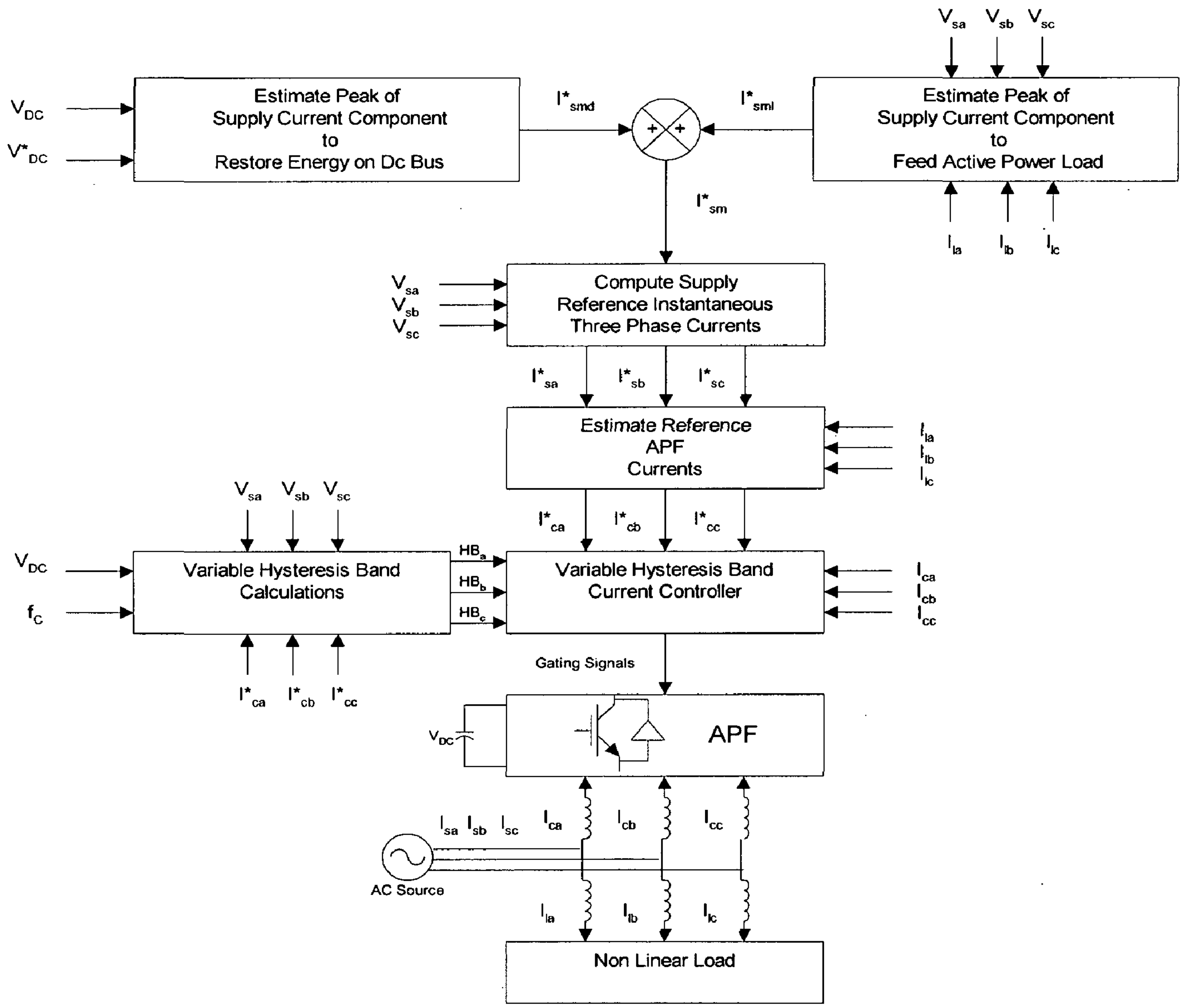

Fig. 5.17 Control Scheme for APF

This component of peak of supply currents (I^*_{smd}) is computed by using average dc bus voltage, value of the capacitor and required reference value of dc bus voltage (v^*_{dc}). The main component of peak of supply currents (I^*_{sml}) to feed load currents is computed using sensed load currents and supply voltages. The total peak value of supply currents (I^*_{sm}) is computed by adding these two components ($I^*_{sml}+I^*_{smd}$).

Three-phase instantaneous reference supply currents (i^*_{sa}, i^*_{sb}, i^*_{sc}) are computed by multiplying this peak magnitude (I^*_{sm}) with unit current templates (u_{sa}, u_{sb}, u_{sc}) derived in phase with supply voltages (v_{sa}, v_{sb}, v_{sc}) .Three-phase instantaneous reference currents of an APF (i^*_{ca}, i^*_{cb}, i^*_{cc}) are computed by subtracting load currents (i_{la}, i_{lb}, i_{lc}) from reference supply currents (i^*_{sa}, i^*_{sb}, i^*_{sc}).

A adaptive hysteresis band rule based carrier-less PWM current control technique is employed over the current errors of the three-phase sensed and reference currents of the APF to derive gating signals to the IGBTs of the VSI bridges. Band width of adaptive hysteresis band current controller is programmed as a function of supply voltage (v_{sa}, v_{sb}, v_{sc}), dc bus voltage (v_{dc}) and slope of reference compensator current (i^*_{ca}, i^*_{cb}, i^*_{cc}) wave to maintain the switching frequency constant. The APF draws the required currents from the ac mains to feed harmonics and reactive power and causes balanced sinusoidal unity power factor supply currents under varying operating conditions.

C. ANALYSIS AND MODELING

The system comprises of ac source, non-linear load, the APF and the new control scheme. The components of the system are analyzed separately and integrated to develop the complete model for simulation.

C1. CONTROL SCHEME

The operation of the control scheme, shown in Fig. 2, has been discussed in an earlier section. Different steps in the scheme are modeled as follows.

Peak Source Current Estimation

The reference current has two components (I^*_{sml} and I^*_{smd}) and the first component (I^*_{sml}) corresponding to load is computed from instantaneous load power. The instantaneous load power is

$$P_L = v_{sa}\, i_{la} + v_{sb}\, i_{lb} + v_{sc}\, i_{lc} \quad (5.1)$$

where i_{la}, i_{lb} and i_{lc} are three-phase load currents, of which some may be zero; v_{sa}, v_{sb} and v_{sc} are three-phase line to neutral voltages of the mains; under ideal conditions,

$$v_{sa}=V_{sm}\,\text{Sin}\,(wt),\ v_{sa}=V_{sm}\,\text{Sin}\,(wt\text{-}2pi/3),\ v_{sa}=V_{sm}\,\text{Sin}\,(wt\text{+}2pi/3) \quad (5.2)$$

where V_{sm} be zero is the peak value of phase voltage and w is the frequency in rad/s .

The average power of the load (Ps) to be supplied by the ac mains can be computed by averaging P_L and expressed as

$$Ps = (3/2)\ V_{sm} I_{ml} \cos \Phi = (3/2)\ V_{sm} I^*_{sml} \quad (5.3)$$

where I_{ml} is the peak of fundamental supply current and cos Φ, is the fundamental power-factor (displacement factor) of the load.

From Eq. (5.3) the supply peak current (I^*_{sml}) for unity power-factor corresponding to load average power is computed as

I^*_{sml} as= Ps / {(3/2) V_{sm}} (5.4)

The second component of supply reference current (I^*_{smd}) is to restore the energy on dc bus for regulating its voltage to constant value, is computed based on energy balance. In the present work, the losses in APF, being very small, are neglected. The nominal stored energy (e^*_{dc}) on the dc bus of the APF is

$e^*_{dc}=C_{dc}(v^*_{dc})^2/2$ (5.5)

where v^*_{dc} is the reference voltage across the dc bus capacitor C_{dc}.

But, the actual average stored energy on dc bus is

$e^*_{dc}=C_{dc}(v_{dca})^2/2$ (5.6)

where v_{dca} is the average value of the actual dc bus voltage.

Thus energy loss of dc bus capacitor is

$\Delta e_{dc} = e^*_{dc} - e_{dc} = C_{dc}\{(v^*_{dc})^2 - (v_{dc})^2\}/2$ (5.7)

This energy difference, encountered in the APF, must be supplied by the three-phase ac mains. The corresponding peak value of supply current (I^*_{smd}) is computed as

$$\int_0^T \{ v_{sa} I^*_{smd} \text{Sin}(wt) + v_{sa} I^*_{smd} \text{Sin}(wt-2pi/3) + v_{sa} I^*_{smd} \text{Sin}(wt+2pi/3)\} \quad (5.8)$$

where T is the half cycle period of the supply frequency over which the averaging is carried out.

The net peak value of supply currents (I^*_{sm}) from Eq. (5.4) and Eq. (5.8) is

$I^*_{smd} = I^*_{smd} + I^*_{smd}$ (5.9)

Source Reference Current Generation

The instantaneous three-phase reference supply currents are computed using Eq. (5.9) as

$I^*_{sa} = I^*_{sm} / u_{sa}$, $I^*_{sb} = I^*_{sm} / u_{sb}$ and $I^*_{sc} = I^*_{sm} / u_{sc}$ (5.10)

Where u_{sa}, u_{sb}, u_{sc} are unit current vectors obtained from Eq. (5.1) and peak supply voltages as

$u_{sa} = v_{sa} / V_{sm}$, $u_{sb} = v_{sb} / V_{sm}$ and $u_{sc} = v_{sc} / V_{sm}$

Reference APF Current Generation

The APF currents are computed using Eq. (10) and sensed load currents i_{la}, i_{lb} and i_{lc} as

$i^*_{ca} = i^*_{sa} - i_{la}$, $i^*_{cb} = i^*_{sb} - i_{lb}$ and $i^*_{cc} = i^*_{sc} - i_{lc}$ (5.11)

Adaptive Hysteresis Based Current Controller

The current controller decides the switching pattern of the APF devices. The switching logic is formulated as follows:

If $i_{ca} < (i^*_{ca} - HB_a)$ upper switch is OFF and lower switch is ON for leg 'a' (SAL=0);

If $i_{ca} < (i^*_{ca} - HB_a)$ upper switch is ON and lower switch is OFF for leg 'a' (SAL=1)

The right leg devices of 'phase a' bridge are switched in a complementary manner to left leg devices, i.e. SAL is the complement of SAR. In the same fashion, the switching of 'phase b' and 'phase c' are derived using HB_b and HB_c the variable width of the hysteresis band.

Variable Hysteresis Band Calculation

The width of the hysteresis band determines the switching frequency of the inverter. As the bandwidth narrows the switching frequency increases. A suitable bandwidth should be selected in accordance with the switching capability of the inverter. The bandwidth should also be small enough to supply the reference current precisely keeping the view of switching losses and EMI related problems [72]. Therefore the range of switching frequencies used is based on a compromise between these factors.

The bandwidth of the hysteresis current controller determines the allowable current shaping error. By changing the bandwidth the user can control the average switching frequency of the APF and evaluate the performance for different value of hysteresis bandwidth. Switching frequency of the hysteresis band current controller is depends on the rate of change of the actual APF current therefore switching frequency does not remain constant and varies along with the current waveform. Also line inductance of the APF and the dc bus voltage are the main parameters determining the rate of change of the actual APF currents. Therefore switching frequency depends also on these two parameters.

Fig. 5.18 shows the PWM current and voltage waves for phase a. When the actual line current of the active power filter tries to leave the hysteresis band, the suitable IGBT is switched to ON or OFF state to force the current to return to a value within the hysteresis band. Then the switching pattern will be trying to maintain the current inside the hysteresis band .The currents i^{-}_{ca} tends to cross the lower hysteresis band at point 1, where upper side IGBT of leg 'a' is switched on. The linearly rising current i^{+}_{ca} then touches the upper band at point 2, where the lower side IGBT of leg 'a' is switched on. The following equations can be written in the respective switching intervals t_1 and t_2.

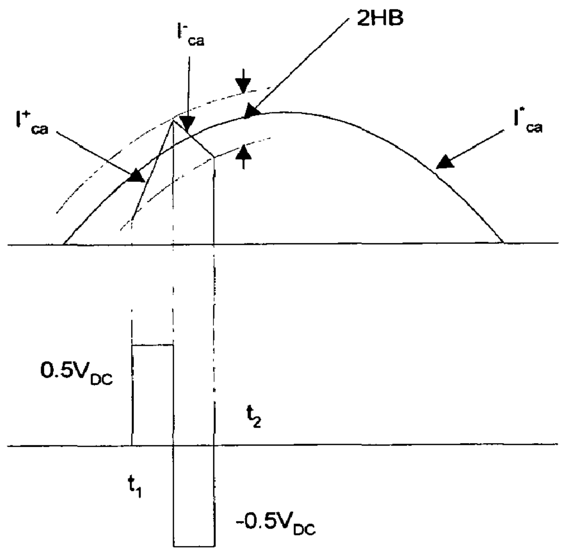

Fig. 5.18 Current and Voltage Waves for Hysteresis Band Current Control

$$L\frac{di_a^+}{dt} = (0.5V_{DC} - V_s)$$
$$L\frac{di_a^-}{dt} = -(0.5V_{DC} + V_s) \qquad (5.12\text{-}5.14)$$
$$\frac{di_a^+}{dt} + \frac{di_a^-}{dt} = 0$$

where L=phase inductance, and i^+_{ca} and i^-_{ca} are the respective rising and falling current segments.

From the geometry of Fig. 3, we can write

$$\frac{di_a^+}{dt}t_1 - \frac{di_a^*}{dt}t_1 = 2 * HB$$
$$\frac{di_a^-}{dt}t_2 - \frac{di_a^*}{dt}t_2 = -2 * HB \qquad (5.15\text{-}5.17)$$
$$t_1 + t_2 = T_C = \frac{1}{f_c}$$

where t_1 and t_2 are the switching intervals, and f_c is the switching frequency.

Adding (5.15) and (5.16) and substituting in (5.17), we get

$$\frac{di_a^+}{dt}t_1 + \frac{di_a^-}{dt}t_2 - \frac{1}{f_c}\frac{di_a^*}{dt} = 0 \qquad (5.18)$$

Subtracting (5.16) from (5.15), we get

$$4HB = \frac{di_a^+}{dt}t_1 - \frac{di_a^-}{dt}t_2 - (t_1 - t_2)\frac{di_a^*}{dt} \qquad (5.19)$$

Substituting (5.14) in (5.19) and (5.18) and simplifying

$$4HB = (t_1 + t_2)\frac{di_a^+}{dt} - (t_1 - t_2)\frac{di_a^*}{dt}$$
$$(t_1 - t_2) = \left(\frac{di_a^*}{dt}\right) \Big/ f_c\left(\frac{di_a^+}{dt}\right) \qquad (5.20\text{-}5.21)$$

Substituting (5.21) in (5.20), gives

$$HB = \frac{0.125V_{DC}}{f_c L}\left[1-\frac{4L^2}{V_{DC}^2}\left(\frac{V_s}{L}+m\right)^2\right] \tag{5.22}$$

Where m=is the slope of command current wave. Hysteresis band (HB) can be modulated at different points of fundamental frequency cycle to control the switching pattern of the inverter. For symmetrical operation of all three phases, it is expected that the hysteresis band width (HB) profiles HB_a, HB_b and HB_c will be the same, but have phase difference. The adaptive hysteresis band current controller changes the hysteresis bandwidth according to instantaneous compensation current variation and capacitor dc bus voltage to minimize the influence of current distortion on modulated waveform. The adaptive hysteresis band current controller is given by Eq. (5.22).

Equation (5.22) shows the hysteresis bandwidth (HB) as a function of switching frequency, supply voltage, dc capacitor voltage and slope of the reference compensator current wave. Hysteresis band can be modulated as a function of capacitor voltage and reference compensator current wave so that the switching frequency is remains nearly constant. This will improve the PWM performances and APF substantially.

Therefore variable hysteresis band for phase 'a', 'b' and 'c' is given as

$$HB_a = \frac{0.125V_{DC}}{f_c L_C}\left[1-\frac{4L^2}{V_{DC}^2}\left(\frac{V_{sa}}{L_C}+\frac{di_{ca}^*}{dt}\right)^2\right]$$

$$HB_b = \frac{0.125V_{DC}}{f_c L_C}\left[1-\frac{4L^2}{V_{DC}^2}\left(\frac{V_{sb}}{L_C}+\frac{di_{cb}^*}{dt}\right)^2\right] \tag{5.23-5.25}$$

$$HB_c = \frac{0.125V_{DC}}{f_c L_C}\left[1-\frac{4L^2}{V_{DC}^2}\left(\frac{V_{sc}}{L_C}+\frac{di_{cc}^*}{dt}\right)^2\right]$$

C2 ACTIVE POWER FILTER

The unity turns ratio transformer in each phase has equivalent inductance (L_c) and resistance (R_c) at ac input. The common dc bus capacitor is C_{dc} .These APF may be modeled by the following state space equations.

$pi_{ca} = -(R_c /L_c) i_{ca}+(v_{sa} - v_{ca})/ L_c$ (5.26)

$pi_{cb} = -(R_c /L_c) i_{cb}+(v_{sb} - v_{cb})/ L_c$ (5.27)

$pi_{cc} = -(R_c /L_c) i_{cc}+(v_{sc} - v_{cc})/ L_c$ (5.28)

$pv_{dc} = (i_{cad}+ i_{cbd} + i_{ccd})/ C_{dc}$ (5.29)

where p is the differential operator (d/dt) and i_{cad}, i_{cbd} and i_{ccd} are the charging current to the dc bus of the APF form the single phase VSI bridges.

The current depends on switching logic and are expressed as

$i_{cad} = i_{ca}$(SAL-SAR), $i_{cbd} = i_{cb}$(SBL-SBR) and $i_{ccd} = i_{cc}$(SCL-SCR)

where SAL,SAR,SBL,SBR SCL and SCR are the switching functions.

Voltages v_{sa} , $v_{sb}$and v_{sc} are the three-phase PWM voltages reflected on the ac input side computed as

$v_{sa} = v_{dc}$ (SAL-SAR), $v_{sb} = v_{dc}$ (SBL-SBR) and $v_{sc} = v_{dc}$ (SCL-SCR)

D. SIMULATIONS RESULTS AND DISCUSSIONS

The detail simulation is carried out using MATLAB/SIMULINK. Performance characteristics of the APF system with proposed control scheme are given in Fig. 5.19-5.21 illustrating the steady state conditions.

Fig. 5.19 shows the supply voltage, source currents, load current, APF current and the dc bus voltage when a load is increased from 10 kW to 20 kW at 0.2 S. The source current responds very quickly and settles to steady state value within a cycle demonstrating the excellent transient response of the APF. The AF current increased almost instantaneously to feed the increased load current demand by taking the energy instantaneously by the dc bus capacitor. DC bus voltage recovers within 0.1 S. Source currents always remain sinusoidal and lower then the load currents in all operating conditions. The THD of the source current is reduced from 26.27 % to 0.66 % under light load (10 kW) and from 24.48 % to 0.73 % during heavy load (20 kW).The APF is quite effective to reduce the THD well below the specified 5 % limit of standard IEEE-519.

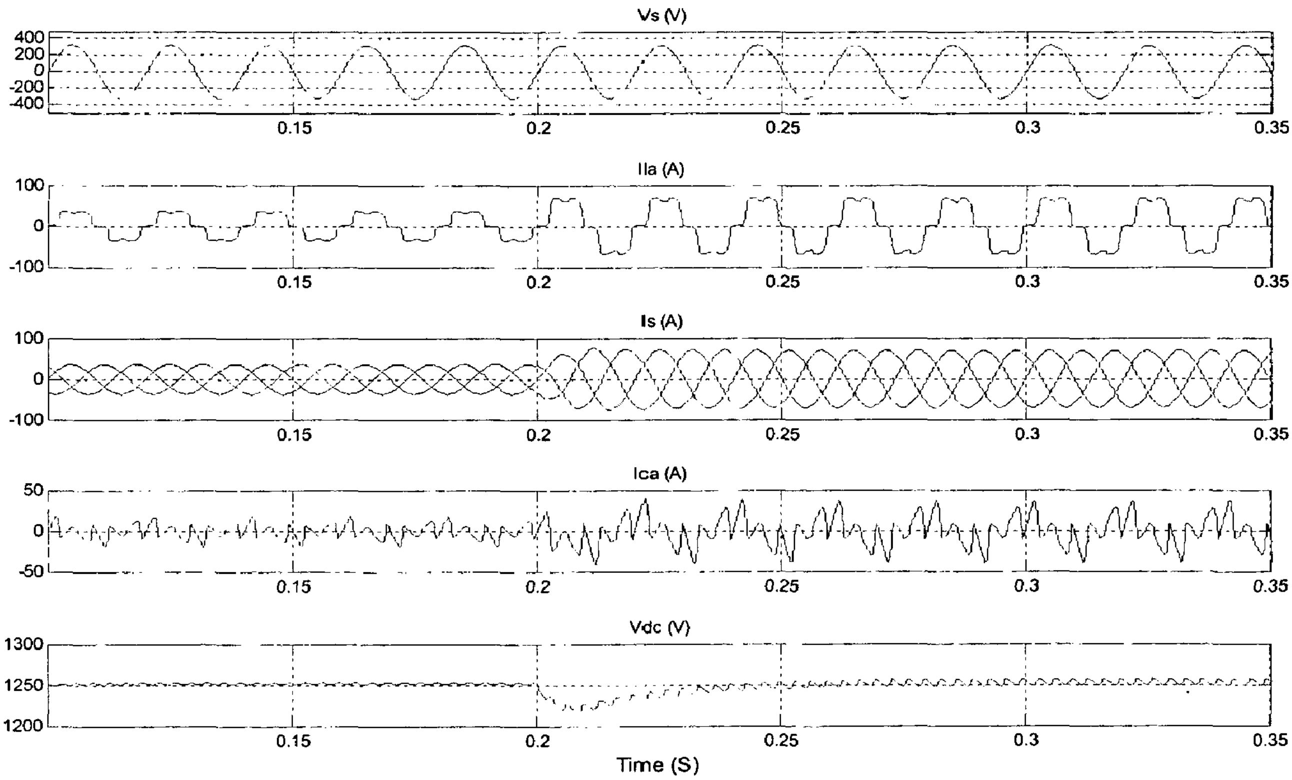

Fig. 5.19 Performance of the APF under Load Change from 9.7 kW to 19.3 kW.

In conventional fix band hysteresis current control and adaptive hysteresis band current control method the switching frequency are shown in Fig. 5.20. In adaptive hysteresis band current control method the switching frequency is constant but in conventional fix band hysteresis current control deviation in switching frequency is clearly shown. In practical applications it is necessary to kept switching frequency to a certain limits, in order to determine switching device and its switching losses.

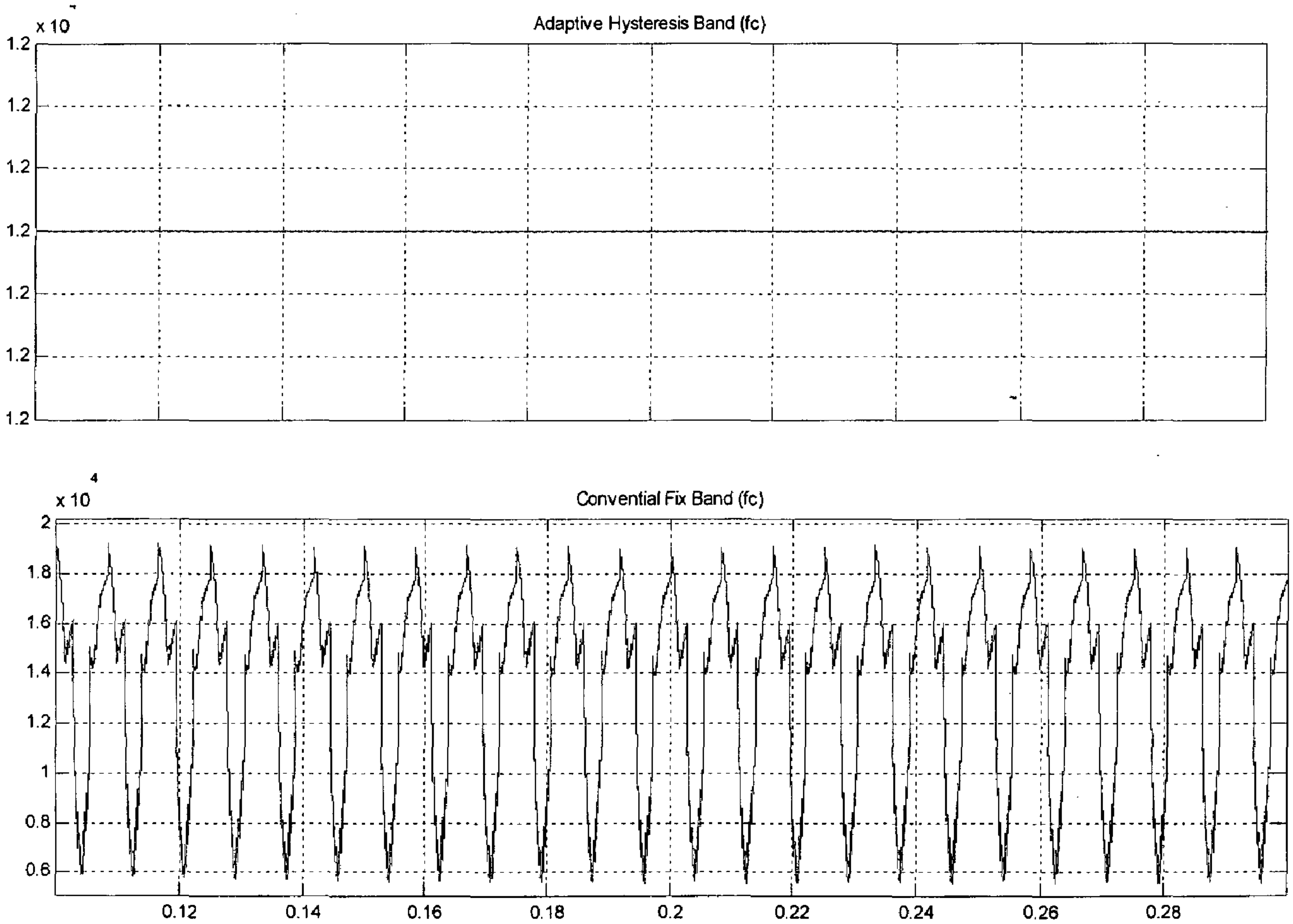

Fig. 5.20 Switching Frequency in Hz

In conventional fix band hysteresis current controller, it is not possible to determine not only hysteresis bandwidth but also switching frequency according to system parameters (L_c and V_{DC}). In adaptive hysteresis band current controller, switching frequency remains constant respecting the system parameters and defined frequency. In Fig. 5.21 variable hysteresis band for phase 'a' (HB_a) is given when a load is light (10 kW).

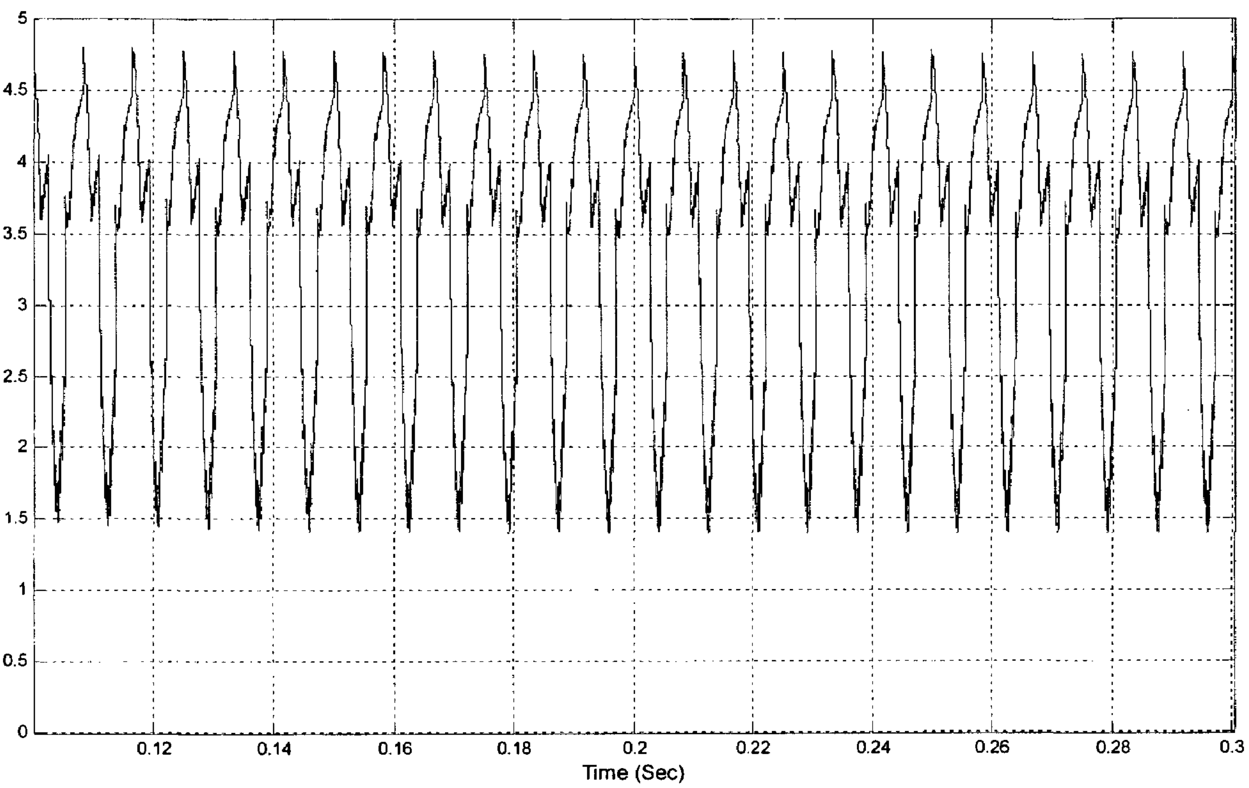

Fig. 5.21 Variable Hysteresis Band (HB_a) for light load (9.7 kW)

The performance of the proposed control algorithm of the APF is found to be excellent and the source current is practically sinusoidal and in phase with the source voltage. The fast response of the APF ensures that the APF is not overburdened during transient's conditions. Switching frequency remains constant and independent of load conditions.

This section demonstrates the validation of a simpler and efficient control approach for the adaptive hysteresis band current controller for the shunt APF. The results of simulation study of new APF control technique presented in this section is observed to eliminate the harmonic and reactive components of load currents resulting in sinusoidal and unity power-factor source currents. The APF enhances the system efficiency because the source need not process the harmonic and reactive power demanded by the load.

The validity of this technique in order to compensate current harmonics was proved on the basis of simulation results. The APF is found effective to meet IEEE-519 standard recommendations on harmonics level.

The section describes an efficient and simple control scheme to realized shunt APF with an adaptive hysteresis band current controller which changes the hysteresis bandwidth as a function of supply voltage, dc bus voltage and reference compensator current to optimize switching frequency and THD of supply current. Although various criteria of optimization are possible, this section illustrates a case where the switching frequency is held constant.

E. SYSTEM PARAMETERS

V_s (rms/phase) = 230 V, F = 50 Hz, Lc = 1mH, Ls = 0.01 H, Inverter Dc Voltage=1250 V C_{DC} =1500 μF, Switching Frequency = 12 kHz.

6. CONCLUSIONS

In the scope of this work, investigation of harmonics on power distribution system is done, i.e. the qualitative overview study of the distribution power system with the goal of understanding harmonics waveform distortion within it, and to provide a detailed analysis, that gives quantitative answers to the distortion due to the specific sources of harmonics and to take preventive measures for control of the same, is done. The qualitative analysis enables one to get a general outlook of the studied power system from the harmonics point of view. It can be of special interest in cases of widespread systems.

Investigation of the cumulative harmonic current characteristics of a large number of single-phase power electronic loads that employ conventional diode bridge rectifiers and DC smoothing capacitors is done. Examination of the effects of shared impedance, as well as variations in power level, impedance magnitude, X/R ratio, and smoothing capacitance is done.

It is shown that there is significant attenuation of current harmonics above the 3rd multiple when a number of identical loads, such as televisions and desktop computers, share a common source impedance. The THD of current in this case is approximately one-half of that obtained using superposition of individual load currents. However, the 3rd harmonic, which is responsible for most harmonic-related neutral conductor overloading problems, experiences only slight attenuation (i.e., 0.7 - 0.8).

By defining a current harmonic diversity factor, it is also shown that the cumulative harmonic currents for the 9th multiple and above experience appreciable phase cancellation due to individual and/or composite variations in power level, impedance magnitude, impedance X/R ratio, and smoothing capacitance. Since the 3rd and 5th harmonics show little phase cancellation, the THD of the summed current is only slightly less than that obtained by using superposition.

The mean harmonic diversity factors shown in Table 4.1 were calculated for ranges of circuit parameter variations that are likely to be encountered by these types of loads in actual distribution systems.

The attenuation and diversity factors calculated give an indication of how much the commonly-used fixed current injection method, using arithmetic sums of harmonic current magnitudes, can overestimate the cumulative harmonic currents produced by distributed single-phase power electronic loads.

Derivation of harmonic domain models suitable for the study of conventional three-phase, six pulse harmonic converters is done. Modulation theory based on switching functions and discrete convolutions are the cornerstone of these models.The harmonic converter models given in this work build up incrementally, starting with the simplified case where no commutation effects are included. This simplicity is used to illustrate the simple relationship that exists between the AC and DC voltages and switching functions. The MATLAB™ code is used for developing the model. The characteristic and non-characteristic harmonics are implicitly included in the model, together with DC ripple, ac and converter imbalances, and pre existing harmonics.

The model comes in the form of a harmonic admittance which shows a very strong cross- coupling between phases and between harmonics. Also, the harmonic interaction and frequency conversion that exists between the ac and DC sides of the converter are implicitly included. The effect of source impedance is presented in detail with effects on harmonics.

Inrush current phenomenon, arising during transformer energization, and containing a slowly decaying transient response, with connection to harmonic domain technique is discussed and simulated.

The performance of the proposed control algorithm of the APF is found to be excellent and the source current is practically sinusoidal and in phase with the source voltage. The fast response of the APF ensures that the APF is not overburdened during transient's conditions. Switching frequency remains constant and independent of load conditions.

Also it demonstrates the validation of a simpler and efficient control approach for the adaptive hysteresis band current controller for the shunt APF. The results of simulation study of new APF control technique presented in this section is observed to eliminate the harmonic and reactive components of load currents resulting in sinusoidal and unity power-factor source currents. The APF enhances the system efficiency because the source need not process the harmonic and reactive power demanded by the load.

The validity of this technique in order to compensate current harmonics was proved on the basis of simulation results. The APF is found effective to meet IEEE-519 standard recommendations on harmonics level.

7. BIBLIOGRAPHY

1. Bollen, M., "Understanding Power Quality Problems, Voltage Sags and Interruptions". IEEE Press, New York, 2000.
2. J.Arrillaga, D.A.Bradley and P.S.Bodger, "Power System harmonics". John Wiley and Sons, 2003.
3. Sankaran, C., "Power Quality". CRC Press, Boca Raton London New York, 2002.
4. A. Enrique and M. Manuel, "Power System Harmonics". John Wiley and Sons, LTD 2001.
5. Joseph S. Subjek, John S. Mcqulkin, "Harmonics – Causes effects, measurement and analysis: An update" IEEE Trans. Industry Applications Vol.26 No.6 November 1990.
6. Owen E.L., "A History of harmonics in Power Systems", IEEE Industry applications Magazine, Jan/Feb 1998.
7. Medina A., "Harmonics Simulation Techniques (Methods & Algorithms)" IEEE Trans. Industry Applications Vol.26 No.6 November 1990.
8. Reformat, M., Woodford, D.; Wachal, R., Tarko, N. J., "Non-linear load modeling for simulations in time domain" 8th IEEE International Conference on Harmonics and Quality of Power ICHQP 1998, Athens, Greece, Oct. 1998, pp. 506-510.
9. EN 61000-4-7, 2002 (Ed.2): Electromagnetic compatibility: Testing and measuring techniques-General guide on harmonics and interharmonics measurements and instrumentation, for power supply systems and equipment connected thereto.
10. Manjure, D. P., Makram, E. B. "Impact of Unbalance on Power System Harmonics" 10th IEEE International Conference on Harmonics and Quality of Power ICHQP 2002, Rio de Janeiro, Brazil, Oct. 2002.
11. Arrillaga, J., Smith, B. C., Watson, N. R., Wood, A. R., "Power System Harmonic Analysis" John Wiley & Sons, Chichester, 1997.
12. Arrillaga, J., Watson, N. R., Chen, S. "Power System Quality Assessment" John Wiley & Sons, Chichester, 2001.

13. "IEEE Recommended Practices and Requirements for Harmonic Control in Electrical Power System," ANSI/IEEE Std. 519-1992.
14. "IEEE task force on the Effects of Harmonics on Equipment", IEEE Transactions on Power Delivery, 8(2), pp 672-680, 1993.
15. N. Mohan, T.M. Undeland, W.P. Robbins. "Power Electronics: Converters, applications and Design", John Wiley & Sons, 2003.
16. A. Mansoor, W.M. Grady, A.H. Chowdhury, M.J. Samotyj, "An Investigation of Harmonics Attenuation and Diversity Among Distributed Single-Phase Power Electronics Loads," IEEE Transaction on Power Delivery, Vol. 10, No. 1, January 1995.
17. Alberto Prudenzi "A Novel Procedure based on Lab Tests for Predicting Single-Phase Power Electronics-Based Loads Harmonic Impact on Distribution Networks," IEEE Transaction on Power Delivery, Vol. 19, No. 2, April 2004.
18. A. Mansoor, W.M. Grady, P.T. Staats, R.S. Thallam, M.T Doyle, M.J. Samotyj, "Predicting the Net Harmonic Currents Produced by Large Numbers of Distributed Single-Phase Computer Loads," IEEE /PES Winter Meeting, January 1995, New York.
19. A. Mansoor and W.M. Grady "Analysis of Compensation factors Influencing the Net Harmonic Current Produced by Single-Phase Non-Linear Loads," International Conference on Harmonics and Quality of Power ICHQP' 98, Athens, Greece, October 14-16, 1998.
20. D.E. Rice, "A Detailed Analysis of Six-Pulse Converter Harmonic Currents", IEEE Transactions on Industry Applications, Vol. 30, No. 2 March/April 1994.
21. M. Sakui, H. Fujita, M. Shioya, "A Method of Calculating Harmonic Current of a Three-Phase Bridge Uncontrolled rectifier with DC Filter", IEEE Transactions on Industry Electronics, Vol. 36, No. 3 1989.
22. L. Hu, R. Yacamini, "Calculation of Harmonic Interface in HVDC System with Unbalance", Proceedings of the International Conference on AC and DC Power Transmission, 1991, pp. 390-394.

23. J. Jesus Rico, E. Acha and M. Madrigal "The study of Inrush Current Phenomenon Using Operational Matrices", IEEE Transactions on Power Delivery, Vol. 16, No. 2, 2001.
24. D. Povh and W. Schultz "Analysis of overvoltages caused by transformer magnetizing inrush current", IEEE Transactions on Power Apparatus and System, Vol. PAS 97, No. 4, July 1978.
25. J.F. Write, F.P. DeCesaro and S.R. Mendis, "Damaging long-term overvoltages on industrial capacitor banks due to transformer energization inrush current", IEEE Transactions on Industry Applications, Vol. 30, No. 4, July 1994.
26. J.P. Bowles," Overvoltages in HVDC transmission system caused by magnetizing inrush current", IEEE Transactions on Power Apparatus and System, Vol. PAS 93, No. 2, July 1974.
27. E. Acha, A. Semlyen and N. Rajakovic, "A Harmonic Domain Computattional Package For Nonlinear Problems And Its Application To Electric Arcs" IEEE Trans. On Power Delivery, Vol.5, No.3, July 1990.
28. H.W. Dommel, A. Yan and S. Wei, "Harmonics from transformer saturation" IEEE Trans. On Power Systems, Vol. PWRD-1, No.2, April 1986.
29. A. Semlyen, E. Acha, and J. Arrillaga, "Newton-Type Algorithms for the Harmonic Analysis of Nonlinear Power Circuits in Periodical Steady State with Special Reference to Magnetic Nonlinearities", IEEE Transactions OIL Power Delivery, Vol. PWRD-3, No.3, July 1988, pp. 1090 1098
30. N. Rajakovic and A. Semlyen, "Harmonic Domain Analysis of Field variables Related to Eddy Current and Hysteresis losses in Saturated Laminations", IEEE Transactions on Power Delivery, Vol. 4, No.2, April 1989.
31. N. Rajakovic and A. Semlyen. "Investigation of the Inrush Phenomenon: A Quasi-Stationary Approach in the Harmonic Domain", IEEE Paper No. 89 WM 082-9-PWRD, presented at the 1989 IEEE/FES Winter Power Meeting.
32. H.W. Dommel, "Harmonics form Transformer Saturation", IEEE Transactions on Power System, Vol.PWRD-1, No. 2, Apirl 1986, pp. 209-215.

33. R. Yacamini, A. Abu-Nasser, "Numerical Calculation of Inrush Current in Single-Phase Transformers", Proceedings of the IEE, Part B, Vol. 128, No. 6, November 1981, pp. 327-334.
34. J. Pedra, C. Felipe, L. Sainz and R. Lopez,"Harmonic Nonlinear Transformer Modeling", IEEE Transactions on Power Delivery, Vol. 19, No.2, April 2004.
35. J. Pedra, C. Felipe, L. Sainz ,M. Salichs and R. Lopez, "Pspice computer model of a three-phase three-legged Transformer", IEEE Transactions on Power Delivery, Vol. 19, pp 200-207, Jan 2004.
36. Timothy L. Skvarenina, "The Power Electronics Handbook, Industrial Electronics Series", CRC Press, 2002.
37. AICTE Sponsored Short term Course on "Power Quality Problems & Solutions: Recent Advances", IIT-Roorkee, May 23-27 2005.
38. Bird, B. M., Marsh, J. F., and McLellan, P. R., "Harmonic reduction in multiple converters by triple-frequency current injection", IEE Proc., 116(10), pp.1730-1734, 1969.
39. Gyugyi, L. and Strycula, E. C, "Active AC power filters", Proceedings of the 1976 IEEE/IAS Annual Meeting, 1976, pp.529-535.
40. Kawahira, H., Nakamura, T., Nakazawa, S., and Nomura, M., "Active power filters", in Proceedings of the 1983 International Power Electronics Conference, Tokyo, Japan, 1983, pp.981-992.
41. Moran, S., "A line voltage regulator/conditioner for harmonic-sensitive load isolation", in Proceedings of the 1989 IEEE/IAS Annual Meeting, 1989, pp947-951.
42. Grady, W. M., Samotyj, M. J., and Noyola, A. H., "Survey of active power line conditioning methodologies", IEEE Trans. Power Delivery, 5(3), pp. 1536-1542, 1990.
43. Akagi, H., "Trends in active power line conditioners", IEEE Trans. Power Electronics, 9, 3, pp. 263-268, 1994.
44. Akagi, H. and Fujita, H., "A new power line conditioner for harmonic compensation in power systems", IEEE Trans. Power Delivery, 10(3), pp. 1570-1575, 1995.

45. Fujita, H. and Akagi, H., An approach to harmonic current-free AC/DC power conversion for large industrial loads: the integration of a series active filter and a double-series diode rectifier, IEEE Trans. Industrial Applications, 33(5), 1233-1240, 1997.
46. Aredes, M., Heumann, K., and Watanabe, E. H., "A universal active power line conditioner", IEEE Trans. On Power Delivery, 13, 2, pp. 545-551, 1998.
47. Akagi, H., "New trends in active filters for power conditioning", IEEE Tram. Industrial Applications, 32, 6, pp. 1312-1322, 1996.
48. Watanabe, E. H., "Series active filter for the DC side of HVDC transmission systems", in Proceedings of the1990 International Power Electronics Conference, Tokyo, Japan, 1990, 1024-1030.
49. Zhang, W., Asplund, G., Aberg, A., Jonsson, U., and Lbfif, O., "Active DC filter for HVDC system—A test installation in the Konti-Skan at Lindome converter station", IEEE Trans. Power Delivery, 8(3), 1599-1605, 1993.
50. B. Singh, K. Al-Haddad and A. Ambrish Chandra, "A review of active power filters for power quality improvement", IEEE Transaction on Industrial Electronics, vol.46, pp.1-12, October 1999.
51. Akagi, H., Tsukamoto, Y., and Nabae, A., "Analysis and design of an active power filter using quad-series voltage-source PWM converters", IEEE Trans Industrial Applications, 26(1), 93-98, 1990.
52. Peng, F. Z., Akagi, H., and Nabae, A., "A new approach to harmonic compensation in power systems-a combined system of shunt passive and series active filters", IEEE Trans. Industrial Applications., 26(6), 983-990,1990.
53. Peng, F. Z., Akagi, H., and Nabae, A., "A study of active power filters using quad-series voltage-source PWM converters for harmonic compensation, IEEE Trans. Power Electronics", 5(1), 9-15, 1990.
54. Bhattacharya, S., Frank, T. M., Divan, D., and Banerjee, B., "Active filter system implementation", IEEE Industrial Applications Mag., 4(5), 47-63, 1998.

55. Krah, J. O. and Holtz, "Total compensation of line-side switching harmonics in converter-fed AC locomotives", in Proceedings of the 1994 IEEE/IAS Annual Meeting, 1994, 913-920.
56. Peng, F. Z., Application issues of active power filters, IEEE Industrial Application Mag., 4(5), 21-30, 1998.
57. Takeda, M., Ikeda, K., and Tominaga, Y, "Harmonic current compensation with active filter", in Proceedings of the 1987 IEEE/IAS Annual Meeting, 1987, 808-815.
58. Peng, F. Z., Akagi, H., and Nabae, A., "Compensation characteristics of the combined system of shunt passive and series active filters", IEEE Trans. Industrial Application, 29(1), 144-152, 1993.
59. Kawaguchi, L, Ikeda, H., Ogihara, Y, Syogaki, M., and Morita, H., Novel active filter system composed of inverter bypass circuit for suppression of harmonic resonance at the Yamanashi maglev test line, in proceedings of the IEEE-IEEJ/IAS Power Conversion Conference, 1997, 175-180.
60. Fujita, H. and Akagi, H., "A practical approach to harmonic compensation in power systems-series connection of passive and active filters", IEEE Trans. Industrial Application, 27(6), 1020-1025, 1991.
61. Balbo, N., Penzo, R., Sella, D., Malesani, L, Mattavelli, P., and Zuccato, "A Simplified hybrid active filters for harmonic compensation in low voltage industrial applications", in Proceedings of the 1994 IEEE/PES International Conference on Harmonics in Power Systems, 1994, 263-269.
62. Zyl, A., Enslin, J. H. R., and Spee, R., "Converter based solution to power quality problems on radial distribution lines", in Proceedings of the 1995 IEEE/IAS Annual Meeting, 1995, 2573-2580.
63. Bhattacharya, S., Cheng, P., and Divan, D., "Hybrid solutions for improving passive filter performance in high power applications", IEEE Trans. Industrial Application, 33(3), 732-747, 1997.
64. Akagi, H., Nabae, A., and Atoh, S., "Control strategy of active power filters using multiple voltage-source PWM converters", IEEE Trans. Industrial Application., 22(3), 460-465, 1986.

65. Takeda, M., Ikeda, K., and Tominaga, Y, "Harmonic current compensation with active filter", in Proceedings of the 1987 IEEE/IAS Annual Meeting, 1987, 808-815.

66. Van Schoor, G. and van Wyk, J., "A study of a system of current-fed converters as an active three-phase filter", in Proceedings of the 1987 IEEE/PELS Power Electronics Specialist Conference, 1987, 482-190.

67. Akagi, H., Kanazawa, Y., and Nabae, A., "Generalized theory of the instantaneous reactive power in three-phase circuits", in Proceedings of the 1983 International Power Electronics Conference, Tokyo, Japan, 1983,1375-1386.

68. Akagi, H., Kanazawa, Y., and Nabae, A., "Instantaneous reactive power compensators comprising switching devices without energy storage components", IEEE Trans. Industrial Application., 20(3), 625-630, 1984.

69. Akagi, H., Fujita, H., and Wada, K.,"A shunt active filter based on voltage detection for harmonic termination of a radial power distribution line", IEEE Trans. Industrial Application, 35(3), 638-645, 1999.

70. Bose B.K."An adaptive Hysteresis-Band Current Control Technique of Voltage-Fed PWM Inverter for Machine Drive System" IEEE Transaction on Industrial Electronics, vol.337, no.5, pp.402-406, October 1990.

71. S.Buso, S.Fasolo, L.Malesani, P.Mattaveli, "A Dead Beat Adaptive Hysteresis Current Control" IEEE Transaction on Industrial Applications, vol.36, no.4, pp.1174-1180, July 2000.

72. Murat Kale and Engin Ozdemir "A Novel Adaptive Hysteresis Band Current Controller for Shunt Active Power Filter" Electric Power System Research, vol.73, February 2005.

73. B.Singh, K.Al-Haddad and A.Ambrish Chandra, "A New Control Approach to Three-Phase Active Filter for Harmonics and reactive Power Compensation" IEEE Transaction on Power Systems, vol.13, no.1, pp.133-138, February 1998.